Distribution Agreement

In presenting this thesis or dissertation as a partial fulfillment of the requirements for an advanced degree from Emory University, I hereby grant to Emory University and its agents the non-exclusive license to archive, make accessible, and display my thesis or dissertation in whole or in part in all forms of media, now or hereafter known, including display on the world wide web. I understand that I may select some access restrictions as part of the online submission of this thesis or dissertation. I retain all ownership rights to the copyright of the thesis or dissertation. I also retain the right to use in future works (such as articles or books) all or part of this thesis or dissertation.

Signature: _____

Printed name: Ryan Martinez

Date:

To Affinity and Beyond: T cell receptor strength and its role in T cell development and function

By

Ryan Martinez

Doctor of Philosophy

Graduate Division of Biological and Biomedical Science

Immunology and Molecular Pathogenesis

_____

Brian Evavold Advisor

_____

Jacob Kohlmeier Committee Member

_____

John Altman Committee Member

_____

Mandy Ford Committee Member

_____

Rustom Antia Committee Member

Accepted:

_____

Lisa A. Tedesco, Ph.D. Dean of the James T. Laney School of Graduate Studies

_____ Date

To Affinity and Beyond

By

Ryan Martinez

Bachelor of Arts

Advisor: Brian Evavold, PhD

An abstract of a thesis submitted to the Faculty of the James T. Laney School of Graduate Studies of Emory University in partial fulfillment of the requirements for the degree of Doctor of Philosophy in Immunology and Molecular Pathogenesis in 2016

Abstract

To Affinity and Beyond

By Ryan Martinez

Functionality of the adaptive immune system depends on its ability to distinguish self and foreign antigens. However there is a balancing act the adaptive system must make, as it needs to recognize a wide range of diverse epitopes, but also distinguish between epitopes with astonishing specificity. The diversity of the adaptive immune system originates from the semi-random rearrangement of multiple gene segments to form a unique lymphocyte receptor. Mechanisms during lymphocyte development remove cells whose receptor either cannot recognize self-antigen or recognize self-antigen too well. Traditionally, this process removes cells that will not contribute to the immune response and those cells most likely to cause autoimmunity, respectively. The remaining lymphocytes then enter the periphery to protect the host from foreign pathogens. This education on self-antigen during development is intriguing, as lymphocytes must be made to recognize all potential antigens during an infection, even though they have never seen the antigens previously. Once the naïve lymphocytes have encountered antigen, many factors contribute to the fate of these cells, but the biophysical characteristics of the lymphocyte receptor interacting with peptide presented by major histocompatibility complex (pMHC) directs the initial signaling events and controls lymphocyte functionality. This receptor:ligand interaction is fundamentally important as it controls many aspects of the development and intrinsic functions of the lymphocyte. In this introduction I will discuss how central tolerance discriminates between self vs non-self as well as how these mechanisms alter the functionality and detection of lymphocytes throughout the immune response.

To Affinity and Beyond

By

Ryan Martinez

Bachelor of Arts

Advisor: Brian Evavold, PhD

A thesis submitted to the Faculty of the James T. Laney School of Graduate Studies of Emory University in partial fulfillment of the requirements for the degree of Doctor of Philosophy in Immunology and Molecular Pathogenesis in 2016

Table of Contents

Introduction

At the most simple of levels, the immune system must be able to differentiate self-vs non-self antigens either at the receptor level or at the downstream-signaling level. The idea of receptor theory was originally proposed in the early 1900s by Dr. Langley and Dr. Ehrlich to explain the differential effects seen by globally administered agents on selective cell types (1). The theory of receptor:ligand pairs has since grown to what is currently understood today and will be discussed further later. The immune system is composed of two basic systems of receptors that act to protect the host organism(2). The first system, termed the innate immune system, is made up of non-specific defenses to prevent pathogenesis and is evolutionarily older as it is the dominant form of immune defense in fungi, insects and primitive organisms (2). The innate system is also critical for instructing and educating the second branch of the immune system, termed the adaptive immune system, to respond to antigens. The two systems employ different receptors to cause the effects necessary for functionality. The innate system has conserved sets of receptors that can detect pathogenic or dangerous antigenic molecules, and through different combinations of innate receptors, integrated signals are created for each pathogen. In reaction to these integrated signals, the innate immune system reacts accordingly to initiate processes to protect the host organism. The signals produced by the innate system will also then activate and direct the adaptive immune system in order to combat and clear the antagonizing agent.

The receptors that activate the adaptive immune systems are more varied than innate receptor sets, hypothesized to contain a possible $1x10^{18}$ distinct receptors in the T cell compartment alone(3). The signals received through their T cell receptors are similar between lymphocytes, but specificity is generated by the unique receptor, as most

lymphocytes are believed to have a singular, functional antigen-recognition receptor. This concept of a unique receptor per lymphocyte is credited to Burnet's clonal selection theory that is fundamental to adaptive immunity (4). In Burnet's seminal work, the clonal selection theory has four postulates as follows:

1. Each lymphocyte has a single, unique antigen-recognition receptor.
2. Lymphocytes with receptors that recognize self-antigens will be deleted.
3. Receptor-ligand binding is necessary for activation.
4. Differentiated cells will bear this same unique receptor.

These postulates are fundamental building blocks to how we currently understand the adaptive immune system, but each has been shown to have shortcomings as more is understood about T cell receptor biology.

To understand further points, I want to set a framework for the terms of biophysical parameter used to describe receptor ligand interaction. Affinity is defined as the probability of a receptor (TCR)-ligand (pMHC) interaction and is one of the most commonly used measurements to predict the T cell response to antigen (5). As with all receptor-ligand interactions, affinity, or the association constant (K_a) is derived from the on-rate (k_{on}) and off-rate (k_{off}) of receptor-ligand equilibrium and is calculated independently of concentrations of ligand and receptor (Affinity=K_a=k_{on}/k_{off}) (5, 6). The affinity of an interaction is not its bond strength, or the force needed to break the bond, though these terms are often incorrectly used interchangeably. An example of this distinction can be seen in the avidin/biotin system, as this receptor-ligand pair has one of the highest affinity interactions measured, but the non-covalent interactions can be easily broken, signifying lower bond strength(7). Along with TCR:pMHC affinity, the

dissociation constant (K_d, inverse of K_a) and half-life ($\tau_{1/2}= \ln(2)/k_{off}$) can also be derived. The combination of these measurements have been used to describe T cell activation and differentiation models (kinetic proofreading, optimal dwell time, etc), but not all methods of biophysical measurements generate similar results(5, 8, 9). Therefore, further understanding of measurement systems is necessary.

Affinity is commonly measured using purified reactants in solution by surface plasmon resonance (SPR), where free ligand is flowed over receptors fixed to a surface(10). This absolute affinity measurement occurs in three dimensions (3D) and allows for the definition of protein interactions in their simplest, purified form with no influence from outside interactions. However, the increased degrees of freedom that occur in solution may not be the optimal method to accurately assess interactions between receptor and ligands that occur on two opposing plasma membranes(5). A better replicate of *in vivo* interactions between proteins at the membrane surface can be accomplished using two-dimensional (2D) receptor-ligand binding techniques such as flow chamber assays, thermal fluctuation assays, single molecule FRET, Zhu-Golan plots, contact area FRAP and the adhesion frequency assay(5). Currently the focus of our lab has been the use of the two-dimensional micropipette adhesion frequency assay (2D-MP), a measurement of the relative 2D affinity of the receptor-ligand interaction on opposing membranes(11). This 2D affinity is termed a relative affinity because it is dependent on the context in which it was measured, whereas 3D methods generate an absolute affinity measurement while ignoring all other cellular participants. This distinction of relative and absolute affinity will be discussed in a later section. When 2D and 3D affinity TCR measurements are compared, an increased affinity with an associated decreased k_{off} can

be appreciated (8, 9, 12, 13). Attempts to correlate affinity values generated by 2D and 3D methods have been achieved with little success, as the parameters controlling relative 2D affinity are still unknown(8). Importantly, the relative affinity measured by 2D-MP better correlates with functional responses than 3D methods and refers to the affinity in the proper cellular context(8, 12).

The advent of recombinant pMHC tetramer reagents has allowed for the identification of antigen-specific T cells and the subsequent use of these reagents for indirect assessment of biophysical interactions of TCR:pMHC (14). The binding of the tetramer reagent is dependent on valency to increase its avidity as monomeric pMHC complexes do not attach well to TCR (15, 16). This lack of monomer interaction with TCR is most likely due to the reliance of pMHC tetramer staining on higher affinity interactions (17, 18). The k_{off} and k_{on} for each arm of the pMHC tetramer binding to TCRs are known to reflect avidity interactions, with the binding of one pMHC monomer arm enhancing the k_{on} of the subsequent monomer arm and reducing the k_{off} of the entire reagent (19). The use of pMHC tetramer to measure k_{off}, $k_{on,}$ and $\tau_{1/2}$ assumes that the amount of pMHC tetramer bound to a cell is directly proportional to the affinity of that cell, with more tetramer bound to higher-affinity cells than to lower-affinity T cells (14, 18–20). However, this assumption may not always yield a direct correlation, with many groups demonstrating tetramer binding intensity does not equate to functional responses or SPR measurements (21–24). One possibility explanation for discrepancies with SPR is that the functional cellular membrane can affect tetramer binding. Another possibility for these discrepancies is that TCR density affects binding because tetramer relies on an avidity interaction. While many have normalized the TCR to pMHC concentrations on

each cell(16, 25, 26), others do not account for the number of TCRs expressed at the cell surface (21, 27, 28). The effect of TCR density can be appreciated, as the analysis of the tetramer+ populations reveals lower TCR expression as they exhibit only 20-40% of the TCR density compared to the bulk T cell population (Unpublished data). This indicates tetramer+ T cells may have different TCR levels than the remaining T cell population but it is unknown if this is a cause or an effect of being a tetramer binder.

The measurement of TCR:pMHC affinity by 2D-MP is an extremely sensitive method that follows first order kinetics and is dependent upon T cell intrinsic factors (5). Measured TCR affinities can be altered when reagents are used to change lipid composition and actin cytoskeleton(8). Adjustments of the membrane and supporting scaffolding should change 2D-affinity, as the characteristics of the opposing membranes during receptor-ligand interactions are fundamental for the measurement of relative 2D affinities. Much of the sensitivity of the 2D-MP assay comes from the flexibility of the red blood cell (RBC) membrane, which can be distended by the formation of a single TCR:pMHC bond(5, 29). As biotinylated pMHC is bound to the RBC through streptavidin interactions, clustering and valency of ligand could play a role in binding. Varying the concentration of pMHC on the RBC surface does not change the calculated affinity of activated T cells, signifying concentration does not affect the 2D measurements (8, 11). In experiments altering the valency of pMHC on the RBC through use of mutant streptavidin, no changes in 2D affinity were noted (8). This is in contrast to pMHC tetramers which rely on both concentration and valency of the reagent to measure antigen-specificity(30). Together, this suggests concentration and valency do not play a

role in the measurement of affinity by 2D-MP. In addition, it demonstrates the micropipette values are a measure of affinity and not avidity.

The measurement of TCR:pMHC biophysical interactions are performed under conditions with no applied force(5, 8). Application of force to or by the TCR may be important in the functionality of T cells, as the TCR/CD3 complex has been postulated to function as a mechanosensor (31, 32). Methods using 2D measurements can interrogate the role of force on the TCR anchored in the membrane, allowing for the study of these interactions and how they can affect kinetic parameters. Recent work has demonstrated the application of force to the TCR:pMHC interaction increases the lifetime of the bond by reducing the k_{off} of the bond(32). By applying force, the increased cumulative lifetimes correlate with a higher likelihood of calcium-mediated activation, though this is best appreciated when the accumulation of bonds are in the first minute of force application(32).

An important distinction between CD4 and CD8 T cells is the contribution of coreceptor to the overall strength of binding between pMHC and TCR (16, 33). CD4 and CD8 coreceptors are thought to stabilize TCR:pMHC bonds while also recruiting Lck to the TCR complex for the initiation of the downstream signaling cascade (34, 35). Intriguingly, CD8 has a higher affinity for its coreceptor than CD4, though both interactions are of weaker affinity(9, 34). For CD8 T cells, coreceptor contributes to the binding of TCR to pMHC when assessed by pMHC tetramer, 2D-MP and SPR (33, 36–38). The removal of CD8 contribution leads to decreased avidity and functional responses (39–41). In addition, the binding of the lowest affinity T cells are the most affected by the loss of CD8, signifying CD8 helps to increase the likelihood of low-affinity TCR:pMHC

interaction and signaling(12, 39). In contrast, the role of CD4 is very different as there is little to no contribution to the TCR:pMHC interaction as measured by 2D-MP, pMHC tetramer and SPR (9, 34). This is not to say CD4 is not important in functional responses, as CD4 is required to recruit Lck for optimal initiation of T cell signaling (15, 42, 43), but at least under the conditions used in tetramer and 2D assays, there is little contribution to biophysical parameters(9). Importantly, detection of CD4 T cells by pMHCII tetramer would be expected to miss more of the lower affinity TCRs due to the lack of coreceptor contribution as compared to pMHCI tetramer and CD8 T cells. These differences in CD4 and CD8 coreceptor binding impact the use of tetramers to count antigen-specific T cells as well as measuring the kinetic rates of the TCR:pMHC interaction.

Detection of Antigen-specific CD4 T cells

The identification of T cells is important as the biophysical TCR:pMHC interactions discussed are correlated with functional responses. The current gold standard for identifying antigen-specific T cells are using either pMHC tetramer reagents or readouts of functional responses, but both are sub-optimal in identifying the true number of antigen-specific T cells (44–47). For example, not all T cells of the same specificity make cytokine upon stimulation as demonstrated by the use of TCR-Tg T cells(48, 49). Further, a CD4 T population has a number of distinct fates with associated effector functions, such that any one cytokine will underestimate the total number of antigen-specific cells. Interestingly, the number of pMHC tetramer+ T cells sometimes equates to the number of cytokine producing cells, even though not all T cells will produce the target cytokine (27, 45, 47). For the most part intracellular staining for cytokines is incompatible with tetramer staining making it unclear if cytokine-producing cells overlap

with tetramer binders, or if they are distinct populations. To more accurately identify the number of antigen-specific T cells, groups have used activation markers such as CD11a, LFA-1 or CD49d that are up regulated on antigen-specific T cells after infection (45, 50). When these cells are quantitated using these functional cell surface markers, they far outnumber the number of tetramer or cytokine-producing cells(45, 50). The 2D-MP further corroborates the underestimation of antigen-specific T cells by pMHC tetramers (17, 18). When compared to the total population of antigen-specific T cells, pMHC tetramer+ T cells make up only the highest affinity population(18). Most T cell repertoires have a normally distributed TCR:pMHC affinity range, with the rarest cells being the highest and lowest affinity. Based on this data, tetramer+ cells are above average in affinity and would therefore only make up a fraction of the total T cells in an immune response(51). This would be especially apparent for CD4 T cells since the coreceptor does not aid in tetramer avidity.

The 2D-MP assay is currently the most sensitive available to capture the entire affinity range of a T cell repertoire and not just the highest affinity T cells. To perform the 2D-MP assay, single T cells are randomly chosen for affinity measurements from a purified population of cells. As this is a sampling process that is time intensive, it is important to understand the numbers of cells needed for analysis to reflect representative data of the entire population. To address how many cells need to be measured to find the average affinity of an antigen-specific polyclonal population, we have combined previously published measurements of a polyclonal T cell population for a single antigen (MOG_{38-49}:I-A^b) and performed random sampling experiments (Figure 1). When noting the moving average from 10 repetitions of the randomly sampled MOG-specific T cell

affinities, it is apparent the sampling affinity often reaches the average affinity rapidly, ie, within 10 binding pairs. By the time 16 binding T cells have been analyzed, the average affinity measured is +/- 5% of the affinity of the entire pooled population. This measurement is for a polyclonal population with a 2,000-fold range in affinity, meaning a repertoire with considerably less diversity (TCR-Tg or tetramer+ T cells) needs even fewer points measured to identify the average affinity. Therefore, to measure the average affinity of a normally distributed polyclonal repertoire only 10-16 T cell affinities need to be measured to be within 5% of the average affinity of the repertoire.

Signaling in low-affinity T cells

In both kinetic segregation and proofreading models, the binding of TCR:pMHC is key to activation, with the k_{off} and k_{on} and $\tau_{1/2}$ controlling the strength of signal the T cell receives(52–56). Higher-affinity interactions with prolonged $\tau_{1/2}$ have an increased likelihood of forming a stable conjugate and triggering the T cell signaling cascade, though an optimal $\tau_{1/2}$ most likely exists due to the hypothesized need for serial engagement (6, 53, 56). Using this logic, the lowest-affinity T cells should have a reduced probability of initiating T cell signaling, but these cells do efficiently propagate the signaling cascade as low-affinity T cells do expand, and differentiate during the immune response (17, 18, 50). Thus, mechanisms must exist that allow for low-affinity T cells, with the reduced probability of initial TCR:pMHC bond formation, to receive sufficient signals to compete with high-affinity counterparts.

Developing thymocytes discriminate positive- and negative-selecting signals through both qualitative and quantitative signaling pathways. Qualitatively, studies have

suggested reduced but sustained Erk signaling is necessary for positive selection while strong Erk, p38 and Jnk activation are necessary for negative selection(57–60). In positive selection, the protein Themis reduces TCR signaling by recruiting the phosphatase SHP-1 to inhibit Lck activation and reduces strong, transient, Erk activation, a property associated with negative selection(60, 61). Without Themis, low-affinity pMHC can produce strong agonist signals resulting in increased negative selection(61). This is of interest, as negative regulatory mechanisms must be preventing low-affinity ligands from being selected like high-affinity ligands. Currently, it is unknown what controls the function of Themis or how it discriminates between high- and low-affinity pMHC to ultimately regulate downstream signals. One potential quantitative mechanism for discriminating high- and low-affinity pMHC was found in thymocyte negative selection. During negative selection, thymocytes bind to pMHC and scan coreceptors (CD4 and CD8) to find one coupled to Lck(62). CD8 coreceptors on thymocytes have a lower amount of coupled Lck than CD4 coreceptor, so a longer TCR:pMHC $\tau_{1/2}$ is necessary for CD8 T cell negative selection(62). If a TCR:pMHC bond is maintained during the duration for a coreceptor-Lck conjugate to be found, the T cell is determined to be high-affinity and will undergo Bim-dependent apoptosis(63). These differences in signaling between positive and negative selection demonstrate how similar stimuli (pMHC) can generate distinct results depending on the TCR interaction parameters.

Naive CD4 and CD8 T cells demonstrate a distribution of reactivity to multiple foreign-antigens that is established during thymic selection on self-antigens. In both naïve CD4 and CD8 T cells, multiple studies have been able to identify heterogeneity in reactivity of T cells for self- and foreign-pMHC(26, 64–67). These ranges of reactivity

relate to markers of self-pMHC stimulation (CD5, Nur77, basal TCRζ phosphorylation) (26, 64, 67, 68) as well as indicators of activation in response to foreign-pMHC (ERK phosphorylation, IL-2 production)(67). Conflicting experimental evidence exists when attempting to correlate self-reactivity with foreign-reactivity(26, 64, 67). Some have demonstrated CD5 positively correlates with foreign TCR reactivity (measured by pMHC tetramer and function)(26, 64), while others have demonstrated CD5 expression can be altered without changes to TCR affinity as measured by SPR (67). Nonetheless, based on the TCR affinity for self-pMHC, the immune system is able to diversify the reactivity of signaling machinery by controlling the basal phosphatase and kinase activity.

The first step of signaling after TCR triggering is phosphorylation of CD3 and TCRζ intracellular chains by Lck and the recruitment of the kinase Zap70. Phosphorylation of Zap70 by Lck propagates the initial signals and causes downstream activation of the MAP kinase (Erk), NF-κB and calcineurin pathways(69). To inhibit signaling cascades, phosphatases such as SHP-1/2 and CD45 prevent the sustained activation of kinases(69). For low-affinity TCR:pMHC interactions, the peak of T cell signaling molecules (Erk, Jun, Ras) are delayed or absent and TCR signaling is decreased (61, 65, 70). This late and reduced activation of Erk in low-affinity T cells allows for the sustained recruitment and activity of SHP-1, decreasing the activation of Lck and reducing the T cell signaling response(61, 70, 71). Another phosphatase, PTPN22, has also been shown to inhibit Erk phosphorylation in T cells stimulated with low-affinity pMHC(72). It is surprising that even with these negative signaling events, low-affinity TCRs are able to signal and even upregulate activation genes CD69 and CD25 to similar levels as higher-affinity T cells (70, 73). Similar to thymocyte selection, this

demonstrates peripheral T cells have mechanisms to detect biophysical TCR interactions that can then be translated to signaling cascades, as well as possess compensatory mechanisms to enhance low-affinity TCR interactions or even decrease higher-affinity T cell interactions(74). Potentially, force generation by TCRs could be a mechanism by which low-affinity T cells are able to increase bond $\tau_{1/2}$ and receive similar signals as high-affinity counterparts(32, 75, 76). Conversely, it may be that different pathways are induced by low-affinity TCR:pMHC binding that are currently not understood. Overall, low- and high-affinity T cells use similar mechanisms and machinery to signal, but the outcomes seem to vary in their response.

Functionality of low-affinity T cells

The development and function of T cells has been highly associated with TCR:pMHC affinity, with high- and low-affinity T cell interactions often performing different roles. Thymocyte selection is dependent upon TCR:pMHC affinity interactions, with positive selection requiring low-affinity interactions and negative selection deleting thymocytes greater than a threshold affinity (77, 78). The number of antigen-specific T cells for a single epitope is tightly controlled by central tolerance and therefore by TCRs affinity for self-pMHC presented in the thymus (79–83). The initial numbers of DP thymocytes for a single epitope are defined by the size of their positively selecting niche of self-peptides and further culled by their reactivity to self-antigen via negative selection(27, 66, 83–85). Work suggests positive selection is important in the generation of a functional T cell repertoire, as alterations in the size of the selecting niche can cause T cell dysfunction or increased reactivity to antigen (66, 86). Analysis of the autoimmune prone NOD mouse has suggested its positive selecting niche is reduced, causing

competition for positive selection survival signals and enriching for T cells that have a higher affinity TCR:self-pMHC interaction (85). This reduced positive selection niche and concurrent increase in TCR affinity will not be fully compensated by negative selection, as negative selection is not as effective as once believed (66, 85, 87–89). The precursor frequency of a given antigen-specific T cell repertoire reproducibly generated by thymocyte selection is important as antigens with higher precursor frequencies can reach peak numbers more rapidly and provide better immune protection (27). Antigen-specific T cell repertoires with lower precursor frequencies will have a greater fold expansion, but will still not outnumber the higher precursor frequency repertoires (90). Based on this functional data, one could assume the repertoires with larger precursor frequency have a higher affinity for pMHC, as this would mean they have undergone less negative selection. Recent work supports this hypothesis as epitopes with lower precursor frequency demonstrate more similarity to mouse self-peptides as well as reduced pMHCII tetramer binding(27). Therefore, a balance exists between positive and negative selection and their preference to favor low- and high-affinity interactions between pMHC and TCR will ultimately determine the numbers and affinity of antigen-specific T cells.

All the advantages of TCRs with high-affinity for pMHC would suggest they can easily outcompete the lower affinity T cells(91), but this does not seem to be occurring when the full affinity repertoire is analyzed(17, 18, 50). One caveat to many model systems is the focus on a single TCR and the use of different APLs to model the fate of polyclonal T cells in response to lower-affinity antigens(62, 73, 92–94). In TCR-Tg mice, each T cell undergoes similar thymic selection mechanisms, and therefore possesses similar reactivity to antigen. Groups have shown different repertoires undergo different

TCR selection and peripheral tolerance mechanisms, including negative selection, agonist selection, clonal diversion and inhibitory molecule upregulation(68, 74, 77, 95, 96). For example, every OT-I TCR-Tg T cell will be positively and negatively selected by the same self-antigens, while in a polyclonal system, T cells with a range of affinities will recognize the OT-I cognate peptide (SIINFEKL) and will be positively and negatively selected by numerous different peptides. In the polyclonal setting, there will be a range of affinities for SIINFEKL and an accompanying range of tolerance mechanisms to control responses to this antigen. Therefore, a single TCR binding to different affinity pMHC complexes during selection is not the same as a polyclonal set of different TCRs binding to a set of pMHC. This distinction between effects at a clonal as opposed to a polyclonal level could alter functionality and impact interpretation on the role of lower-affinity ligands during an immune response.

After primary antigen exposure and triggering of signaling cascades, division of CD4 and CD8 T cells will cause 100-1000 fold expansion (64, 90, 97). Interestingly, low-affinity T cells are easily detectable throughout the response, signifying they are capable of expanding as well as high-affinity T cells (18, 50). Higher-affinity CD8 TCR interactions cause asymmetric division that is associated with increased functionality of the proximal daughter cells(94). These CD8 T cells have similar initial rates of division, but eventually the highest affinity T cells maintain division while the lower-affinity T cells begin to contract(73, 94). The contraction of lower-affinity T cell is not due to increased death or lack of memory formation, as a similar frequency of low-affinity pMHC primed CD8 T cells differentiates into memory T cells(93, 94). Along with differences in division rates, the migration kinetics of T cells are controlled by affinity,

with the lower-affinity APL stimulated T cells demonstrating increased numbers of TCR-Tg T cells in the blood at earlier time points(73). Studies in high- and low-affinity CD4 T cells demonstrates the time to the first division of high-affinity CD4 T cells is much faster than low-affinity cells, though after several divisions, the low-affinity cells reach the same absolute number as high-affinity T cells(70). Together, these data demonstrate low- and high-affinity T cells behave similarly during initial expansion, but most likely have roles in the immune response at distinct times and locations.

Evidence demonstrates T cell affinity controls effector and memory differentiation of antigen-specific populations. Using the OT-I CD8 T cell APL system, groups have demonstrated low-affinity priming generates a greater frequency of Eomes+ memory T cells(93). It was determined TGF-βR expression, a negative regulator of T cells, is not downregulated in low-affinity T cell responses, creating a balance of the generation (IL-12R) and ablation (TGF-βR) of memory T cells (93). In CD4 T cells, TCR:pMHC affinity has been correlated with memory (20, 98, 99), T helper subset (T_H1 vs T_H2), and T follicular helper (T_{FH}) differentiation(97, 98, 100, 101) as well as prevention of exhaustion by chronic antigen exposure(102). Lower-affinity TCR interactions have been shown to be biased to generate long-lived memory cells(20, 98, 99), while for T_H1 vs T_H2 differentiation, greater strength of TCR stimulation increases the likelihood of T_H1 differentiation (100, 101). For T_{FH} cells, increased and decreased TCR:pMHC affinity has been correlated with differentiation, thought to be due to TCR-dependent IL-2/IL-2R alterations (28, 97, 98). The finding that T_{FH} cells can differentiate from TCRs with low and high-affinity TCR:pMHC interactions is perplexing, but demonstrates active mechanisms maintain the differentiation diversity of the low and

high-affinity T cells. Nonetheless, comparing and contrasting the findings of CD4 and CD8 T cells demonstrates the complexity of each system, but also demonstrates unique roles and pathways for high- and low-affinity TCR:pMHC interactions to presumably maintain functional diversity.

The activation and regulation of metabolic pathways is essential for the initiation and maintenance of the immune response(103–106). In CD8 T cells, the TCR:pMHC interaction controls initial metabolic reprogramming by upregulating IRF4 and Myc in a TCR:pMHC affinity dependent manner(106). The transcription factors Myc and IRF4 coordinate the switch from fatty acid oxidation to aerobic glycolysis, which is essential for maintenance of the immune response(104, 106). Low-affinity TCR interactions led to less Myc and/or IRF4 expression, reducing the uptake of metabolic intermediates and changing the amount of T cell death during the response (104, 106). Therefore, TCR:pMHC affinity is necessary for instructing metabolic reprogramming and a generating a greater functional response, but it is still unclear what function affinity based metabolic reprogramming plays for the differentiation and maintenance of low-affinity T cells.

Maintenance of affinity diversity

The maintenance of clonotype diversity in the immune system is essential for the health of the organism(107). By maintaining clonotype diversity, TCR affinity diversity is also preserved, with a single epitope being recognized by multiple T cells to create a normally distributed TCR:pMHC affinity population. For each epitope, a range of T cell precursors exist whose frequency is controlled by central tolerance mechanisms(27, 108).

As the preimmune frequency for a single epitope approaches zero, the capacity of the repertoire to protect the host from this epitope diminishes(3, 95). This theoretical lower limit of T cells that can effectively protect the host is defined as a protecton and is dependent upon the size of the organism and the migration velocity of T cells(109). Larger organisms need a larger protecton because their bodies have a greater volume to patrol and protect against pathogen dissemination.

Along with the size of the organism, the protecton is dependent upon the amount of cross-reactivity between TCRs. To derive the level of cross-reactivity inherent to an individuals TCRs, the entire number of antigen-specific T cells inclusive of lower-affinity ones needs to be defined. Recent studies have identified T cells with cross-reactivity using multiple high-affinity dependent methodologies such as pMHC tetramers, but the rules regulating cross-reactivity are still being formulated(3, 27, 110, 111). Previous studies have suggested the highest-affinity T cells are the most cross-reactive, as these cells have been shown to accept the most degeneracy in TCR:pMHC interaction and still function(112–114). However, single T cells can have both increased and decreased functional responses to peptides, meaning that just because a TCR binds to one pMHC with low-affinity, it can not bind to another pMHC with higher affinity(110). Theoretically, a single TCR should possess a range of affinity for peptides presented by MHC, meaning that cross-reactivity is not unique to only high- or low-affinity TCRs. Groups have identified low-affinity T cells during the immune response, signifying these cells must be represented in the naïve mouse, yet these lower affinity T cells are currently not being included in the calculations (17, 18, 50). If inclusion of lower affinity T cells leads to a greater number of T cells in an antigen-specific repertoire, then the amount of

cross-reactivity would correspondingly change(3). Therefore, protecton size and cross-reactivity calculations may be inaccurate due to the exclusion of these cells.

Low-affinity T cells are effective immune mediators and can have dominant roles in the immune response under specific conditions(65, 93, 115–117). When T cell clones are compared for their ability to cause autoimmunity, combat infection or prevent tumors, low-affinity T cells are often comparable in accomplishing these tasks (22, 65, 102, 116, 117). For example, when a lower-affinity CD8 T cell clone specific for an influenza antigen is transferred into a mouse expressing the antigen in a tumor, little immune response occurs(117). However, when this mouse is infected with influenza and/or given CD4 T cell help, the low-affinity T cells can respond with enhanced function(117). Along with influenza, groups have demonstrated adjuvants such as CFA, MPL and *Listeria monocytogenes* can generate a larger population of low-affinity T cells (20, 116, 118, 119). Besides adjuvants, the form of antigen can control low-affinity T cell expansion, as the use of protein antigen has been demonstrated to recruit more low-affinity T cells into the immune response(99). Why antigen and adjuvant influence the affinity diversity of the T cell response is still unclear, though these factors point to the type of antigen presenting cells (APCs) as a possible manipulator of low- and high-affinity T cell skewing. This suggests high- and low-affinity T cells may compete for TCR signaling, but mechanism such as antigen processing and presentation may maintain and influence the affinity diversity.

Alteration of APC by using different adjuvants or forms of antigen is one way to potentially alter T cell diversity, but can diversity of affinity be regulated in a T cell intrinsic fashion? As previously mentioned, the 2D affinity measurement by 2D-MP is a

relative affinity, dependent unknown factors as well as the contact area restricting the receptor and ligand interactions. Our work reveals slightly different affinities (<10-fold) for thymocytes, peripheral naïve TCR-Tg T cells, and activated T cells demonstrating that the context of the membrane environments plays a role (13, Unpublished data). Thymocytes, naïve, and activated T cells are different sizes, which may alter contact area between the T cell and RBC during the 2D-MP measurement. At the macroscopic level, the contact area difference between thymocytes and naïve T cells seems negligible, but in fact could result in differences as lymphocytes contain excess membranes, which is stored in ruffles and protrusions that could change during development and activation state(120). If there are differences in the ruffling of the membrane along with size differences, the membrane surface area in contact containing the TCR and pMHC could vary between different populations of cells. Of note, within a given population of cells the surface area would be similar allowing for accurate affinity measures. These effects on membrane surface would also be predicted to influence lymphocyte function *in vivo*, which could be why 2D affinity so accurately predicts the level of functional response.

In addition, 2D affinities are dependent on the local membrane structure that is maintained by the actin cytoskeleton and controlled by the membrane lipid composition. During TCR activation, the actin cytoskeleton is remodeled(121). This cytoskeleton change could alter the 2D-MP affinity, as the integrity of the membrane structure and orientation of the surface proteins will also fundamentally change. Inhibition of actin polymerization has been demonstrated to reduce 2D affinity as well as functional responses(8, 9). The actin inhibitors again demonstrate how 2D affinity measurements accurately readout the functionality of the TCR interaction with pMHC (8, 12). A T cell

could manipulate its 2D affinity through changes in the cytoskeletal support and protein attachment to actin. Alternatively, 2D affinity could be regulated to a degree by alterations in lipid content as CD4 T cell subsets contain differential organization of lipids(122, 123). Lipid composition has not been studied in relation to 2D affinity, but lipid order and organization has been demonstrated to be important in T cell functional responses, implicating the affinity may be different (122, 123).

Other surface proteins could influence the ability of the TCR to interact with pMHC and the 2D affinity. In the kinetic segregation model of T cell activation, the size of the CD45 molecule regulates the interaction of TCR:pMHC, with its exclusion from the synapse a necessary step to initiate the T cell signaling cascade(54, 55). T cell expression of a smaller isoform of CD45 would reduce steric hindrance and could increase the TCR:pMHC affinity measured by 2D-MP. Therefore, when the 2D affinity is calculated in the context of the cellular membrane, multiple T cell intrinsic factors can tune its measured value. *In vivo*, this fine-tuning of 2D affinity could be envisioned as a mechanism allowing for small alterations in the likelihood of TCR engagement (affinity for pMHC) while maintaining the diversity of the immune response.

Evidence demonstrates lower-affinity T cells most likely have overlapping and distinct roles when compared to T cells with higher-affinity interactions. Low-affinity T cells use much of the same signaling machinery for generating an immune response, but also must possess unique pathways or factors to sustain function and prevent excessive negative regulation during signaling. During differentiation, low-affinity T cells can again be found to have shared and unique roles when compared to higher-affinity T cells.

Low and high-affinity T cells must function together to efficiently generate a complete immune response and maintain the diversity of TCR affinity to efficiently protect the host.

Chapter 1

Targeted loss of SHP1 in murine thymocytes dampens TCR signaling late in selection

Abstract

SHP1 is a tyrosine phosphatase critical to proximal regulation of TCR signaling. Here, analysis of CD4-Cre SHP1$^{fl/fl}$ conditional knockout thymocytes using CD53, TCRβ, CD69, CD4 and CD8α expression demonstrates the importance of SHP1 in the survival of post selection (CD53^{+}), single-positive thymocytes. Using Ca^{2+} flux to assess the intensity of TCR signaling demonstrated that SHP1 dampens the signal strength of these same mature, post-selection thymocytes. Consistent with its dampening effect, TCR signal strength was also probed functionally using peptides that can mediate selection of the OT-I TCR, to reveal increased negative selection mediated by lower-affinity ligand in the absence of SHP1. Our data show that SHP1 is required for the survival of mature thymocytes and the generation of the functional T-cell repertoire, as its absence leads to a reduction in the numbers of CD4^{+} and CD8^{+} naïve T cells in the peripheral lymphoid compartments.

Introduction

T-cell development and function is dependent on the regulation of T cell receptor (TCR) signaling as well as downstream transcriptional alterations (54). Early in the TCR signaling pathway, protein kinases and phosphatases regulate the functionality of signaling intermediates to either modify or enhance downstream effects (69). SHP1, encoded by *Ptpn6*, is expressed in hematopoietic cells and is an important phosphatase in

many cellular signaling pathways (124). In naturally occurring SHP1 deficient mice (*me/me*), groups have found SHP1 to be important in the processes of thymocyte development (both positive and negative selection), naïve T-cell homeostasis, T helper (T_H) differentiation, functionality and Treg suppression (125–133). These T-cell defects occurred in *me/me* mice with the global loss of SHP1 in all hematopoetic cells. Therefore, specific T cell intrinsic effects of SHP-1 remain to be determined.

The conditional deletion of SHP1 has not been reported to effect thymocyte development (134, 135). As SHP1 is a key proximal regulator in TCR signaling, its lack of participation in thymocyte selection is surprising as thymocyte development is highly reliant upon the strength of TCR signaling in discriminating weak from strong peptide-MHC (pMHC) interactions (68, 129). SHP1 interacts with many different proteins in a host of signaling pathways. For example, SHP1 is recruited to LAT via GRB2 to interact with the protein Themis, which is involved in a negative feedback loop to alter the threshold of thymocyte positive and negative selection (61, 136–140). The lack of Themis prevents the recruitment of SHP1 to the GRB2:LAT complex, correlating with excessive signaling in response to lower-affinity ligands (61). The outcome of the Themis:GRB2:SHP1 interactions is to preserve lower-affinity TCRs in the repertoire by generating a negative feedback loop to limit thymocyte deletion (141). Yet, global analysis of the thymic compartment in SHP1 deficient mice did not reveal any effects on thymocyte development (134). Here we have probed thymocyte development in greater detail and contrary to previous reports, find that SHP1 is necessary to reduce TCR signaling and prevent the deletion of mature thymocytes. Furthermore, the absence of SHP1 during development leads to an altered peripheral T-cell repertoire with a loss of

naïve T cells and over representation of memory-like T cells. Therefore, SHP1 expression in developing thymocytes is intrinsically essential for the generation of a normal naive T-cell repertoire and the rescue of developing thymocytes from negative selection.

Results

Thymocytes selection is dependent upon TCR binding to self-pMHC, with the translation of biophysical TCR:pMHC interactions dictating signal strength and thymocyte fate (68, 142, 143). Defects in the proximal TCR signaling intermediates have been demonstrated to alter T-cell selection and therefore the repertoire of T cells in the periphery (61, 68, 77, 78). To determine if SHP1 alters thymocyte selection, we interrogated polyclonal CD4-Cre SHP1$^{fl/fl}$ thymocyte development based on expression of TCRβ and CD69, with no differences noted in the absence of SHP1 (Figure 1A). Thymocytes were further analyzed based on defined maturation phases using TCRβ and CD69, with thymocytes progressing through selection by upregulating TCR and CD69 before down regulating CD69 upon completion of selection (144). Within the TCR and CD69 subsets, distinct thymocyte developmental stages were identified using CD4 and CD8α that included double negative (DN), double positive (DP), post selection DP, CD8α intermediate (CD8α int), CD4 single positive (CD4SP) and CD8α single positive (CD8SP) (Figure 1B) (144). When the individual subsets of maturing thymocytes were analyzed the most mature (TCRβ^{Hi}CD69^{-}) stage revealed significantly reduced numbers of SHP1 deficient cells in the post-selection CD8αInt, CD4SP and CD8αSP populations (Figure 1C). Comparison of the maturation stages before expression of CD4 (before Cre expression) and selection (DN and pre selection DP) were not found to be different

(Supplemental Figure 1). Thus, SHP1 controls the survival of thymocytes during late stages of development.

As SHP1 deficiency revealed a defect in post-selection thymocytes, we next probed thymocytes for CD53 expression, a marker that distinguishes pre ($CD53^-$) and post ($CD53^+$) selected cells (Figure 2A) (145). Loss of SHP1 in CD4-Cre $SHP1^{fl/fl}$ mice revealed a reduced frequency of post-selection ($CD53^+$) thymocytes as compared to WT mice (Figure 2A). Enumeration of thymocyte subsets based on CD4 and CD8 expression in the $CD53^+$ post-selection population of $SHP1^{fl/fl}$ and CD4-Cre $SHP1^{fl/fl}$ mice revealed a 2.9 fold and 2 fold reduction in CD8αSP and CD4SP thymocytes respectively (Figure 2B). These data confirmed that SHP1 controls the survival of thymocytes at later developmental stages. To corroborate the survival defect of mature thymocytes was SHP1 dependent, mixed bone marrow (BM) chimeras with CD4-Cre $SHP1^{fl/fl}$ (Thy1.2/CD45.2) and WT (Thy1.2/CD45.1) were created. After reconstitution, total thymocytes from BM chimeras were analyzed for maturation using TCRβ and CD69 expression and the contribution of WT and SHP1 KO thymocytes were compared at each developmental stage (Figure 3A,B). Initially, the frequency of SHP1 deficient thymocytes was significantly higher than WT thymocytes (Figure 3B,C). However, once the thymocytes matured to the $TCR\beta^{Hi}CD69^{Hi}$ stage, no significant differences were noted (Figure 3B,C). Upon completion of the final maturation stage, WT thymocytes were found significantly over-represented (Figure 3B,C). This suggests that loss of SHP1 initially impacts survival of $TCR\beta^{Hi}CD69^{Hi}$ thymocytes, as this stage is where WT thymocytes begin to show a survival advantage even though there are no significant

differences between the cell types. Thus, even in the same developing environment, thymocytes deficient in SHP1 have a defect in survival.

The reduced levels of thymocyte survival could result from either a decrease in positive selection or an increase in negative selection or a mixture of both. Decreased positive selection could arise from decreased TCR signaling strength, while increased negative selection would occur if there was increased signaling caused by TCR selection events (78). Both of these possibilities have been reported using *me/me* mice (128, 146). To distinguish these possibilities, thymocyte subsets were assayed for their ability to flux calcium (Ca^{2+}), a measurement that is positively correlated with TCR signal strength (147). Using the ratiometric Ca^{2+} dye Indo-1, post-selection DP and CD8α intermediate thymocytes deficient in SHP1 were found to flux greater amounts of Ca^{2+}, as measured by area under the curve (AUC) and peak value measurements (Figure 4A). Interestingly, Ca^{2+} flux in SHP1 deficient thymocytes was not increased until after selection ($CD53^{+}$) and then returned to levels similar to $SHP1^{fl/fl}$ mice as thymocytes matured (Figure 4B). These findings demonstrate the deficiency of SHP1 during selection permits increased TCR signaling. As greater negative selection would be predicted by greater TCR signaling, this data indicates the lack of SHP1 dominantly affects negative selection of the developing thymocytes, thereby causing the decrease in thymocyte cell number (Figure 1C).

To further study the development of thymocytes lacking SHP1, we created OT-I TCR-Transgenic (Tg) mice with T cells lacking SHP1 (OT-I CD4-Cre $SHP1^{fl/fl}$). The OT-I TCR-Tg system allows for the study of SHP1's influence on selection of thymocytes with differing selecting affinities, as altered peptide ligands (APLs) have

been defined for the native SIINFEKL:H2-K^b (N4) epitope. A range of APLs have been defined that cause positive or negative selection of the OT-I thymocytes (62, 83, 94). To determine how SHP1 affects the selection of OT-I thymocytes, OT-I and OT-I CD4-Cre $SHP1^{fl/fl}$ were mixed with a fluorescent nucleic acid stain impermeant to viable cells (Sytox Green) and OVA:H2-K^b or APL:H2-K^b tetramer to induce thymocyte selection as read out by apoptosis (affinity hierarchy for ligands used is N4> Q4R7) (62, 94, 148). Q4R7 has been previously shown to be the lowest-affinity APL that can negatively select the OT-I TCR(147). These stimulated thymocytes were then analyzed using the IncuCyte Zoom system to quantitate dead (Sytox $Green^+$) thymocytes by imaging the cells every hour (Figure 4C). Comparison of N4 and Q4R7 between WT OT-I thymocytes revealed affinity-dependent cell death, while OT-I's lacking SHP1 were not able to display a similar dependence (Figure 4C). Quantification of cellular death was calculated by taking the area under the curves (AUC) for the H-2K^b-tetramer treatments and normalizing the data to the WT N4 ligand (Figure 4D). SHP1 was not needed to discriminate high-affinity ligands (N4), but was essential for separating the effect of the lower-affinity ligand (Q4R7) that has been used to map selection events for the OT-I TCR. In this regard, our data is similar that reported for $Themis^{-/-}$ mice (Figure 4D) (61). Therefore, SHP1 is essential in discriminating high- and low-affinity pMHC ligands during thymocyte selection.

Since the number of SP thymocytes is decreased in the absence of SHP1, CD4 and CD8 T cell counts could also be reduced as naïve peripheral T cells are populated by emigrating SP thymocytes (149). However, previous work using the same CD4-Cre model reported increased frequency of memory ($CD44^+$) T cells without taking into

account potential T cell numerical differences(134). Analysis of splenic CD4 and CD8 T cell numbers demonstrated a reduction of both cell types in the absence of SHP1 (Figure 5A, 5B). In contrast to the previous work, enumeration of naïve ($CD44^-$) and memory ($CD44^+$) T cells found the reduction of CD4s and CD8s in the absence of SHP1 originated from the loss of naïve T cells (Figure 5A,B) (134). Of note, SHP1 deletion caused changes in CD8, but not CD4 memory T cells. The lack of naïve T cells was confirmed to be driven by SHP1 expression in T cells by using mixed BM chimera experiments as described above. When WT and SHP1 deficient T cells were analyzed and counted in the same animals, a reduction in the number of T cells was appreciated, which was driven by the loss of naïve ($CD44^-$) T cells (Figure 5C). In parallel, analysis of memory ($CD44^+$) T-cell compartments in the BM chimeras showed no enhancement of CD8 memory generation in the absence of SHP1, but did show significant differences for CD4 T cells (Figure 5C). Contrary to previous reports(134), our results demonstrate SHP1 controls selection of thymocytes and in the peripheral compartment predominantly effects the maintenance of the naïve T-cell population with only minimal alterations to memory T cells.

Discussion

Here we demonstrate the phosphatase SHP1 dampens TCR signaling of developing thymocytes and is critical for the development of mature, single positive thymocytes. As predicted by *Themis*$^{-/-}$ experiments, SHP1 functions to discriminate lower-affinity TCR signaling and dampen the negative selection to weaker ligands (61). SHP1's negative regulation was found to be key in early post-selection thymocytes, as defined by CD53, but was not found to be necessary for controlling TCR signaling of

later-stage, SP thymocytes. Conversely, thymocyte enumeration showed delayed effects of the increased TCR signaling with similar numbers of early selection thymocytes but differences in later stages. The decrease in late-stage thymocytes extended into the peripheral T-cell compartment, showing a decrease in the number of naïve T cells. By defining SHP1s role during thymocyte development, this work validates findings from *Themis*$^{-/-}$ mice and reiterates SHP1s is an essential phosphatase for the generation of functional T cells.

The conclusion that SHP1 is necessary for thymocyte development and functionality demonstrates distinct roles for SHP1 throughout the life cycle of a T cell. This is apparent in the comparison of experiments where SHP1 is deleted in DP thymocytes (CD4-Cre) (134) or in mature SP thymocytes (dLck-Cre), leading to distinct outcomes (135). Comparisons of these models reveal several key differences. First, when SHP1 deletion occurs in immature DP thymocytes, no proliferative differences of peripheral T cells are noted, whereas SHP1 deletion in mature thymocytes produced a proliferative advantage of these T cells. Second, SHP1 deletion during thymocyte development caused the enrichment of memory-like CD8 T cells and IL-4 producing CD4 T cells, with few naïve T cell alterations identified when SHP1 was deleted post-thymocyte selection (134). Yet, it was previously unexplained why these two Cre systems gave different results, as it was incorrectly established that use of the CD4-Cre system did not cause thymocyte alterations (134). With the new understanding that SHP1 plays a role in thymocyte selection, these two findings can be reconciled. The absence of SHP1 during thymocyte development causes alterations to the peripheral T-cell repertoire by reducing the number of naïve T cells, but leaving the memory T-cell compartment

unaltered or increased. This implies the naïve populations of antigen-specific T cells are reduced in number and diversity, potentially altering the functionality of the immune response to pathogens. Therefore, fine tuning of TCR signals executed by SHP1 is important to prevent the reduction of naïve T cells and to generate a T-cell repertoire with the capacity to fully protect the host.

Our work on the role of SHP1 during thymocyte selection has revealed disparities with other work (134). Several factors may be playing a role in these discrepancies. The previous study only reported CD4 and CD8 expression of thymocytes as opposed to our more extensive analysis (134). Furthermore, the numbers of peripheral lymphocytes was not calculated in the previous work(134), leading the incorrect conclusion of increases in memory T-cell populations. Even with genetically identical mice in both experiments, factors such as age, sex and housing conditions could impact the findings. This could be due to SHP1 functioning differently due to sex/age of mice, or due to difference in microbiota between facilities (150). It is also possible that deletion of SHP1 may be incomplete, or with different levels of redundancy with SHP2 between laboratories. Therefore, several unknown confounding factors may exist, but our more detailed analysis revealed SHP1s role in selection and repertoire generation.

The role of SHP1 in the generation and maintenance of memory T cells is complex. Even with the decreased number of naïve T cells, we find SHP1 acts to maintain or increase numbers of memory CD4 and CD8 T cells. SHP1 could potentially be controlling memory T-cell differentiation in several ways. SHP1 could prevent the steady state naive to memory transition by reducing the signaling generated by tonic TCR:pMHC interactions needed for T cell maintenance and survival (151, 152).

Alternatively, SHP1 may control the activation sensitivity of naïve T cells, allowing them to proliferate to larger populations and generate greater numbers of antigen-experienced T cells. Excessive generation of antigen-experienced T cells in the absence of SHP1 has been shown previously (135), but it is unclear if it can explain our observations in the CD4-Cre model as we are measuring memory T-cell contribution at the steady state. Either way, both hypotheses would end in the generation of a memory T-cell population with reduced TCR clonotype diversity, reiterating SHP1 acts to diversify the T-cell immune population.

Identifying the role of SHP1 during selection corroborates data from mice lacking Themis, as *Themis*$^{-/-}$ thymocytes are not able to recruit SHP1 to GRB2 or phosphorylate SHP1 (61, 139). These changes in SHP1 associated with a loss of Themis lead to altered negative selection thresholds, allowing lower-affinity TCR:pMHC interactions that normally positively select thymocytes to result in deletion (61, 136–138). This change in the threshold between positive and negative selection is likely due to an alteration in the negative feedback loop generated by Themis/SHP1. The negative feedback loop allows for the generation of constant TCR signaling output, even with increases in TCR affinity, and is essential to demarcate the sharp, digital response between positive and negative selection(61, 141). Interestingly, the peripheral T-cell phenotype found in CD4-Cre SHP1$^{fl/fl}$ mice and *Themis*$^{-/-}$ mice is very similar, with loss of naïve T cells and enhanced survival of memory-like T cells (137, 138). However, the CD4-Cre SHP1$^{fl/fl}$ mouse does not exactly phenocopy *Themis*$^{-/-}$ thymocytes. *Themis*$^{-/-}$ thymocytes are noted to have a selection defect at the CD3^{hi}CD69^{+} (TCR^{Hi}CD69^{+}) stage of development, while we do not find any difference using this gating strategy (Figure 1A). As well, signaling defects

were found in *Themis*$^{-/-}$ thymocytes before selection(61), but we only found differences in TCR induced Ca^{2+} flux after positive selection (Figure 4A,B). We believe two factors could be playing a role in these differences. First, SHP2 can bind to Themis similar to SHP1 and potentially regulate signaling in a similar fashion and partially rescue the phenotype (139). Generation of SHP1/SHP2 double knockout thymocytes would address this issue. Second, as the system we studied is a conditional knockout where SHP1 is deleted upon CD4 upregulation, SHP1 may still be partially present and functional during the initial selection. The half-life of SHP1 after Cre-induced excision is unknown, though previous work suggested SHP1 is undetectable via western blot by the DP thymocyte stage(134). Therefore, the timing of SHP1 deletion is likely important for the generation of this selection phenotype. As for the IL-4 producing CD4 T cells found in the CD4-Cre SHP1$^{fl/fl}$ mice (134), we hypothesize these cells arise due to an altered TCR repertoire caused by excessive negative selection. Of interest TCRs with lower interactions with antigen tend to develop into T_H2 cells (100). Nonetheless, the role of SHP1 is fundamental in discriminating TCR strength of thymocytes and generation of a functional naïve TCR repertoire.

Materials and Methods

Mice

CD4-Cre SHP1$^{fl/fl}$ and SHP1$^{fl/fl}$ mice have been described previously and were purchased from Jackson Laboratories and bred on site (134). OT-I mice were purchased from Jackson Laboratories and the OT-I CD4-Cre SHP1$^{fl/fl}$ mice were bred on site. C57BL/6 (WT) mice were purchased from the National Cancer Institute. All mice in experiments were 6-8 weeks old except for those used in the IncuCyte assay, which were

4-6 weeks old, and both males and females were used in experiments. All animals were housed in an Emory University Department of Animal Resources facility (Atlanta, GA) and used in accordance with an Institutional Animal Care and Use Committee–approved protocol.

Flow Cytometry

Mouse thymus or spleens were processed into a single cell suspension and stained with fluorochrome-labeled antibodies for 30 min on ice. Antibodies used are listed per manufacturer: CD3ε (145-2C11), CD8α (53-6.7) (Tonbo biosciences), CD4 (RM4-5), CD69 (H1.2F3), Thy1.2 (30-H12), CD45.1 (A20) (Biolegend), CD11b (M1/70), CD11c (HL3), CD19 (1D3), CD53 (OX-79) (BD Pharmigen), CD44 (IM7), F4/80 (BM8), TCRβ (H57-597) (eBioscience). For thymocytes, viable cells (as identified by FSC and SSC) were gated and then analyzed as described in the figures. For splenocytes, viable cells (as identified by FSC and SSC) were gated on and T cells ($CD3\varepsilon^{+}$) were identified that were lineage (CD19, CD11b, CD11c, F4/80) negative and then analyzed as described in the figure captions. Cells were counted using AccuCheck microbeads (Invitrogen). Data was acquired on a LSRII (Becton Dickinson) and analyzed using FlowJo (Treestar).

Calcium Flux Measurements

Calcium flux measurements were performed as previously described. Briefly, thymocyte cell suspensions from $SHP1^{fl/fl}$ or CD4-Cre $SHP1^{fl/fl}$ mice were made and rested for 60 min at 37°C. One of the samples was stained with Cell Trace Violet (CTV) for 10 min at room temperature while the other sample received equal amounts of vehicle-only control (DMSO). Cells were then washed and equal number of cells were

mixed together at a density of $2x10^6$ cells/ml in R10 media (RPMI1640, 10% (v/v) FCS, 2mM L-glutamine, 0.05mM 2-mercaptoethanol and 0.05mg/ml gentamicin sulfate). The mixed thymocytes were incubated with the calcium indicator Indo-1 AM (Molecular Probes; 1mM final concentration) for 15 min at room temperature. Cells were washed once in R10 and stained for 15 min at room temperature with fluorescently conjugated antibodies and biotinylated anti-CD3ε (Tonbo Biosciences; 145-2C11) antibody. Cells were washed once in cHBSS (Ca^{2+} and Mg^{2+} free Hank's balance salt solution supplemented with 1% (v/v) FCS, 1mM $MgCl_2$, 1mM EGTA and 10mM HEPES, pH 7.3) and resuspended in cHBSS. Samples were warmed to 37°C for 2 min and then analyzed on a LSRII (Becton Dickinson). $CaCl_2$ (2mM) was added 30 seconds into analysis followed by streptavidin (10 mg/ml) at 60 seconds to activate the samples.

Bone Marrow Chimeras

Bone marrow cells harvested from the femur, tibia and sacrum were processed into a single cell suspension and depleted of T cells using Thy1.2-PE conjugated antibody and anti-PE magnetic microbeads as per manufacturer protocol (Miltenyi Biotec). Recipient mice (Thy1.1/CD45.2) mice were irradiated (950 rad) and injected i.v. with $1x10^7$ bone marrow cells from C57BL/6 (Thy1.2/CD45.1) and CD4-Cre $SHP1^{fl/fl}$ (Thy1.2/CD45.2) mice mixed at a 50:50 ratio. Recipient mice were treated with drinking water containing 2% sucrose, 0.5 mg/ml Neomycin, 0.0125 mg/ml Polymyxin B for 7 days after irradiation and were analyzed 6-8 weeks after irradiation.

Incucyte Sytox Assay

Thymocytes from OT-I or OT-I CD4-Cre $SHP1^{fl/fl}$ mice were harvested and processed into a single cell suspension in complete R10 media without phenol red (recipe

above). Cells were enriched for viable cells by density centrifugation using Lymphocyte Separation Medium (density= 1.077-1.080 g/mL at room temperature) by overlaying 2mL of room temperature cell suspension over 1mL of room temperature Lymphocyte Separation Medium and centrifuging for 15min at 400 x g. The interface was removed and washed in complete RPMI. A 96 flat-bottom plate was prepared for the assay by adding 25μl CellTak (BD) per well at a concentration of 22.4μg/ml diluted in PBS. The CellTak was incubated for 20 minutes at room temperature, and then washed using dH_2O. Next, cells were resuspended at $1.5x10^6$ cells per mL in complete R10 media supplemented with 125nM Sytox Green (Life Technologies). 100μl of cells were plated on the pretreated plate and mixed with 100μl of complete RPMI media with H-$2K^b$ tetramers (1μl of tetramer per well) or left unstimulated. Cells were then tacked to plate using centrifugation (acceleration: 5, deceleration: 5) by accelerating the plate to 450rpm, stopping the spin, rotating the plate 180°, and then spinning again to 450rpm. Cells were next placed into IncuCyte (Essen Bioscience) machine and imaged once every hour using the 20x phase and fluorescent channel 1 objectives. Analysis of images was performed after experiments using the following settings. Phase: Background=0.3, Cleanup (Holefill=0 μm^2, Adjust Size=-3 pixels). Green: TopHat parameters (radius=100μm, Threshold=2.000 GCU), Edge split on (Edge sensitivity=4), Cleanup (Holefill=0 μm^2, Adjust Size=-3 pixels), Filters (Max=650 μm^2, Mean Intensity=5.000 μm^2). Unstimulated samples were analyzed for $Sytox^+$ cells and this background was subtracted from H-$2K^b$ treated $Sytox^+$ events before analysis.

Statistical Analysis

All data were analyzed using Prism (Graphpad) Software. Outliers were excluded if identified by Grubs Test.

Acknowledgments

The authors would like to thank Laurel Lawrence for maintaining the mice used in these experiments as well as Shayla Shorter, Hunter Martinez and Emily Cartwright for helpful discussion. This work was supported by NIH grant T32 AI007610, RO1 AI096879, RO1 AI110113, F31 NS086130 and T32 AI070081.

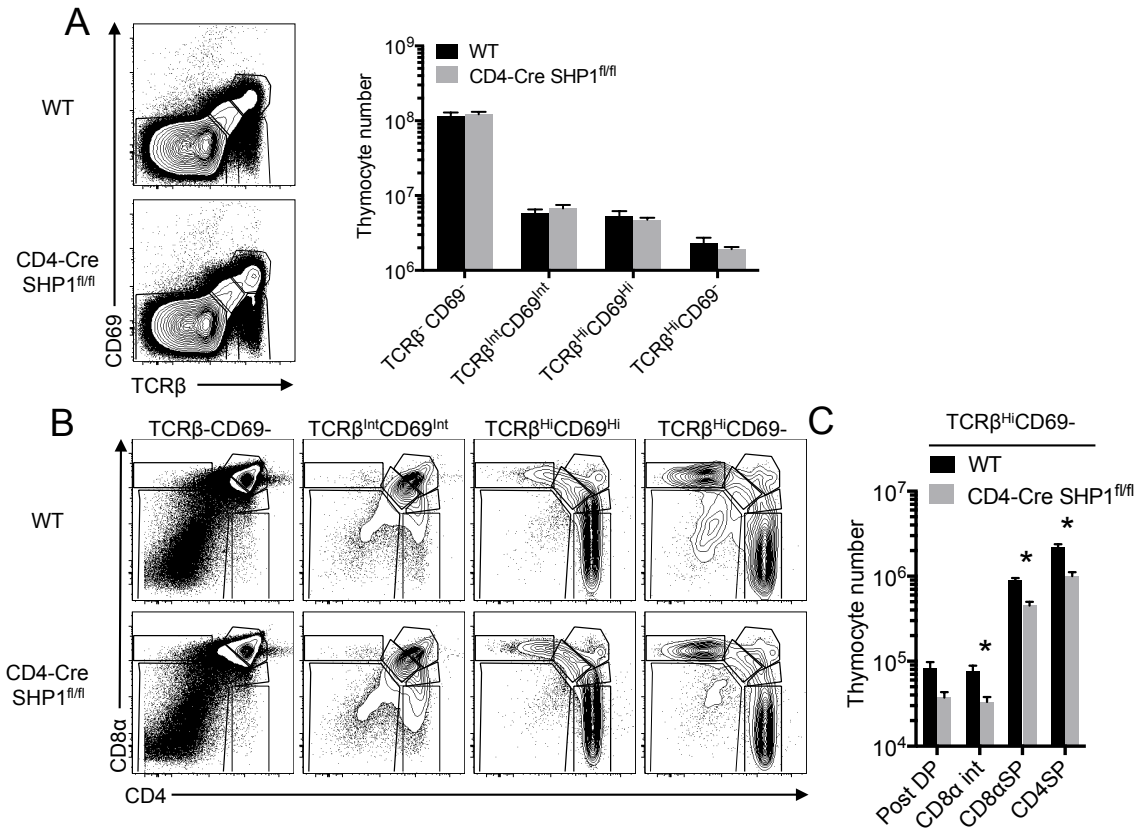
A
WT
CD4-Cre SHP1fl/fl
CD69
TCRβ
WT
CD4-Cre SHP1fl/fl
Thymocyte number
TCRβ- CD69-
TCRβIntCD69Int
TCRβHiCD69Hi
TCRβHiCD69-
B
TCRβ-CD69-
TCRβIntCD69Int
TCRβHiCD69Hi
TCRβHiCD69-
WT
CD4-Cre SHP1fl/fl
CD8α
CD4
C
TCRβHiCD69-
WT
CD4-Cre SHP1fl/fl
Thymocyte number
Post DP
CD8α int
CD8αSP
CD4SP

Figure 1.

Figure 1. SHP1 is necessary for thymocyte development.

(A) Representative flow cytometry and gating from WT (upper) and CD4-Cre SHP1$^{fl/fl}$ (lower) thymocytes showing TCRβ and CD69 expression. Enumeration of TCRβ and CD69 thymocyte subsets in WT and CD4-Cre SHP1$^{fl/fl}$ mice demonstrate no difference in subset number (mean+/-SEM, n=6-10 mice, three experiments). (B) CD8α and CD4 expression of thymocyte subsets by the maturation markers TCRβ and CD69 with WT (top row) and CD4-Cre SHP1$^{fl/fl}$ (bottom row). (C) Enumeration of the developing thymocytes reveals decreased numbers of single positive thymocytes in the TCRβ^{Hi}CD69^{-} stage (mean+/-SEM, n=6-10, 3 total experiments, CD8α int p=0.01, CD8αSP p=5.1x10^{-5}, CD4SP p=7.51x10^{-5}, Multiple Sample T-test with correction for multiple comparisons using the Holm-Sidak method).

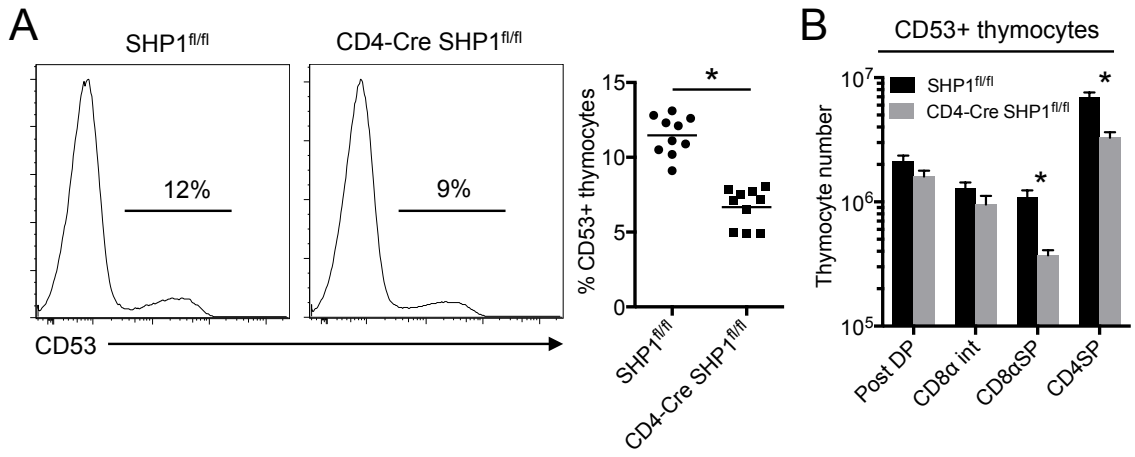
A
SHP1fl/fl
CD4-Cre SHP1fl/fl
12%
9%
CD53
% CD53+ thymocytes
15
10
5
0
*
SHP1fl/fl
CD4-Cre SHP1fl/fl
B
CD53+ thymocytes
Thymocyte number
10^7
10^6
10^5
SHP1fl/fl
CD4-Cre SHP1fl/fl
*
*
Post DP
CD8α int
CD8αSP
CD4SP

Figure 2.

Figure 2. Thymocyte survival is decreased in the absence of SHP1.

CD53 was analyzed on bulk SHP1$^{fl/fl}$ and CD4-Cre SHP1$^{fl/fl}$ thymocytes. (A) Representative histogram of CD53 expression from a SHP1$^{fl/fl}$ and CD4-Cre SHP1$^{fl/fl}$ mouse with the decreased frequency of selected thymocytes in the absence of SHP1 (points represent single mice, 3 independent experiments, *p<0.0001, Student's T-test). (B) Numerical comparison of CD53+ thymocyte CD4/CD8 subsets, demonstrating the lack of survival of SP, post-selection thymocytes (mean+/-SEM, n=6-10 mice, three experiments, CD8αSP p=0.0001, CD4SP p=0.00015, Multiple T-test with correction for multiple comparisons using the Holm-Sidak method).

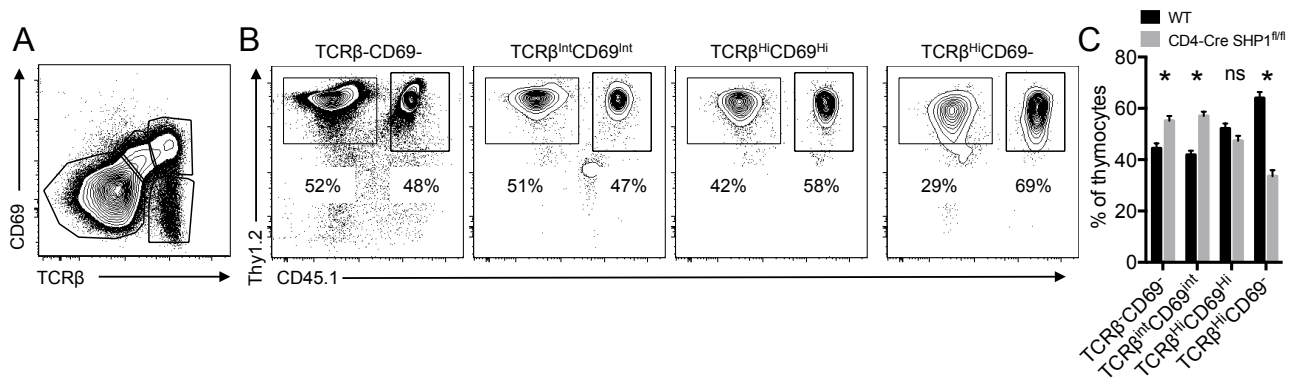
A
CD69
TCRβ
B
TCRβ-CD69-
TCRβ^IntCD69^Int
TCRβ^HiCD69^Hi
TCRβ^HiCD69-
Thy1.2
CD45.1
52%
48%
51%
47%
42%
58%
29%
69%
C
WT
CD4-Cre SHP1^fl/fl
% of thymocytes
80
60
40
20
0
* * ns *
TCRβ-CD69-
TCRβ^IntCD69^Int
TCRβ^HiCD69^Hi
TCRβ^HiCD69-

Figure 3.

Figure 3. Intrinsic dependence of SHP1 in the survival of mature thymocytes.

Mixed BM chimeras revealed SHP1 is necessary for thymocyte maturation. (A) Representative TCRβ and CD69 expression of total thymocytes in mixed BM chimeras. (B) Contribution of WT (Thy1.2+/CD45.1+) and CD4-Cre SHP1$^{fl/fl}$ (Thy1.2+/CD45.1-) at maturation stages defined by TCRβ and CD69 (Representative plots, n=10 mice, two experiments). (C) Tabulated frequency of the thymocyte contribution at each stage in thymocyte development, showing CD4-Cre SHP1$^{fl/fl}$ thymocytes initially start at greater frequency, but do not survive upon maturation (mean+/-SEM, n=10 mice, two experiments, TCRβ^{-}CD69^{-} p=0.0009, TCRβ^{int}CD69^{int} p=2.6x10^{-6} , TCRβ^{Hi}CD69^{-} p=3.14x10^{-}8, Multiple T-test with correction for multiple comparisons using the Holm-Sidak method).

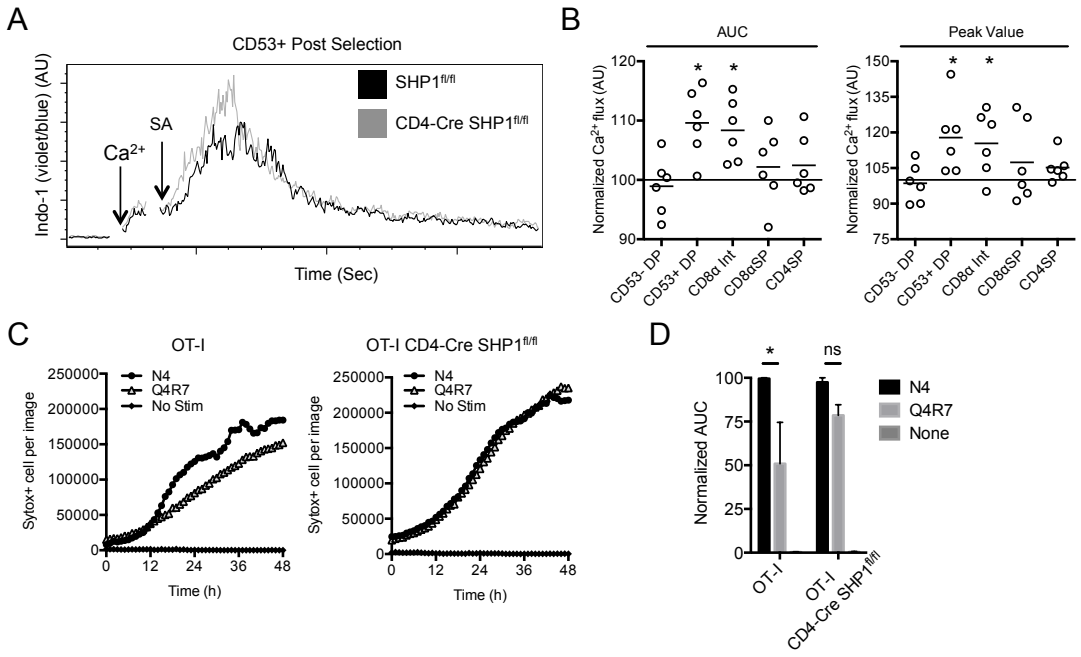
A
CD53+ Post Selection
SHP1fl/fl
CD4-Cre SHP1fl/fl
Ca2+
SA
Indo-1 (violet/blue) (AU)
Time (Sec)
B
AUC
Peak Value
Normalized Ca2+ flux (AU)
CD53- DP
CD53+ DP
CD8α Int
CD8αSP
CD4SP
C
OT-I
OT-I CD4-Cre SHP1fl/fl
N4
Q4R7
No Stim
Sytox+ cell per image
Time (h)
D
Normalized AUC
None
OT-I
OT-I CD4-Cre SHP1fl/fl
ns

Figure 4.

Figure 4. Increased thymocyte TCR signaling in the absence of SHP1.

TCR reactivity was measured in SHP1$^{fl/fl}$ and CD4-Cre SHP1$^{fl/fl}$ thymocytes. (A) Ratiometric calcium changes of Indo-1 dye of post selection (CD53+) DP SHP1$^{fl/fl}$ and CD4-Cre SHP1$^{fl/fl}$ thymocytes after Ca^{2+} and streptavidin (SA) addition. (B) Normalized Indo-1 calcium flux calculated by dividing the area under the curve (AUC) and peak value from SHP1$^{fl/fl}$ and CD4-Cre SHP1$^{fl/fl}$ thymocytes. Normalization reveals significantly increased Ca^{2+} signaling in CD4-Cre SHP1$^{fl/fl}$ thymocytes as the black line designates equal Ca^{2+} flux (n=6, three experiments, AUC: CD53+DP p=0.009, CD8αint p=0.01,Peak Value: CD53+DP p=0.035, CD8αint p=0.04, One-sample T-test for each point with a reference value of 100). (C) IncuCyte analysis of cell death demonstrates SHP1 is essential for discrimination of low-affinity TCR:pMHC interactions in the OT-I TCR Tg system. Total Sytox green+ cells per image were counted every hour and graphed as a function of time (one representative sample, two experiments). (D) Normalized AUC data from (C) reveals increased amounts of negative selection in thymocyte lacking SHP1 (mean+/-SEM, two experiments, means calculated from combined technical replicates from the two experiments, Two-Way ANOVA with Sidak's multiple comparison test, *p<0.05)

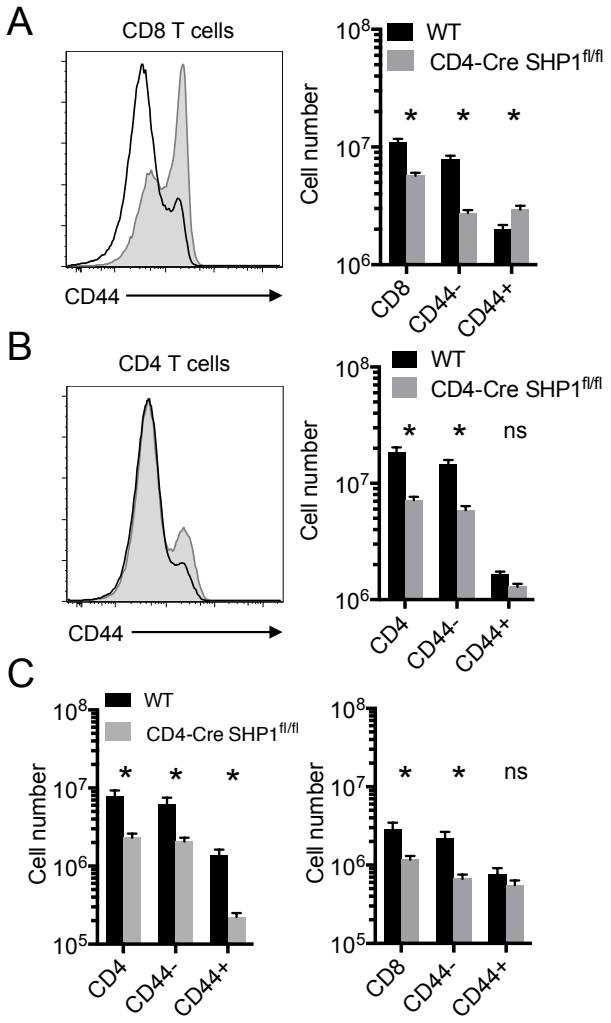
A
CD8 T cells
CD44
WT
CD4-Cre SHP1fl/fl
Cell number
CD8
CD44-
CD44+
B
CD4 T cells
CD44
WT
CD4-Cre SHP1fl/fl
Cell number
ns
CD4
CD44-
CD44+
C
WT
CD4-Cre SHP1fl/fl
Cell number
CD4
CD44-
CD44+
ns
CD8
CD44-
CD44+

Figure 5

Figure 5. SHP1 controls the homeostasis of naïve T cells.

Analysis of frequency and number of CD4 and CD8α T cells in WT and CD4-Cre $SHP1^{fl/fl}$ mice. (A-B) Flow cytometry shows increased expression of CD44+ T cells in CD4-Cre $SHP1^{fl/fl}$ (filled gray histogram) when compared to WT (open black histogram) of both CD8 and CD4 T cells. Upon enumeration, decreased T cell counts are found in CD4-Cre $SHP1^{fl/fl}$ mice stemming from lack of naïve, CD44- T cells (mean+/-SEM, n=6-10 mice, three experiments, CD4: CD4 total $p<0.0001$, CD44- $p<0.0001$, CD8: CD8 total $p<0.0001$, CD44- $p<0.0001$, CD44+ $p=0.0037$, Multiple T-tests with correction for multiple comparisons using the Holm-Sidak method). (C) Generation of CD4-Cre $SHP1^{fl/fl}$ and WT mixed bone marrow chimera indicates the maintenance of naïve T cells is SHP1 intrinsic and not an environmental effect (mean+/-SEM, n=10, two experiments, CD4 $p=0.00469$, CD44- $p=0.0088$, CD44+ $p=0.00034$, Multiple T-tests with correction for multiple comparisons using the Holm-Sidak method).

Chapter 2

Dual positive selection mechanisms limit autoimmune demyelinating disease

Abstract

To understand tolerogenic mechanisms preventing autoimmunity, we probed the development of polyclonal T cells specific for myelin oligodendrocyte glycoprotein (MOG), a tissue restricted target during demyelinating disease. We found that clonal deletion of MOG-tetramer+ thymocytes was not a primary tolerance mechanism. Instead, T cell tolerance to MOG was implemented in the responding T cells via two positive selection processes. First, the presence of MOG self-antigen generated less potent albeit more numerous MOG-specific T effector precursors. Second, MOG induced a more efficacious MOG-tetramer+ Foxp3+ regulatory T cell population. These positive selection mechanisms induced transcriptional alterations of the effector and regulatory antigen-specific T cell populations, with the enhanced functionality of the MOG-specific Tregs being coupled to Foxo1 regulated genes. Our results refine thymocyte maturation processes by demonstrating positive selection on a single self antigen can alter T cell population dynamics through complementary tolerance mechanisms and reduce autoimmune disease propensity in the absence of obvious negative selection.

Introduction

CD4 T cell development is dependent upon the ability of the T cell receptor (TCR) to interact with self-peptide and major histocompatibility class II (self-pMHCII) complexes in the thymus(78). As self cross-reactivity is a fundamental property of all TCRs, mechanisms such as negative selection and regulatory T cells are in place to

prevent autoimmune disease(153–156). The efficiency of negative selection is shown to be most effective in preventing self-reactive T cell activation to ubiquitously or highly expressed self-peptides(157, 158). Thymic epithelia expression of the transcription factor AIRE is critical in the production of many of these self-peptides(88, 153, 159, 160). However, other self-proteins are minimally expressed in the thymus or periphery (159, 160), making it less clear how tolerance protects against autoimmunity to self antigens with reduced thymic expression and therefore less negative selection.

In models of autoimmune demyelination a range of tolerance mechanisms and thymic myelin antigen expression can be appreciated(159, 161); illustrating that tolerance is not simply the presence or absence of myelin self-antigen in the thymus. Clinically MHC/HLA is a risk factor for autoimmune disease, yet the presence of autoreactive CD4 T cells does not predict autoimmunity. This is demonstrated by healthy patients having myelin-specific CD4 T cells in their peripheral blood without clinical signs of demyelination(162, 163). Increased development of Foxp3+ regulatory CD4 T cells (Tregs) could potentially explain some of the differences between healthy controls and patients as Tregs have been found to be dysfunctional during autoimmunity (164, 165). However, Treg deficiencies alone cannot fully explain the break in tolerance to self-antigens (157, 158). The role of MHC/HLA as a risk factor suggests antigen specific-tolerance mechanisms are in place to prevent activation of self-reactive T cell activation in healthy patients. For example, findings of intact negative selection in the autoimmune prone NOD mouse led to the possibility of altered positive selection as a defective tolerance mechanism for self reactive CD4 T cells(85). Therefore, further study of

positive selection may be needed to understand how self-pMHCII specific CD4 T cells are selected and tolerized in the presence of limited amounts of self-antigen.

To define tolerance to self-antigens with restricted tissue and thymic expression, polyclonal CD4 T cells were analyzed for specificity to encephalitogenic myelin oligodendrocyte glycoprotein (MOG) using mice sufficient and deficient in MOG expression. In both cases MOG-tetramer+ T cells were readily identified, although CD4 T cells from MOG deficient animals were more encephalitogenic. The size of the naïve MOG-specific CD4 T cell repertoire suggested a lack of thymocyte negative selection. Instead, MOG expression appears to support positive selection for a subset of CD4 T cell clones specific for MOG itself. This subset of MOG-selected thymocytes leads to transcriptionally altered effector CD4 T cells made up of a diverse family of TCRs that display increased tolerance and reduced ability to demyelinate. Moreover, the presence of MOG selected for antigen-specific Foxp3+ Tregs that possessed greater ability to prevent autoimmune demyelination through changes associated with the transcription factor Foxo1. Therefore, a single self-antigen with low availability in the thymus induces dual tolerance mechanisms by positively selecting for a unique antigen-specific TCR population with reduced encephalitogenic potential along with a greater frequency of Tregs with enhanced suppressive capabilities.

Results

Targeted loss of MOG self-antigen causes more severe autoimmunity

Self-peptide specific CD4 T cells mediate autoimmune disease within the target organs based on the expression of cognate protein. To confirm MOG deficiency leads to loss of MOG-specific T cell tolerance (166), naïve CD4 T cells from C57BL/6 (WT) or

MOG KO mice were transferred into TCR$\alpha^{-/-}$ recipients followed by induction of EAE demyelinating disease. The adoptive transfer model of EAE was used as KO mice will not develop MOG-induced demyelination due to the lack of MOG expression on myelin. Mice receiving MOG KO CD4 T cells showed an earlier onset (MOG KO: day 11 and WT: day 16) and increased severity of disease as compared to mice receiving WT CD4 T cells (Figure 1A). Clinically, MOG KO CD4 T cells mediated rapid and severe paralysis that resulted in the cessation of experiments due to >20% loss of body weight by day 16-18, which coincidentally was the time of disease onset for mice receiving WT CD4 T cells (Figure1B). Increased disease severity was accompanied by a greater number of MOG-tetramer+ T cells in both the CNS (Figure 1C) and spleen (Figure 1D) with increased CD4 T cell production of the pro-inflammatory cytokine IFN-γ in the CNS (Figure 1E, 1F). Therefore, T cells developing in the presence of tissue-specific MOG demonstrate strong tolerance induction with decreased MOG reactivity, delayed gain of effector function, and reduced expansion of tetramer+ encephalitogenic T cells.

Tissue-specific self-pMHCII selects conventional and regulatory T cells

Subsets of higher-affinity thymocytes specific for self-pMHCII undergo negative selection while also inducing antigen-specific Foxp3+ Tregs to prevent autoreactivity (87, 156, 167, 168). To determine if tissue-specific tolerance employed both of these thymocyte tolerance mechanisms, naïve pMHCII tetramer enrichments were performed as this technique identifies the highest-affinity T cell most likely to be negatively selected or diverted to Foxp3+ Tregs(156, 168). Naïve WT mice lacked the classic signature of negative selection as they displayed increased numbers of MOG-tetramer+ CD4 T cells in peripheral lymphoid organs as compared to MOG KO mice (WT:195+/-28 vs

KO:75+/-9 cells, Figure 2A, gaiting strategy Supplementary Figure 1). When naïve MOG-tetramer+ T cells were analyzed in mice devoid of negative selection (Bim KO)(63) or those devoid of AIRE expression (AIRE KO), no significant differences in number were found when compared to WT (Figure 2A). The lack of MOG protein expression only affected repertoires specific for MOG itself as no decrease was apparent in the naïve T cell repertoire for the foreign LCMV epitope GP_{66-77}:I-A^b in WT and MOG KO mice (Figure 2B). Further, alterations of MOG-tetramer+ CD4 T cell development in MOG KO mice originated during thymocyte selection, as differences were evident in MOG-tetramer+ CD4 single positive (CD4SP) thymocytes (Figure 2C). Enhanced conversion of Foxp3+ Tregs generated from TCR:self-pMHCII interactions could possibly explain the decrease in total MOG-specific CD4 T cell number in KO mice (WT: 14.3% MOG KO: 4.8%) (Figure 2D) (169). However, the MOG-tetramer+ Treg numbers did not solely account for the difference identified in the total tetramer+ cells as KO mice still contained reduced numbers of MOG-specific $Foxp3^{gfp-}$ conventional CD4 T cells (Tconv) (Figure 2E). Thus, the absence of MOG led to the absolute reduction of tetramer+ CD4 T cells with decreased selection of both conventional and regulatory MOG-tetramer+ CD4SP thymocytes and CD4 T cells.

MOG is necessary for the development of a subset of MOG-specific TCRs

Since MOG altered selection of tetramer+ TCRs, similar developmental analysis was carried out on in the presence or absence of MOG using two MOG-tetramer+ retrogenic TCRs (Rg-TCRs), termed B8 and 1C9 (170). B8 and 1C9 MOG reactivity was confirmed through proliferation assays and were both identified as Tconv T cells (Data not shown). Examination of Rg thymocytes in WT mice revealed both 1C9 and B8 Rg-

TCRs could develop into CD4SP thymocytes, though at different efficiencies (B8: 5%, 1C9: 0.5%) (Figure 3A-D)(171). In MOG KO mice B8 Rg TCRs had significantly reduced efficiency of selection with reduced B8 CD4SP thymocytes (Figure 3C). Selection of the 1C9 TCR was unaffected by the absence of MOG (Figure 3D). Enumeration of the developing of CD4SP B8 and 1C9 thymocytes mirrored frequency data (B8: WT-$5.4x10^5$, KO-$8.8x10^4$ cells) (Figure 3B,D), with B8 TCRs demonstrating MOG dependence. The MOG tetramer negative 2D2 TCR-transgenic was similarly analyzed and displayed no dependency on MOG for selection (Data not shown). These data indicate MOG can act as a positive selecting ligand for a subset of MOG-specific Tconv clones. Therefore, a single self-pMHCII during thymocyte development can select for a subset of T cells specific for itself.

The MOG dependent B8 Rg-TCR clone presented here as well as other's previous work(167, 168) have shown selection can alter the TCR populations. To determine if MOG alters the TCR repertoire, MOG-tetramer+ CD4 T cells from both WT $Foxp3^{gfp}$ and MOG KO $Foxp3^{gfp}$ mice were index sorted followed by single cell TCR sequencing(172). Index sorting allows for the discrimination of a Treg (gfp+) or Tconv (gfp-) MOG-tetramer+ CD4 T cell sorted into each well. Analysis of TCRβ sequences revealed minimal repeats within the MOG-specific CD4 T cell repertoire in either WT or MOG KO mice (WT: 319 sequences, 7 mice, KO: 170 sequences, 6 mice, Figure 4A). The paucity of repeated clonotypes ruled out proliferation of peripheral MOG-specific CD4 T cells as a factor for the increase of MOG-specific T cells in WT mice (Figure 2A). Analysis of the V region TCRβ gene segments between WT and MOG KO mice revealed naïve MOG-tetramer+ CD4 T cells from MOG KO mice used more TRBV5 and less

TRBV1 when compared to WT mice (Figure 4B). Ignoring D regions due to limited contribution to diversity, MOG-tetramer+ V and J gene pairing was compared from WT and MOG KO mice and graphed on a heat map as a function of the percent difference between the mouse types (V:J low frequency pairings not shown, Figure 4C). The heat map demonstrates MOG KO sequences are enriched for a single TRBV5 gene with several TRBJ pairings (2-3, 2-5, 2-7, etc), while WT sequences are enriched for a larger diversity of V:J gene pairings including TRBV13-2:TRBJ2-4, TRBV13-1:TRBJ2-7, and TRBV3:TRBJ2-5 (Figure 4C). This data demonstrates the WT MOG-tetramer+ CD4 T cell clonotypic repertoire is diverse and suggests the TCR repertoire is modified in the presence of self-pMHCII, selecting for a greater diversity of V:J gene pairings.

MOG induces intrinsic tolerance mechanisms in MOG-tetramer+ T cells to prevent autoimmunity

To determine if the MOG selection changes caused differences in MOG tetramer+ CD4 T cell functionality, the expansion of the WT and MOG KO CD4 T cells was studied. Even though there were ~50% fewer naïve MOG-tetramer+ CD4 T cell precursors in the MOG KO repertoire (Figure 2A), MOG-tetramer+ CD4 T cells from MOG KO mice expanded 3.8-fold higher than that of WT at day 14 post MOG/CFA immunization (Figure 5A,B). Higher precursor number of tetramer+ CD4 T cells has been reported as a correlate of T cell expansion during an immune response(27), but was not seen here for MOG. The difference in expansion between WT and KO was not explained by the extravasation of MOG-specific CD4 T cells into the CNS of WT mice expressing MOG (Data not shown). This data indicates that mechanisms other than precursor number controlled MOG-tetramer+ clonal expansion. MOG-tetramer+ CD4 T

cells from KO mice had a distinct expansion advantage 21days post immunization compared to WT mice when MOG-tetramer+ CD4 T cells from WT (Thy1.1) and MOG KO (Thy1.2) mice were mixed together at equal numbers ($5x10^6$ CD4 T cells from each donor), transferred into TCR$\alpha^{-/-}$ hosts and induced for EAE (Figure 5C). Therefore, MOG-tetramer+ T cells have an intrinsic expansion advantage following development in the absence of MOG.

As the selection of MOG self-reactive CD4 T cells led to unique TCR clones with reduced response to antigen, selection may have also altered the naïve state of these cells. To determine if the presence of MOG altered the naïve transcriptional profile, naïve MOG-tetramer+ CD4 T cells from WT and KO mice were analyzed using RNA hybridization (NanoString) to an immunological gene panel. Analysis revealed differential expression of 40 of 547 immunological genes measured (Figure 5D) with WT T cells in general possessing decreased levels of expression. For example, the MOG-tetramer+ Tconv from KO mice displayed increased basal levels of IL-2 and Maf, which has been reported to play important roles in autoimmune disease progression(173). Altogether, these data illustrate MOG self-peptide positively selection generates a unique naïve MOG-tetramer+ population.

To assess if T cell development in the presence of MOG alters the intrinsic demyelination ability on a per cell basis, we transferred equal numbers (600 cells each) of previously immunized MOG-tetramer+ CD4 Tconv cells (Foxp3^{gfp-}) from WT or MOG KO mice into TCR$\alpha^{-/-}$ mice and induced EAE (Figure 5E). The transferred MOG-tetramer+ Tconv from MOG KO mice resulted in significantly higher incidence of demyelination as compared to WT Tconv (Figure 5E). This indicates an increased

capacity of the unique MOG KO Tconv cells to cause demyelination, even when Tconv cells are removed from Treg suppression. Therefore, CD4 T cells specific for MOG self-antigen possess intrinsic functional differences initiated by thymic selection.

MOG specific Tregs differ in suppressive capacity

Antigen-specific Tregs provide the optimal levels of control for an immune response(174, 175). We focused on the Treg population in WT and KO mice and found the frequency of MOG-tetramer+ CD4 Tregs in WT and KO mice was relatively constant during the MOG/CFA immune response (~15 and ~5% respectively, Figure 6A). To determine whether the reduced numbers of MOG-tetramer+ Tregs in the KO animals could explain the reduced levels of disease seen in the adoptive transfer model (Figure 1A), MOG-tetramer+ Tregs and Tconv from day 14 EAE immunized mice were sorted, transferred into new TCR$\alpha^{-/-}$ hosts and EAE was induced. The transfer of MOG-tetramer+ Tconv cells (600 cells) from MOG KO mice produced a high incidence of EAE, which was significantly reduced by the addition of Tregs (Foxp3^{gfp+}) from WT mice (300 cells) (Figure 6B). However, the addition of the same number of Tregs from MOG KO mice did not reduce EAE incidence (Figure 6B). Note that in both cases the Tregs are MOG-specific based on tetramer reactivity. To define how the MOG-tetramer+ Tregs differed, RNA-seq was performed on MOG-tetramer+ Foxp3^{gfp} Tregs from WT and MOG KO mice 14 days after EAE immunization (Figure 6C). Of the 479 genes differentially regulated (Figure 6C), gene ontology analysis revealed metabolic differences between WT and KO MOG-tetramer+ Tregs, with gene set enrichment analysis further supporting these findings (Figure 7A,B). Foxo1, a transcription factor regulated by Akt, is key in controlling Treg functionality and metabolism(176, 177). Due

to the relationship between Foxo1, metabolism and suppressive function of Tregs, the differentially regulated genes identified here were compared to the previously defined genes regulated by Foxo1 in Tregs(176). Analysis of genes differentially regulated in the absence of Foxo1 demonstrated significant transcriptional overlap with those in MOG KO Tregs, indicating MOG KO Tregs possessed reduced Foxo1 activity(176) (Figure 7C). Phenotypic analysis of MOG-tetramer+ Tregs recapitulated Foxo1 transcriptional data with those Tregs from WT mice expressing Foxo1-upregulated genes (FR4, CD73) and Tregs from KO mice expressing genes upregulated in the absence of Foxo1 (KLRG1, Ki-67) (Figure 8A,B). Analysis of total Foxo1 was found to be similar between MOG-tetramer+ Foxp3- and Foxp3+ T cells in WT and MOG KO hosts, though Tregs from MOG KO mice were trending to have reduced expression (Figure 8C). This could be the result of Foxo1 phosphorylation by Akt which reduces Foxo1 function by causing nuclear exclusion of the transcription factor followed by degradation(178). MOG-tetramer+ Treg cells were analyzed for phosphorylated Foxo1 (pFoxo1), the form of Foxo1 excluded from the nucleus, finding increased pFoxo1 in MOG KO tetramer+ Tregs (Figure 8D). Thus, Tregs specific for the same antigen can have differing functional fates and suppressive potential with selection in the presence of MOG leading to genes associated with Foxo1.

Discussion

The data presented here shows selection generates two populations of MOG-tetramer+ CD4 T cells. The first subset is dependent on MOG expression for positive selection, as demonstrated by the B8 TCR (Figure 3A,C). The second subset is positively selected independent of MOG expression by cross-reactive self-peptides, represented by

the 1C9 or 2D2 TCRs (Figure 3B,D, data not shown). Together, these two subsets of selected TCRs comprise the MOG-specific CD4 T cell population in WT mice. The MOG positively selected T cells have profound effects on the total effector and regulatory T cell population, increasing their numbers while reducing the encephalitogenecity of effectors and enhancing disease suppressing capabilities of the Tregs. It is unclear if the population of TCRs generated independently of MOG on cross-reactive self-peptides in WT and KO animals possess similar functional characteristics, TCR clonotypes, or levels of negative selection. However, their presence does not take away from the fact that the MOG expression has a dominant effect by positively selecting a subset of MOG-specific CD4 T cells that enforce tolerance amongst the broad MOG-reactive CD4 T cell population.

Positive selection would make for a potent regulator of self-responses to specific antigens, as all cells have to undergo positive selection to become a mature T cell. Although positive selecting epitopes support survival of T cells in the thymus and the periphery, they are typically thought to be unable to activate the full complement of effector functions (62, 179, 180). This lack of functional response is associated with transcriptional alterations induced by the presence of the positive selecting ligand, thereby dampening the response of T cells reactive to self. Our study raises questions as to how the powerful tolerance mechanisms induced by positive selection to MOG or other self-pMHCII antigens are overcome. In the B6 mice with MHC class II generally resistant to spontaneous autoimmunity, EAE is induced using robust stimulatory conditions. Demyelinating disease only develops under extreme inflammatory conditions triggered by two injections of pertussis toxin (causing alterations in G-coupled protein

interactions altering innate and adaptive immune function) and MOG peptide emulsified in Complete Freund's Adjuvant containing increased levels of heat-killed mycobacterium (181). Delivery of MOG with other adjuvants such as LPS is ineffective at inducing EAE (unpublished data). Thus, our findings suggest T cells can be activated by their positive selecting ligand, albeit only under strong inflammatory signals that override the transcriptional alterations put in place to prevent aberrant autoimmunity.

Although it is possible the MOG self-protein could mediate some level of negative thymocyte selection, several findings are contraindicative for this mechanism of tolerance. Besides MOG not being strongly expressed in the thymus(159, 182, 183), multiple retrogenic TCRs generated from αβTCRs with a range of avidity for MOG:MHCII showed no evidence of clonal deletion of thymocytes (171), including our tetramer positive B8 and 1C9 T cells. Immune responses with high tetramer+ naïve precursor CD4 T cell numbers, as seen for MOG, are poorly negatively selected(27). Furthermore, effective deletion of MOG-specific T cells by negative selection has only been reported when groups have targeted MOG overexpression to the thymus(184). Our data support the lack of dominant negative selection by showing MOG can positively select MOG-specific CD4 T cells. Finally, mice lacking traditional negative selection modulators (Aire KO, Bim KO) have no alterations in the MOG-tetramer+ CD4 T cell numbers. The lack of compelling data to support negative thymocyte selection by MOG leads to the conclusion that altered positive selection can act as a tolerance mechanism

MHC confers the largest relative risk for autoimmune diseases and is believed to be linked due to poor thymocyte negative selection by at risk MHC alleles (185). Analysis of the autoimmune prone NOD mice by Benoist and colleagues did not find

impaired negative selection of αβ TCRs, but instead proposed altered thymocyte positive selection as the causative effect behind the increased autoimmunity associated with this strain (85). During T cell development, the number of cells that can undergo positive selection in the thymic cortex is dependent on pMHC availability and thymocyte density (83, 186), with alterations in the size of the positive selecting niche leading to T cell dysfunction (66, 86, 187). We found the presence of MOG led to a 2.5 fold increase in the number of naive MOG-tetramer+ T cells, demonstrating its role as a positive selecting ligand. Although somewhat counterintuitive, the increased numbers of precursor cells were intrinsically less capable of expanding. It is interesting to speculate whether this same process is observed in MS patients and healthy controls as all individuals, regardless of disease status, have T cells that are nominally reactive to self-antigens yet most individuals do not progress to pathogenesis (188). We hypothesize these self-reactive T cells in healthy controls are simply the remnants of self-pMHCII positive selection which are less capable of causing autoimmunity due to reduced reactivity to self and the enhanced frequency of highly suppressive Tregs.

Positive selection also influences the generation and function of regulatory T cells (169). Previous work demonstrated differences in the suppression between antigen-specific and non-specific Tregs, with Tregs of matching antigen-specificity being the most efficient regulators (174, 175). Our data adds additional insight to the functionality of antigen-specific Tregs as we categorized two types of antigen-specific Tregs. The first was those Tregs that selected/responded to the same antigen (MOG selected/MOG responding) and the second were those that were selected on and responded to two different peptides (unknown selected/MOG responding). Both of these Tregs were MOG-

tetramer+, but Tregs selected in the presence of MOG were more capable of suppressing MOG induced disease and expressed a unique transcriptome associated with Foxo1 regulation. As the MOG KO mouse treats MOG as a foreign antigen it also brings into focus the function of Tregs in a foreign antigen-specific T cell response. Interestingly, Treg function is important for maximal anti-viral responses as the complete absence of antigen-specific Tregs delays recruitment of effectors as well as poorly induces memory CD8 T cells due to reduced production of Il-10 (189, 190). Note these Tregs were selected on self-antigen that differs from their cognate antigen, similar to our MOG KO Tregs. This data supports a role for these types of Tregs not in preventing autoimmunity, but instead in regulating the optimal response and expansion of higher-affinity T cells during infection.

This idea of two unique types of suppressive Tregs leads to questions of their use in therapeutic treatments. To effectively intervene in autoimmune disease, one should target antigens from proteins that have specifically positively selected Tregs, and not just myelin-specific or pan-antigen specific Tregs that may have been selected by cross-reactive epitopes. Studies characterizing the expression of thymic antigens have found minimal to no expression of MOG in thymic resident dendritic cells, macrophages and cTEC or mTEC with or without AIRE expression (159, 160, 183, 191). Using the available datasets from these papers (GEO: GSE2585, GSE4494, GSE70798), one can identify numerous tissue-specific antigens implicated in autoimmune disease that are expressed such as insulin 2, transglutaminase, thyroperoxidase, MBP, and PLP, several of which mediate thymocyte negative selection(161). Numerous proteins with expression patterns similar to MOG can be identified, which include other auto-reactive antigens

such as hypocretin, thyroid stimulating hormone receptor, thyroglobulin, and thyroid stimulating hormone β chain. This data evokes two key concepts. First, other mechanisms must be accounting for the introduction of self-antigen and MOG into the thymus environment, where it clearly has an effect. Second, expression patterns of tissue-restricted antigens suggest MOG is only one of a multitude of self-antigens in which positive selection may mediate effector and regulatory tolerance mechanisms that effectively limit autoimmune disease. Therefore, these two tolerance mechanisms mediated by thymic selection are fundamental for the production of a normal T cell repertoire with a reduced ability to cause autoimmunity.

Methods

Mice

B6 mice were purchased from NCI while Foxp3^{gfp} and TCR-α$^{-/-}$ mice were purchased Jackson Laboratories and bred on site. MOG KO Foxp^{gfp} mice were generated by breeding Foxp3^{gfp} and MOG KO mice on site (166). EAE scoring was on the 5-point scale: 0=not sick, 0.5= distal limp tail, 1= proximal weak tail, 2= hind limb weakness, 3= complete hind limb paralysis, 4= inability to flip over, 5=death or moribund. Mice in EAE experiments were sacrificed at >20% body weight reduction (192).

Peptide Priming

$MOG_{35–55}$ (MEVGWYRSPFSRVVHLYRNGK) peptide were synthesized in house (Protein Technologies, Inc.). For MOG/CFA immunization, 200μg of the peptide was emulsified in 375μg of Complete Freund's Adjuvant (CFA) and 150μl of the emulation was injected subcutaneously on days 0 and 7. On days 0 and 2, 300ng of pertussis toxin was injected intrapertioneally.

MOG-specific CD4 T cell identification

$MOG_{38–49}$:I-A^b and GP_{66-77}:I-A^b reagents were provided by the NIAID TCF. Tetramer enrichment and staining was preformed as previously described (108). Briefly, spleen and lymph nodes were processed into a single cell suspension and stained with fluorophore-conjugated tetramers (4μg/ml) for 60 min at room temperature. Samples were then mixed with anti-fluorophore magnetic beads (anti-PE or anti-APC, Miltenyi Biotec) for 30 min on ice and then isolated by MACS. Samples were mixed with AccuCheck (Thermo Fischer Scientific) beads followed by flow cytometry acquisition for absolute cellular counts. For analysis of CD4 T cells in the CNS, lymphocytes were isolated as previously described (18). CD4 T cell purifications of CNS resident lymphocytes were performed following manufacturer protocol using the CD4 T cell positive isolation kit (Miltenyi Biotec). For cytokine staining, cells were stimulated as previously described (193) and treated with the BD Cytofix/Cytoperm kit (BD Biosciences) as per manufacturer protocol. For analysis of Foxo1, surface stained cells were fixed following the manufacturer protocol using the BD Phosflow kit (BD Biosciences). Briefly, cells were fixed using the Lyse/Fix Buffer (BD Biosciences) and incubating for 10 min at 37°C. Cells were permeabilized using Perm Buffer II (-20°C, BD Biosciences) for 30 min on ice and stained overnight on ice with antibodies against Foxo1 (1:150, C29H4, Cell Signaling Technology) or pFoxo1 (1:100, 9464S, Cell Signaling Technology). The following day rat anti-rabbit F'Ab AF488 (1:50) was used to detect the Foxo1 proteins. Antibodies used for flow cytometry are shown in Supplementary Table 1. Samples were collected on an LSR II (Becton Dickinson) and analyzed using FlowJo (Treestar).

CD4 T cell Adoptive Transfer

CD4 T cells from the spleens or WT of MOG KO mice were purified following manufacturer instructions using the CD4 T cell negative isolation kit (Miltneyi Biotec). Purified CD4 T cells were analyzed and counted by flow cytometry using AccuCheck microbeads (Invitrogen) and $5x10^6$ purified CD4s were then injected IV into recipient mice.

Proliferation Assays

Splenocytes from retrogenic mice were processed into a single cell suspension in RPMI media. $6x10^5$ splenocytes were plated with 10-fold serial dilutions of MOG_{35-55} peptide in RPMI media and incubated for 48hrs at 37°C. ^{3}H-thymidine was added to the samples (0.4 μcuries/well final concentration) and 24 hours later the samples were harvested onto a filtermat using a 96 well Harvester (Packard Filtermate 196, Packard). Filtermats were analyzed using a MicroBeta TriLux (PerkinElmer) and counts per minute (CPM) were reported.

Single cell TCR sequencing

Single cell sequencing was performed as previously described(172). In brief, naïve MOG-tetramer+ CD4 T cells were isolated as previously described and index-sorted by a FACS Aria II (Becton Dickinson) into cDNA master mix. Nested TCRβ PCR was performed and samples were sent to Beckman Coulter Genomics for sequencing. Sequences were tabulated and parsed by in-house designed software and then analyzed by IMGT (194–196). Heatmaps were created by taking the differences of the average for each unique TRBVJ pairings between WT and MOG KO tetramer+ T cells.

TCR retrogenic mice

TCRs in this study were derived from mice primed with MOG_{35-55}/CFA. Bulk CD4 T cells were cultured on MOG_{35-55} to select for antigen-reactivity and individual clones were isolated by limiting dilution cultures and confirmed for antigen specificity with MOG_{38-49}:I-A^b tetramers. TCR were sequenced and inserted into the pMIGII retroviral construct for retrogenic mouse generation from transduced bone marrow as previously published(170). Successfully transduced bone marrow cells derived from a $Rag^{-/-}$ mouse ($2x10^6$ cells, with >30% transduction as measured by GFP expression) were transferred IV into lethally irradiated WT B6 or MOG KO mice (950 rads). Experimental animals were given antibiotic water for one week after irradiation (2% sucrose, 0.5 mg/ml Neomycin, 0.0125 mg/ml Polymyxin B). Mice were analyzed 8 weeks after injection.

Bone Marrow Chimera generation

Bone marrow was isolated bilaterally from the femur, tibia and hip and depleted of T cells based on Thy1.2 expression. To remove Thy1.2+ cells, Thy1.2-PE antibody and anti-PE magnetic microbeads (Miltenyi Biotec) were used following manufacturer instructions. $2\text{-}5x10^6$ bone marrow cells were injected IV into lethally irradiated mice (950 rad). Mice were given antibiotic water for one week after irradiation (2% sucrose, 0.5 mg/ml Neomycin, 0.0125 mg/ml Polymyxin B). Analysis was performed 8 weeks after transfer.

RNA-seq Library Preparation

Total RNA was isolated using the QIAGEN RNEasy Micro Kit. Libraries were generated using the CLONTECH SMARTer V3 kit, briefly, all RNA obtained from 500 cells was used for cDNA synthesis and 15 cycles of PCR were perform to amplify the

cDNA. Barcoding and sequencing primers were added using NexteraXT DNA kit. Libraries were validated by microelectrophoresis, quantified, pooled and clustered on Illumina TruSeq v3 flowcell. Clustered flowcell was sequenced on an Illumina HiSeq 1000 in 100-base single-read reactions.

Gene ontology analysis was conducted on differentially expressed genes (DEGs) using the R/Bioconductor package GOstats (v2.32.0)(197). Gene Set Enrichment Analysis (GSEA v2.1.0)(198) was performed using the pre-ranked list option based on the *t*-statistic determined by DESeq2(199).

NanoString

Tetramer+ Foxp3^{gfp}- CD4 T cells were sorted into 5µl iScript RT-qPCR sample preparation reagent (Bio Rad, Hercules CA) and frozen immediately to -80°C. Samples were submitted to NanoString for analysis with the Gene Expression Assay-Single Cell Application using the Mouse Immunology Panel. Reverse Transcription reactions were performed following NanoString's protocol (MAN-C0027) for Multi-Target Enrichment (MTE). cDNA was transferred to PCR strip tubes for amplification for 14 cycles. 8µl of amplified cDNA was added to each nCounter hybridization reaction. Raw counts for each assay were collected using the NanoString data analysis software nSolver. Data was normalized using positive control normalization as well as RNA content normalization. Normalized data was then evaluated using nSolver Analysis tool v2.6 for analysis of differentially regulated genes. Dataset included in Supplementary data (NanoString Dataset 1).

Statistics

All data were analyzed using Prism (Graphpad) Software. Samples were excluded if the MOG-tetramer+ Treg frequency was >50%. Data were analyzed by 2-tailed Student's *t* tests, One-Way ANOVA with Tukey's test for multiple comparisons, Fisher's exact test, Two-Way ANOVA with Sidak's multiple comparison test and Log rank test followed by the Benjamini-Hochberg test for multiple comparisons.

Study Approval

All animals were housed in an Emory University Department of Animal Resources facility (Atlanta, GA) and used in accordance with an Institutional Animal Care and Use Committee approved protocol.

Data Availability

RNA-Seq data is available via reference accession GSE79124

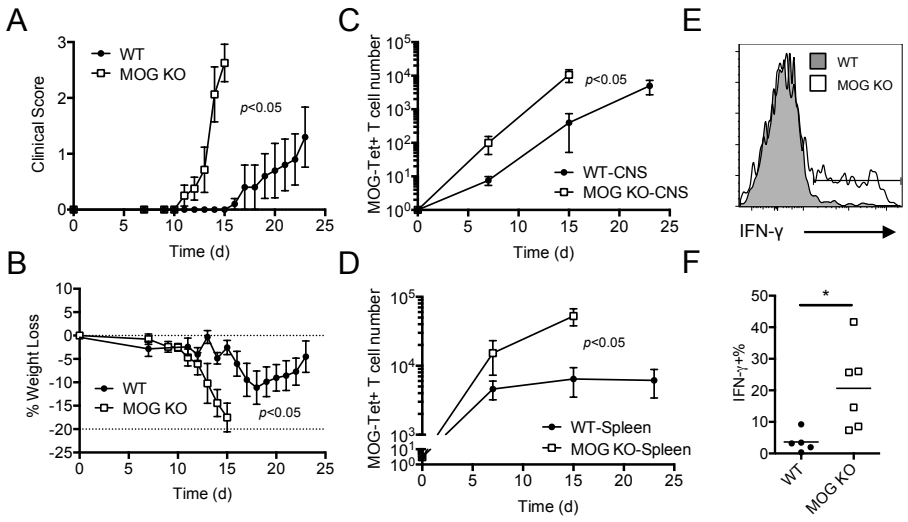
A
Clinical Score
WT
MOG KO
p<0.05
Time (d)
B
% Weight Loss
WT
MOG KO
p<0.05
Time (d)
C
MOG-Tet+ T cell number
p<0.05
WT-CNS
MOG KO-CNS
Time (d)
D
MOG-Tet+ T cell number
p<0.05
WT-Spleen
MOG KO-Spleen
Time (d)
E
WT
MOG KO
IFN-γ
F
IFN-γ+%
*
WT
MOG KO

Figure 1.

Figure 1. CD4 T cells from MOG KO mice have an increased encephalogenic potential. $5x10^6$ CD4 T cells from naïve WT and MOG KO mice were adoptively transferred into TCR$\alpha^{-/-}$ mice and EAE was induced. (A-B) TCR$\alpha^{-/-}$ mice receiving MOG KO CD4 T cells showed more rapid onset and increased severity of EAE clinical symptoms (A) and weight change (B) (n=3-5 with 2 repeats, data are represented as mean +/- SEM, Two-Way ANOVA with Sidak's multiple comparison test). (C-D) Along with increased disease severity, there was an increased rate of accumulation of CNS (C) and spleen (D) resident, MOG-tetramer+ CD4 T cells in MOG KO recipient TCR$\alpha^{-/-}$ (n=5-6 per time point, data represented as mean +/- SEM, Two-Way ANOVA with Sidak's multiple comparison test). (E-F) IFN-γ production of CNS CD4 T cells from TCR$\alpha^{-/-}$ host receiving either WT or MOG KO CD4 T cells stimulated with MOG_{35-55} peptide and PMA on day 15 post EAE induction. (n=4-5, representative flow plot, Student's T-test, *p<0.05).

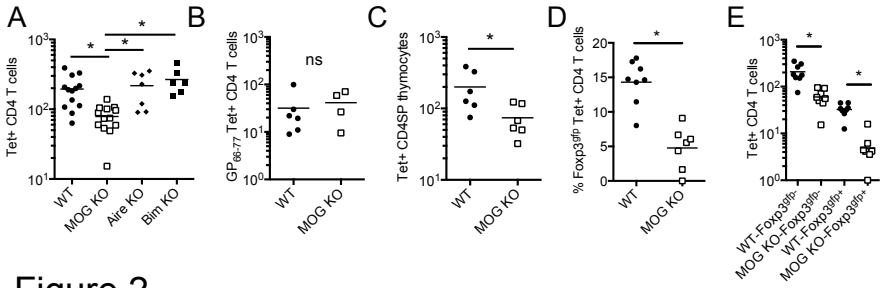
A
B
C
D
E
Tet+ CD4 T cells
WT
MOG KO
Aire KO
Bim KO
ns
Tet+ CD4SP thymocytes
% Foxp3gfp Tet+ CD4 T cells
WT-Foxp3gfp-
MOG KO-Foxp3gfp-
WT-Foxp3gfp+
MOG KO-Foxp3gfp+

Figure 2.

Figure 2 MOG positively selects MOG-tetramer+ Treg and Tconv CD4 T cells.
(A) Double tetramer enrichment was used to identify naïve MOG-tetramer+ CD4 T cells in WT, MOG KO, Aire KO and Bim KO. MOG-tetramer+ CD4 T cells were quantitated from peripheral lymphoid organs (Data represented as single mouse per point, n=6-13 mice, 6 experiments, One-Way ANOVA with Tukey's multiple comparison test, *p<0.05). (B) Naïve enrichment of GP66-tetramer+ CD4 T cells in WT and MOG KO mice (Data represented as single mouse per point, n=5 mice, 2 experiments, Student's T-test ns=no significance). (C) MOG-tetramer+ CD4 T cells were quantitated from thymi of naïve mice (Data represented as single mouse per point, n=3-6 mice, 4 experiments, Student's T-test, *p<0.05) (D) Frequency of Foxp3^{gfp}+ Tregs in naïve MOG-tetramer+ CD4 T cells from the pLO (Data represented as single mouse per point, n=7-8, 3 experiments, Student's T-test p<0.05). (E) Enumeration of naïve MOG-tetramer+ CD4 T cells from Foxp3^{gfp} WT or MOG KO Foxp3^{gfp-} and Foxp3^{gfp+} (Data represented as single mouse per point , n=7-8 mice from 3 experiments, One-Way ANOVA with Tukey's multiple comparison test, *p<0.05).

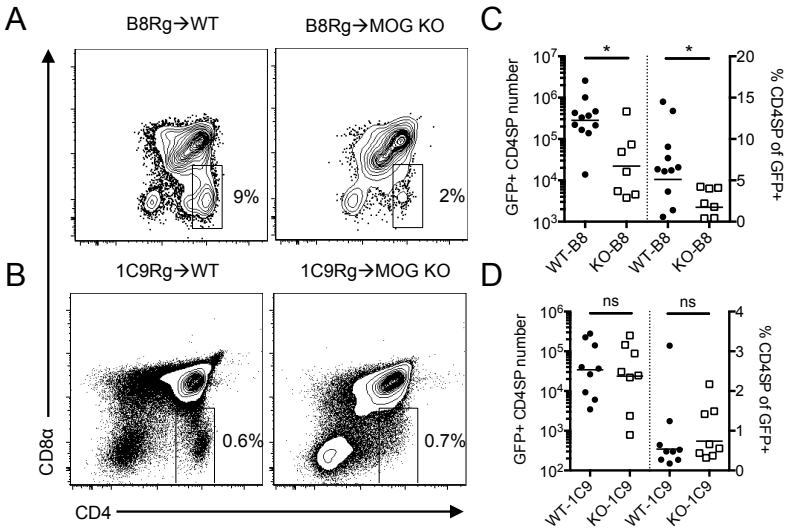
A
B8Rg→WT
B8Rg→MOG KO
9%
2%
B
1C9Rg→WT
1C9Rg→MOG KO
0.6%
0.7%
CD8α
CD4
C
GFP+ CD4SP number
% CD4SP of GFP+
*
*
WT-B8
KO-B8
WT-B8
KO-B8
D
GFP+ CD4SP number
% CD4SP of GFP+
ns
ns
WT-1C9
KO-1C9
WT-1C9
KO-1C9

Figure 3.

Figure 3 MOG dependent development in a subset of MOG-specific TCR clonotypes MOG-specific TCRs were allowed to develop in the presence and absence of MOG to determine their dependence on MOG. (A) Representative flow cytometric plots of GFP+ thymocytes possessing the B8 TCR 6-8 weeks after BM reconstitution in WT and MOG KO mice (n=7-11 mice, two experiments). (B) Representative flow cytometric plots of GFP+ thymocytes possessing the 1C9 TCR 6-8 weeks after BM reconstitution in WT and MOG KO mice (n=7-11 mice, two experiments). (C-D) Frequency and enumeration of selected CD4SP retrogenic thymocytes deriving from either the B8 (C) or 1C9 (D) TCR (n=7-11 mice, two experiments, Student's T-test *p<0.05, ns=no significance).

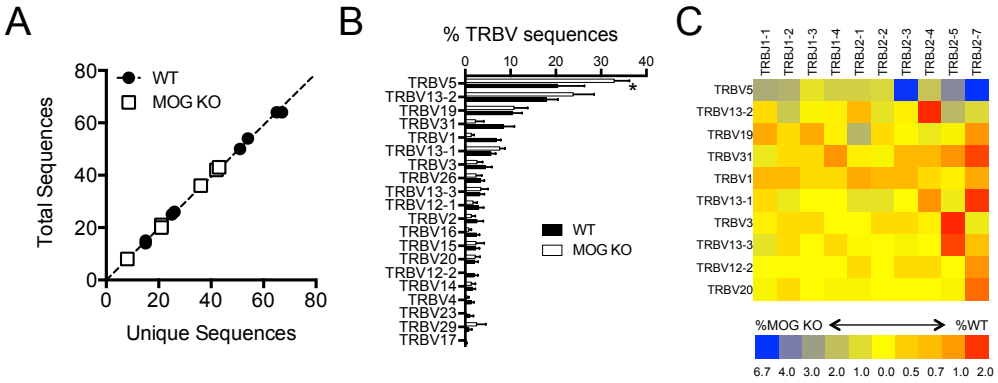
A
WT
MOG KO
Total Sequences
Unique Sequences
B
% TRBV sequences
TRBV5
TRBV13-2
TRBV19
TRBV31
TRBV1
TRBV13-1
TRBV3
TRBV26
TRBV13-3
TRBV12-1
TRBV2
TRBV16
TRBV15
TRBV20
TRBV12-2
TRBV14
TRBV4
TRBV23
TRBV29
TRBV17
WT
MOG KO
C
TRBJ1-1
TRBJ1-2
TRBJ1-3
TRBJ1-4
TRBJ2-1
TRBJ2-2
TRBJ2-3
TRBJ2-4
TRBJ2-5
TRBJ2-7
%MOG KO
%WT
6.7 4.0 3.0 2.0 1.0 0.0 0.5 0.7 1.0 2.0

Figure 4.

Figure 4 MOG selection alters the TCR repertoire.

Naïve MOG-tetramer+ CD4 T cells were single cell index sorted and TCRβ sequencing was performed. (A) Comparison of the total number of TCR sequences (WT=319, KO=170 sequences) to unique number of TCR sequences reveals few repeats within the MOG-specific CD4 T cell repertoire (each dot represents an individual mouse). (B) Frequency of expression of TRBV family members by either WT or MOG naïve MOG-tetramer+ T cells (data represented as mean +/- SEM, n=8-10 mice per group, Two-Way ANOVA with Sidak's multiple comparisons test, $*p<0.05$). (C) Heatmap of differentially paired TRBV and TRBJ family members between WT and MOG KO MOG-tetramer+ CD4 T cells. Data represented as % overexpression in either MOG KO (blue) or WT (red).

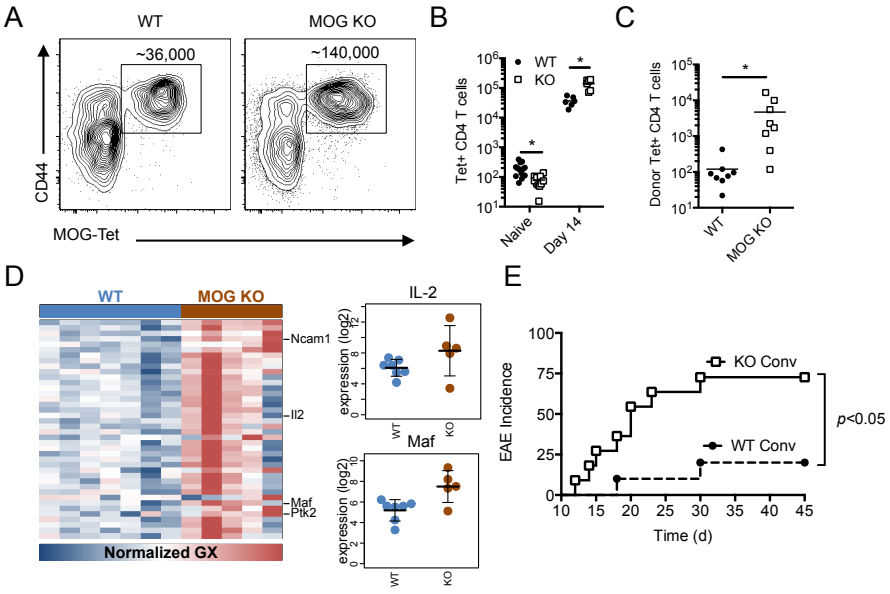
A
WT
MOG KO
~36,000
~140,000
CD44
MOG-Tet
B
WT
KO
Tet+ CD4 T cells
Naive
Day 14
C
Donor Tet+ CD4 T cells
WT
MOG KO
D
WT
MOG KO
Ncam1
Il2
Maf
Ptk2
Normalized GX
IL-2
Maf
expression (log2)
E
EAE Incidence
KO Conv
WT Conv
p<0.05
Time (d)

Figure 5.

Figure 5 Dual tolerance mechanisms control MOG-tetramer+ CD4 T cell expansion (A) Representative flow cytometric plots of d14 MOG/CFA immunized, MOG-tetramer enriched CD4 T cells from WT or MOG KO mice. (B) Enumeration of MOG-tetramer enriched naïve WT (n=13) and MOG KO (n=13) or day 14 WT (n=6) and MOG KO mice (n=6). Naïve enrichments were taken from Figure 2A (Data represented as individual points and the mean, Student's T-test, $*p<0.05$). (C) Expansion of WT and MOG KO MOG-tetramer+ CD4 T cells in TCR$\alpha^{-/-}$ mice after mixed adoptive transfer ($5x10^6$ each) of purified CD4 T cells at day 21 post induction (n=8, 3 experiments, points are single mice with the bar representing the mean, Student's T-test $*p<0.05$). (D) Heatmap of Differentially Expressed Genes (DEGs) determined using NanoStrings. Columns represent biological replicates of WT (blue) and MOG KO (red) MOG-tetramer+ naïve T cells and rows represent DEGs. Data are $\log_2$ transformed and z-score normalized (Two experiments). Beeswarm plots of select DEGs. Black bars represent the mean +/- 1 standard deviation. (E) Incidence of EAE onset mediated by adoptively transferred MOG-tetramer+ effector CD4 T cells (600 cells) (Log rank test).

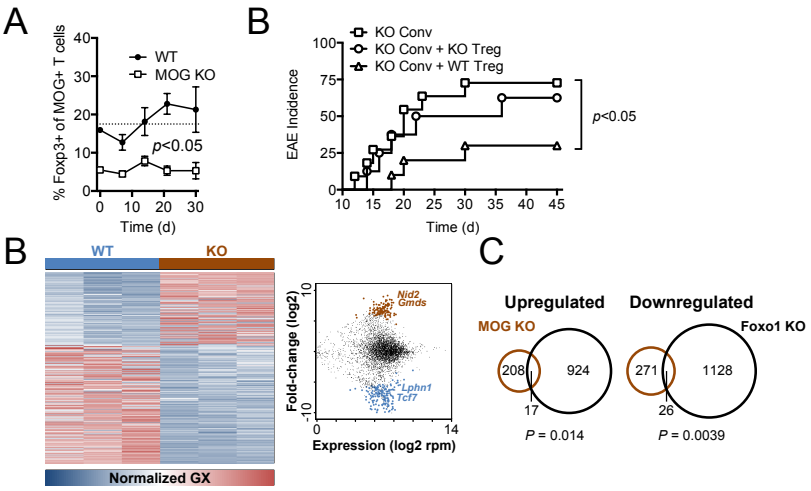
A
% Foxp3+ of MOG+ T cells
WT
MOG KO
p<0.05
Time (d)
B
KO Conv
KO Conv + KO Treg
KO Conv + WT Treg
EAE Incidence
p<0.05
Time (d)
B
WT
KO
Normalized GX
Fold-change (log2)
Nid2
Gmds
Lphn1
Tcf7
Expression (log2 rpm)
C
Upregulated
Downregulated
MOG KO
Foxo1 KO
208
924
17
P = 0.014
271
1128
26
P = 0.0039

Figure 6.

Figure 6 Treg suppression of EAE is dependent upon the Treg selection epitope

(A) Kinetic analysis of MOG-tetramer+ T cells during the EAE immune response in both WT and MOG KO mice (n=6-13 mice per time point, naïve data taken from figure 2B, Two-Way ANOVA). (B) Incidence of EAE onset mediated by adoptively transferred MOG-tetramer+ conventional CD4 T cells (600 cells) with or without MOG-tetramer+ Tregs (300 cells) (n=9-10 mice per group, 3 experiments, log rank test followed by the Benjamini-Hochberg test for multiple comparisons). (C) Heatmap of Differentially Expressed Genes (DEGs) determined by RNA-seq. Columns represent biological replicates of WT (blue) and MOG KO (brown) Tregs and rows represent DEGs. Data are $\log_2$ transformed and z-score normalized. Scatter plot of average expression (x-axis) by fold-change between WT and Mog KO. Positive fold-changes represent increases in Mog KO. Differential genes are shown in blue and red. (D) Venn diagrams of DEGs up- and down-regulated in MOG KO (brown) and Foxo1 KO (black) Tregs. Foxo1 KO DEGs were those previously published(176). Significance of overlap was determined by Fisher's exact test.

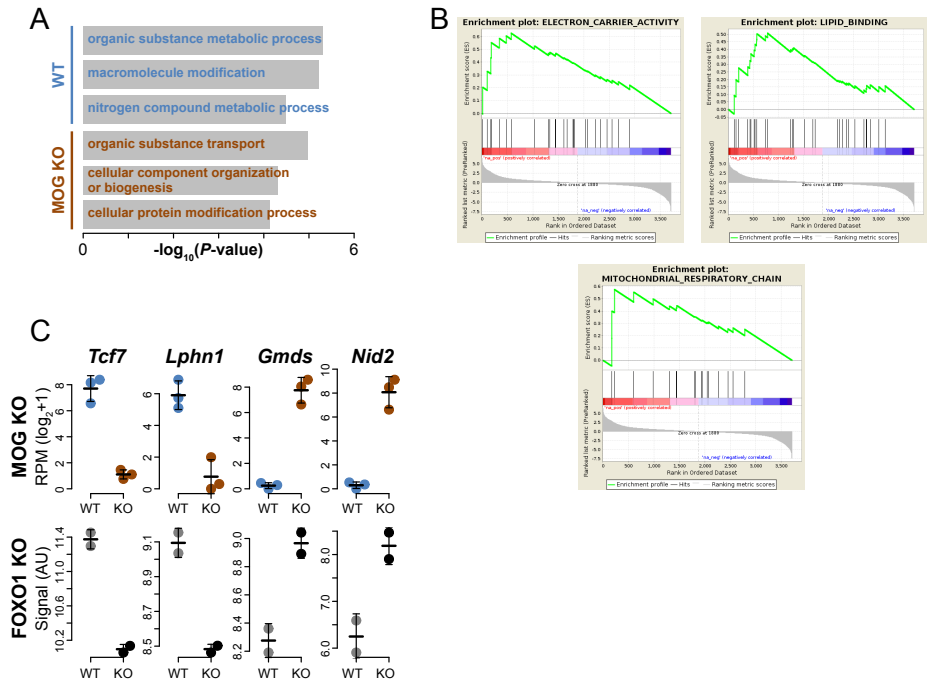
A
WT
MOG KO
organic substance metabolic process
macromolecule modification
nitrogen compound metabolic process
organic substance transport
cellular component organization or biogenesis
cellular protein modification process
0
-log10(P-value)
6
B
Enrichment plot: ELECTRON_CARRIER_ACTIVITY
Enrichment plot: LIPID_BINDING
Enrichment plot: MITOCHONDRIAL_RESPIRATORY_CHAIN
C
Tcf7
Lphn1
Gmds
Nid2
MOG KO
RPM (log2+1)
FOXO1 KO
Signal (AU)
WT
KO

Figure 7.

Figure 7 Differentially regulated transcriptome in WT and MOG KO Tregs. (A) Gene ontology of MOG-tetramer+ Tregs from WT and MOG KO mice. (B) Gene set enrichment analysis (GSEA) of WT and MOG KO Tregs. Positive fold-changes represent increases in WT Tregs (C) Beeswarm analysis of DEG between MOG-tetramer+ Tregs and Foxo1 regulated genes, showing similar expression patterns in MOG KO and Foxo1 Tregs. Data for MOG-tetramer+ cells are $\log_2$ transformed and z-score normalized. Data from Foxo1 KO Tregs were previously published(176) and were downloaded from GSE40645.

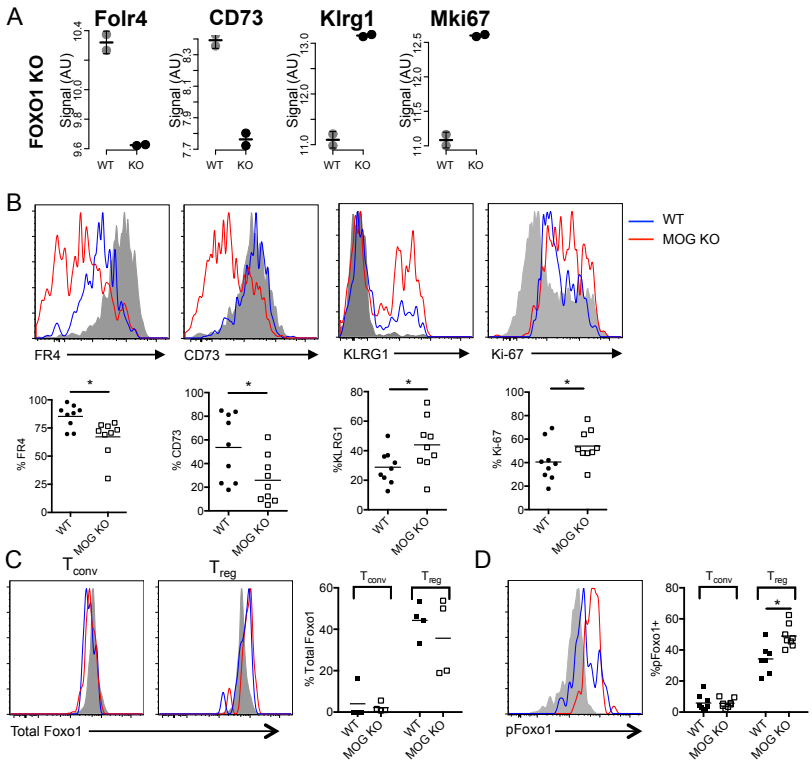
A
Folr4
CD73
Klrg1
Mki67
FOXO1 KO
Signal (AU)
WT
KO
B
WT
MOG KO
FR4
CD73
KLRG1
Ki-67
% FR4
% CD73
%KLRG1
% Ki-67
C
T conv
T reg
Total Foxo1
% Total Foxo1
D
pFoxo1
%pFoxo1+

Figure 8.

Figure 8 Foxo1 is associated with self vs foreign Treg suppressive capabilities

(A) Beeswarm analysis of DEG between Foxo1 KO Tregs, showing predicted expression for WT and MOG KO Tregs. Data from Foxo1 KO Tregs were previously published(176) and were downloaded from GSE40645. (B) Representative flow cytometric plots of MOG-tetramer+ Tregs in WT (blue line) or MOG KO (red line) mice with comparison to tetramer- Foxp3+ CD4 T cells (filled grey histogram) (n=6-9 mice, 3 experiments). Comparison of protein expression between MOG-tetramer+ Tregs in WT (filled circles) and MOG KO mice (Open squares) based on % positive expression (Points represent individual mice, n=6-9 mice, 3 experiments, Student's T-test *p<0.05). (C) Expression of total Foxo1 expression of MOG-tetramer+ Tconv and Tregs in WT (blue line) and MOG KO (red line) compared to tetramer- CD4 T cells (filled grey) (n=4 mice, each point is a single mouse, one experiment, Two-Way ANOVA with Sidak's multiple comparison test, *p<0.05). (D) Expression of phosphorylated Foxo1 in MOG-tetramer+ Tconv and Tregs in WT (blue line) and MOG KO (red line) compared to tetramer- Foxp3+ CD4 T cells (filled grey) (n=7-8 mice, two experiments, each point is an individual mouse, Two-Way ANOVA with Sidak's multiple comparison test, *p<0.05).

Supplementary Materials:

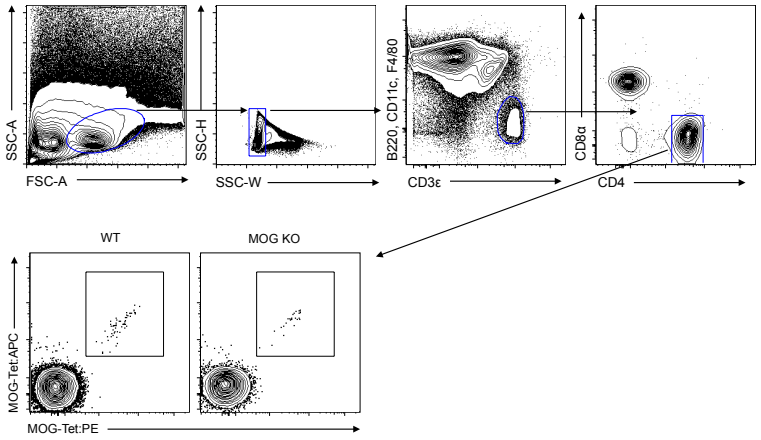

Supplementary Figure 1.

Supplementary Figure 1: Gating strategy for MOG-tetramer+ CD4 T cells.

For naïve mice tetramer staining was performed as shown to identify B220-,CD11c-, F4/80-,CD3ε+, CD8α-,CD4+, MOG-tetramer double positive (APC and PE) T cells.

Chapter 3

Large numbers of lower-affinity CD4 T cells enter and participate in the primary immune response

Abstract

A robust primary immune response has been corelated to the precursor number of antigen-specific T cells as identified using pMHCII tetramers. However, pMHCII tetramers only identify the highest-affinity T cells. To better study the entire CD4 T cell repertoire inclusive of low-affinity T cells missed by tetramers, we employed a T cell receptor-signaling reporter and micropipette based assay to quantify both naïve precursors and expanded populations. *In vivo* limiting dilution assays revealed hundreds more precursor T cells than previously thought, with higher-affinity tetramer+ T cells comprising only 5-30% of the total antigen-specific naïve repertoire. Additionally, the lower-affinity T cells maintained their predominance as the primary immune response progressed; finding no enhanced survival of T cells with high-affinity TCRs. These findings demonstrate that affinity for antigen does not control CD4 T cell entry into the primary immune response as a diverse range in affinity is maintained from precursor through peak of T cell expansion.

Introduction

The number of antigen-specific CD4 T cells in the naïve mouse correlates with the effector potential of the population. Defining the total number of antigen-specific T cells in an organism therefore has important ramifications for understanding immune

response outcomes (3, 79, 81, 107, 142, 200). Currently, peptide-major histocompatibility complex (pMHC) tetramers (Tet) provide the gold standard for the identification of antigen-specific CD4 T cells(14, 27). Tetramers are limited to identifying CD4 T cells with higher-affinity T cell receptor (TCR):pMHC interactions (16–18) and bind via an avidity dependent mechanism without dependence on CD4 co-receptor (9, 16, 35, 40, 201–203). Thus, unbiased assessment of the total number of antigen-specific T cells has been challenging for CD4 T cells due to the high-affinity predisposition by tetramers. Therefore, the contribution of lower-affinity T cells in the naïve and expanded T cell repertoires is currently unknown, in part due to the difficulty of accurately quantifying these T cells in the naïve repertoire.

Previous studies have suggested T cells with higher-affinity TCR:pMHC interactions possess enhanced survival or preferred selection during the primary or secondary immune response (20, 91, 204), with others reporting affinity independence of T cell maintenance during an immune response(205). These experiments only analyzed biased populations by restricting αβ TCR diversity and/or sampling through the use of pMHC tetramers, thereby potentially missing clones participating in the response. Further works using TCR-transgenic (Tg) models and altered peptide ligands support the concept that optimal responses occurred in the case highest-affinity interactions (73, 206). Yet, none of these analyses have encompassed the full polyclonal repertoire, leaving the question on the contribution of lower- and higher–affinity T cells in the expanded T cell population unanswered.

To study the contribution of low- and high-affinity CD4 T cells to the primary immune response, the number of naïve and expanded total T cells must be determined.

Multiple groups have identified the presence of lower-affinity (Tet-) T cells but these cells are difficult to adequately quantitate at any point during the immune response (16, 18, 118). To accomplish this task we repurposed the Nur77^{gfp} TCR signaling reporter as a method for identifying lower-affinity, Tet- antigen-specific CD4 T cells. To define the number of precursor T cells we used the Nur77^{gfp} reporter in an *in vivo* limiting dilution assay (LDA), finding Tet- CD4 T cells made up the majority of the naïve antigen-specific T cell population. Upon expansion, the ratio of high- to low-affinity antigen-specific CD4 T cells was significantly reduced, signifying high-affinity TCRs did not confer a clonal expansion advantage. As well, comparison of the total naïve precursor numbers to expanded CD4 T cells found a significant positive correlation, indicating total precursor number predicts expansion when the entire range of TCR affinity is analyzed. These data demonstrate T cell responses are population based with a range of naïve affinities that are maintained throughout an immune response to preserve affinity and diversity.

Results

Limiting dilution reveals greater number of tetramer negative than tetramer positive cells

The transfer of bulk CD4 T cells at the Tet+ limiting dilution level has proven fruitful in the study of single CD4 T cell expansion and differentiation (97, 207). However, polyclonal antigen-specific CD4 T cells with lower-affinity TCR:pMHCII interactions are not detected by traditional pMHCII tetramer staining used in these assays (17, 18, 70). Consequently, lower-affinity, antigen-specific CD4 T cells are missed in these single clonotype pMHCII tetramer based analyses. To better define the response inclusive of lower-affinity T cells, the TCR-specific signaling reporter Nur77 was used as a readout of antigen specificity (63, 65, 208). To determine the extent that lower-affinity

T cells participate in an immune response, we transferred T cells from Nur77^{gfp} mice at the levels reported to be limiting for Tet+ LCMV GP_{66-77}-specific CD4 T cells ($6x10^6$ CD4 Thy 1.2 T cells) into congenically distinct Thy1.1 recipients) (97). At day 7 post immune challenge with peptide antigen in CFA adjuvant (GP66/CFA) (Fig. 1A), GP66-Tet+ CD4 T cells were enriched and designated as donor (Thy1.2) or host (Thy1.1) derived based on their respective Thy1 expression (Fig. 1B). At this number of transferred T cells, four of the seven mice possessed a GP66-Tet+ donor clone, in close agreement with published results (97). To identify if these mice also contained lower affinity Tet- cells, the samples were depleted of GP66-Tet+ T cells by tetramer pulldown, and the remaining T cells (Fig. 1C) were stimulated in vitro for 18-24 hours with specific (GP_{61-81}) or non-specific peptide antigen ($Aasf_{24-32}$, MOG_{35-55}, $NP_{311-325}$) (Fig. 1A). To assess antigen-specificity, the nuclear receptor Nur77 was used as its expression has been shown to be TCR signaling strength dependent (208). Based on Nur77 expression, six of the seven transferred Tet- CD4 T cell populations stimulated with GP66 demonstrated Nur77/CD69 expression with a greater than 3 standard deviation increase above the mean of the non-specific controls Nur77/CD69 expression (Fig. 1C,D). There was a low-level background of Nur77 expression that was priming antigen independent (Fig. 1D), but the normalized percent increase of Nur77/CD69 expression for the GP66 stimulated samples caused the greatest increase. These findings show lower-affinity, Tet- populations are present at least as frequent as Tet+ cells, as demonstrated by similar number of mice with antigen-specific populations (4/7 mice for Tet+, 6/7 mice for Tet-).

Proliferation and expansion is a functional property of antigen-specific responding T cell populations, but it does not describe the role of these low- and high-

affinity T cells in the immune response. Using tetramer and Nur77 as our readout of affinity and antigen specificity, we measured the expression of Bcl-6, the lineage defining transcription factor for follicular helper T cells (T_{FH}) in high- and low-affinity antigen-specific T cells specific for MOG_{35-55} antigen. Previous reports have shown T_{FH} cells can arise from both high- and lower-affinity TCR interactions, allowing for both of these cell types to be studied for T_H differentiation(98). Antigen-specific T cells showed expression of Bcl-6 regardless of whether they were Tet+ or Tet-, although a greater frequency of higher-affinity, Tet+ T cells expressed Bcl-6 compared to lower-affinity, Tet- antigen-specific T cells (Fig. 1E). Antigen-inexperienced (CD44-) T cells and antigen-experienced but not antigen-specific (CD44+Nur77-) T cells demonstrated little to no expression of Bcl-6 (Fig. 1E). Our data support the findings that T_{FH} differentiation can occur for TCRs with a range of affinities (28, 98). As well, the data show that high- and low-affinity T cells have shared but distinct functions in the total T cell population.

Tetramer negative in vivo limiting dilutions reveals low-affinity T cell predominate in the naïve repertoire

Although the above data identified Tet- CD4 T cells during an immune response, it did not quantitate the initial precursor number of these lower-affinity T cells. We next set out to enumerate the precursor frequency of naïve antigen-specific CD4 T cells independent of pMHCII tetramer by using the Nur77 reporter in an *in vivo* LDA (209). Varying numbers of CD4 T cells from $Nur77^{gfp}$ mice were transferred into T cell deficient $TCR\alpha^{-/-}$ mice and recipients were immunized with peptides emulsified in CFA (Fig. 2A). Lymphopenic hosts were used as this allowed for larger blast sizes for individual T cell clones, thereby increasing the sensitivity of the assay as it is dependent

upon population increases in expression of Nur77. At 21 days post immunization, splenocytes from recipient mice were re-stimulated *ex vivo* for 18-24 hours with specific- or non-specific peptide antigens before assessment for $Nur77^{gfp}$ and CD69 expression (Fig. 2B). Representative flow plots of transferred CD4 T cells that demonstrated positive responses (top row, Fig. 2B) and negative responses (bottom row, Fig. 2B) are shown for $NP_{311-325}$ primed mice. $NP_{311-325}$ stimulated samples containing a $Nur77^{gfp+}CD69^{+}$ population greater than three standard deviations above the mean of two non-specific peptides (GP_{61-81} non-specific peptide control shown) were tabulated as positive and graphed as a function of the number of CD4 T cells present in the hosts after transfer (Fig. 2C). The points at which 37% of the hosts do not possess a clone equates to where a single precursor cells is present in the population (dotted line, Fig. 2C) and is based on a 20% park rate into lymphopenic mice with a total of 4×10^7 CD4 T cells per mouse. The precursor frequencies were calculated for six different epitopes with included 95% confidence levels (MOG_{35-55} self antigen: 1099 (669-1805) cells, MTB $85b_{280-294}$: 1206 (682-2133) cells, LCMV GP_{61-81}: 627 (322-1218) cells, Chlamydia $Aasf_{24-32}$: 350 (169-725) cells, Influenza $NP_{311-325}$: 285 (179-454) cells, and Salmonella $FliC_{427-441}$: 192 (92-402) cells) which were chosen as they spanned the range of previously published tetramer precursor frequencies (Fig. 2D) (27). Comparison of the LDA and naïve tetramer enrichments revealed Tet+ numbers accounted for 5-30% of the total naïve antigen-specific repertoire, demonstrating tetramer only identifies a minor subset of each antigen-specific T cells in a naïve population. Control LDA experiments were performed for $NP_{311-325}$ antigen in WT mice, finding similar results as in $TCR\alpha^{-/-}$ mice (Fig. 2E,F, gating strategy Fig. S1). These findings demonstrate Tet- T cells are present in the naïve

T cell repertoire at greater frequencies than Tet+ CD4 T cells and proliferated in an antigen-specific manner that could be read out by the Nur77 assay.

Lower-affinity T cell clonotypes are identified in the LDA

To confirm the Nur77^{gfp+} CD4 T cells identified Tet- T cells, pMHCII tetramer was used to costain unstimulated LDA samples when calculating precursor numbers (Fig. 3A). Of the 34 mice receiving T cells for calculating the precursor numbers for $NP_{311-325}$, only one mouse possessed Tet+ T cells (Fig. 3A, left panel), while 20 mice possessed antigen specific Nur77^{gfp+} cells and the remaining 13 mice did not respond. Next, the micropipette adhesion frequency assay (MP) was used to determine the affinity of CD4 T cells from mice that were either positive or negative for antigen-specific Nur77 upregulation during LDA. CD4 T cells from LDA positive mice had a significantly greater adhesion frequency for the priming antigen $NP_{311-325}$ (left panel, Fig. 3B), than mice with no measurable antigen-specific Nur77 upregulation, allowing for the calculation of TCR:pMHCII affinity (middle panel, Fig. 3B). The affinity for influenza $NP_{311-325}$ was below that for which we previously reported was necessary for detection by MHC class II tetramers ($>10^{-4}$ μm^4) (right panel, Fig. 3B) (18, 210). When the affinity of T cells from five individual mice were assessed, mouse 2, 3, 4, and 5 displayed a range in affinity of <10-fold (Fig. 3B). TCR affinity ranges of 10-fold or less are characteristic of clonal T cell populations (8, 65, 70, 211), while polyclonal populations can possess a 1000 fold range in affinity (18, 212). Of note, mouse number 1 displayed a wider range of TCR affinity that appeared as distinct higher- and lower-affinity populations, suggesting the presence of two clones. This is consistent with the frequency of T cells ($1.2x10^6$ CD4 T cells transferred) for that animal being above the limiting dilution level

and the potential presence of more than one clone. A polyclonal assessment of TCR affinity for $NP_{311-325}$ was included (Fig. 3B), displaying the wider affinity range (>100-fold) observed in polyclonal responses and demonstrating a similar range to the single clones measured (Fig. 3B). Overall, the micropipette analysis defined the presence of antigen-specific T cells with affinities below the minimum required for tetramer staining, while suggesting their clonality and confirming the antigen specificity of the functional $Nur77^{gfp}$ LDA measurements.

To further demonstrate clonality of the LDA experiments, single-cell TCRβ sequencing was performed on $Nur77^{gfp}$ positive and negative populations from $NP_{311-325}$ LDA mice. All LDA positive mice were highly enriched for a single TCRβ clonotype (>70%) with no TCR sequences shared between the mice (shared sequences identified as same color in individual mice, Fig. 3C). The remaining sequences from each mouse correlated with the background GFP expression identified in all $Nur77^{gfp}$ animals. No TCRb chain predominated in mice lacking antigen-specific T cells clones as defined by LDA or amongst the $Nur77^{gfp-}$ T cells in a mouse with a positive clone identified by LDA (Fig. 3C). These data demonstrate the *in vivo* LDA with TCR repertoire analysis can identify and isolate single, lower-affinity T cell clones and provides an effective method for calculating the precursor number of Tet- CD4 T cells in the naïve repertoire.

Total T cell expansion is correlative with total naïve T cell numbers

As we estimated the total antigen-specific CD4 T cell for six epitopes in the naïve mouse and found them to outnumber Tet+ counterparts, we wanted to next determine the contribution of the low-affinity CD4 T cells upon immune expansion. Naïve Tet+ precursor frequency predicts the immunodominance of an antigen-specific T cell

population (27, 81), but these assays have not included Tet- CD4 T cells or even those antigens enriched for lower-affinity TCRs such as self antigens like MOG. Analysis of foreign antigen-specific Tet+ CD4 T cells after immunization with peptide in CFA confirmed the positive correlation between (r^2= 0.86, p= 0.008) precursor and expanded T cell numbers (different antigens represented by each point, dotted line, Fig. 4A, gating strategy Fig. S2). Yet, when MOG self-antigen specific CD4 T cells are included in the tetramer analysis (solid line, Fig. 4A) the r^2 value decreases to 0.46 with a p value of 0.1, indicating factors other than precursor frequency may contribute to Tet+ T cell expansion to self-antigens (157, 158). Next, MP analysis of T cells from mice immunized 14 days earlier with peptide/CFA showed a strong correlation with the naïve precursor frequency measured by LDA (Fig. 4B). When lower-affinity T cells measured by MP were included in the expanded T cell numbers, the naïve to expanded T cell correlation improves, even with the inclusion of CD4 T cells specific for MOG-self antigen (Fig. 4B). Further comparison of the precursor numbers from tetramer staining and LDA calculations revealed a significant correlation between the methods, suggesting tetramer can be used to roughly estimate the hierarchy within naive populations, though it still vastly underestimates naïve T cell numbers (Fig. 4C). Additionally, MP identifies ~10-150 fold greater numbers of expanded antigen-specific CD4 T cells than by tetramer, significantly altering our understanding of the extent of CD4 T cell expansion.

To determine how TCR:pMHCII affinity influences the expansion of T cells during the primary immune response, the ratio of Tet+ to Tet- T cells were compared for all epitopes in both naïve and immunized samples (Fig. 5A). No increase in the frequency of Tet+ T cells was found at the peak of expansion (day 14 after immunization),

signifying Tet+ T cells did not gain a competitive advantage over lower-affinity T cells. In fact, a significant reduction in the frequency of Tet+ CD4 T cells of the total expanding population was found for all antigens (Fig. 5A). This was not a function of the time point measured, as kinetic analysis of the MOG-specific repertoire revealed higher-affinity T cells contributed the most in naïve state, with significantly less involvement as the immune response progressed (Fig. 5B). The large contribution of lower-affinity CD4 T cells was also found in the $NP_{311-325}$-specific T cell population responding during influenza-x31 infection and NP311/CFA immunization (Fig. 5C). This demonstrates that low-affinity T cell recruitment does not only occur in response to CFA but is equally present during infection. Next, the fold expansion of antigen-specific populations (Tet+ and Tet-, each point is a unique antigen) was graphed separately as a function of precursor frequency (Fig. 5D), finding CD4 T cell populations with smaller precursor numbers exhibiting greater expansion. MOG was removed from the analysis for higher-affinity T cells due to its altered expansion due to tolerance. When the higher- (solid line) and lower-affinity (dotted line) populations were compared at the same precursor frequency, the lower-affinity T cells have the potential to expand to a greater number than the higher-affinity, Tet+ T cells (Fig. 5D). Interestingly, the slopes of the two lines generated are similar (Tet+: -0.47, Tet-: -0.42), signifying the two populations of cells compete within themselves comparably (Fig. 5D). Therefore, TCR:pMHCII affinity does not control the accumulation of CD4 T cells during the immune response, and instead immune activation selects for a diverse range of affinities during primary immune expansion.

Discussion

Precise quantification of T cell precursor numbers and expansion is essential for understanding the function of the adaptive immune system, vaccine design, and adoptive T cell therapeutics. Initially, T cell numbers were defined by *in vitro* limiting dilution analysis based on the frequency of functionally responsive cells (209). TCR-transgenic mice allowed for the study of the naïve frequency and expansion of monoclonal populations, but did not address the diversity present in a polyclonal immune response (213, 214). The advent of pMHC tetramer technology began to address the limitation of monoclonal analysis by providing improved assessment of precursor and expanded T cell numbers in more clonally diverse populations (14, 81). Key insight into the relationship between precursor numbers, expansion and cross-reactivity was provided with the use of the tetramers although tetramer based affinity and avidity interactions do not fully encompass polyclonal T cell responses, especially those enriched for lower-affinity interactions, i.e. ones specific for self-antigen (27, 158). Previous studies had identified these low-affinity, Tet- T cells, but have never developed a way to quantify, identify and phenotype these polyclonal T cells in their naïve or activated state (16, 118). Therefore, this work adds to these initial observations, allowing for the study of low-affinity, Tet- T cells in a polyclonal model, providing increased depth of understanding to CD4 T cell responses.

A major goal of this work was to quantify the precursor number of antigen-specific CD4 T cells inclusive of lower-affinity T cells missed by MHC class II tetramers. In calculating the total naïve T cell numbers, we chose to perform these experiments in T cell deficient mice. As the LDA is a digital response (cells are either present or absent), the lymphopenic environment increases the signal to noise ratio of the

assay by allowing for larger proliferation of the single clone being measured for Nur77 expression after restimulation. The lymphopenic environment has minimal impact on the competition dynamics between high- and low-affinity T cells as LDA calculations were similar between mice with (WT) and without (TCRα-/-) T cells. Therefore, we can conclude the lymphopenic environment has minimal impact on competition dynamics between high- and low-affinity T cells in the LDA calculations. This is in agreement with previous work as groups have suggested the initial precursor frequency of CD4 T cells is low enough to prevent competition between antigen-specific T cells (206). Once T cells have expanded, some infer that competition for resources could favor the dominance of individual clonotypes which many would presume relate to TCR affinity (91, 204). Instead for all polyclonal responses analyzed here, we find a distribution of TCRs where low-affinity CD4 T cells expand from their naïve numbers to remain more numerous in the immune repertoire.

Our data indicate TCR affinity does not predict the peak expansion of T cells in response to primary antigen exposure, though we do not know if affinity affects the efficiency of entry into the immune response. The correlation between affinity and expansion has been proposed before, but conflicting data exists. For example one could conclude that affinity does not correlate with expansion to antigen based on transgenic barcoding experiments(215, 216). In these experiments a single OT-I T cell can have a range of contribution to the expanded repertoire even though each T cell expressed the same clonal TCR(215, 216). As well, high- and low-affinity CD4 T cells show similar efficiency of proliferation in both *in vitro* and *in vivo* work (70, 205). On the other hand, the use of APLs or a fixed TCRβ chain transgenic has demonstrated the magnitude of

expansion and contribution to the total repertoire was correlative with TCR:pMHC affinity (20, 73). It is unclear what factors are different between these experiments, but potentially infection type, TCR-Tg T cell thymocyte development or competition with the endogenous repertoires may affect competition and expansion. Thymocyte development has been shown to play an important role in setting the basal activity T cells(74), but TCR-Tg T cells would not undergo these varied developmental consequences, thereby potentially altering an important negative regulatory loop in T cells with different affinities. Our data based on the polyclonal T cell response to 6 different antigens indicates that TCR affinity does not influence clonal expansion dominance.

The identification of low-affinity CD4 T cells always comes with questions about the functionality of this T cell subpopulation as it is hypothesized that low-affinity equates to sub-optimal and that the enumeration of Tet+ and functional responses leads to similar magnitudes (142, 217). However, these assumptions are not completely accurate. Transcription factor profiling of the CFA immune response has shown Tet+ cells have at most 20% T-bet+ (T_H1 lineage defining transcription factor) expression (27, 157). In contrast, experiments monitoring cytokine secretion by T cells in this same immune response have show IFN-γ ELISPOT data and Tet+ T cell number equate (27, 158). Therefore, Tet+ T-bet+ CD4 T cells cannot be the sole source of IFN-γ production in ELISPOT experiments. Likely, lower-affinity T cells are contributing to this pool of antigen-specific T cells identified by ELISPOT. Recent work using a pMHCII dodecamer (12 pMHCII arms instead of 4) supports this hypothesis as they found Tet-, but dodecamer+ T cells exhibited similar function to Tet+ T cells(218). The dodecamer reagent, while giving increased numbers as compared to tetramers, only showed 2-3x

greater identification of T cells, which is still an underestimation as compared to the 7-8x increase we find using Nur77 in the naïve repertoire and >10x increases found using the micropipette. Please note, that Nur77, like all functional responses, underestimates the numbers of CD4 T cells in an immune response as not every T cell can respond at a given time. For example, analysis of cloned TCRs in a retrogenic system found that several TCRs could cause autoimmune diabetes(65), but within each RG population, only a could upregulate Nur77 even though they all shared the same TCR. Therefore, induction of Nur77 expression, as readout by the reporter, is likely less sensitive than select cytokines or effector functions, but more work will needed to understand the interaction of TCR affinity, T cell signaling thresholds and their correlation with effector function.

Since polyclonal TCR affinities during the CD4 T cell response are maintained from the naïve state, this diversity most likely serves a functional purpose, as biological systems are seldom wasteful. In T cell immunotherapeutics, some TCRs have been engineered for higher-affinity pMHC interactions with the belief that the highest-affinity TCR would generate the most efficacious immunodominant response (6). Of interest, the selection of engineered higher-affinity TCRs has been both successful and disastrous in patients with outcomes that have included death (219, 220). This points to a need for further understanding of what is an optimal affinity range for effective immunity, with recent data showing greater function of TCRs with intermediate affinity (205). Instead of a single unusually high-affinity TCR, a range of affinities might prove more advantageous. Our data demonstrates that population diversity is a property of the immune response and that mechanisms maintain a diverse affinity range of CD4 T cells. For example, population diversity of antigen responsive T cells can be seen in the

production and use of IL-2. While only a subset of T cells produce IL-2, both high- and low-affinity T cells may use this key growth cytokine (98, 221, 222). A counterpoint to the concept of favoring higher-affinity T cells are the findings that lower-affinity T cells possess preferred differentiation patterns, with these T cells more likely to acquire T_H2, T_{FH} or T_{CM} phenotypes (93, 98, 100, 142, 217). As well, data has shown that initial induction of peripherally derived regulatory T cells (pTregs) can arise from lower-affinity TCR:pMHCII interactions(223, 224). By understanding the population characteristics of lower-and higher-affinity CD4 T cells together, unique immune treatments may be developed with targeted characteristics.

Inclusion of lower-affinity TCRs in immune repertoires leads to a large increase in the numbers of CD4 T cells specific for a single epitope, altering our understanding of TCR cross-reactivity. TCR cross-reactivity, defined as a single αβ TCR binding to multiple pMHC, has been shown to be necessary for complete immune protection against pathogens as there are a greater number of potential epitopes (20^9~ 5.12 x 10^{11}) than estimated mouse αβ TCR clonotypes (2 x 10^6) (3, 225). Our findings of increased CD4 T cells specific for a single antigen increases the theoretical amount of TCR cross-reactivity required for complete immune protection by 8 fold (3). Due to the increase in cross-reactivity, the amount of T cells needed to protect an entire mouse, termed the protecton, may be similarly decreased due to the increased number of T cells for a single antigen (200). Future work will need to clarify how affinity impacts cross-reactivity or if there is any correlation at all.

In conclusion, we find the expansion of naïve CD4 T cells in the primary immune response is independent of TCR:pMHCII affinity while also quantitating the total number

of CD4 T cells in an immune response. Quantitation of the total repertoire revealed that up to 90% of the CD4 T cells participating in the immune response are ignored by conventional analyses. It will be of interest to determine if secondary re-challenge alters the detection and affinity diversity generated by this initial T cell expansion. Since lower-affinity CD4 T cells have been shown to have similar roles as higher-affinity T cells (97, 98), the sole use of pMHCII tetramers underestimate the diversity and richness of the immune system by not monitoring these lower-affinity cells. The expansion and continual presence of these T cells likely highlight the need of affinity diversity for maintenance of a healthy immune system and limiting microbial immune evasion (226–228). Future studies are needed to fully understand how low-affinity T cells may impact human immune health as we predict to see similar total numbers of antigen-specific T cells in mice and humans given that they possess similar repertoire diversity and specificity (3, 229).

Methods

Mice

Six to eight week old WT mice were purchased from the National Cancer Institute, while MOG KO mice (166) were a gift from Hugh Reid and were bred on site. Thy1.1, Nur77^{gfp} and TCR$\alpha^{-/-}$ mice were purchased from Jackson Laboratories and were bred on site. WT mice immunized with MOG_{35-55} were monitored for weight loss due to EAE and were sacrificed if weights fell below 20% of initial starting weight. All animals were housed in an Emory University Department of Animal Resources facility (Atlanta, GA) and used in accordance with an Institutional Animal Care and Use Committee–approved protocol.

Peptide Priming

$MOG_{35–55}$ (MEVGWYRSPFSRVVHLYRNGK), $85b_{280-294}$ (FQDAYNAAGGHNAVF) GP_{61-81} (GLKGPDIYKGVYQFKSVEFD), $Aasf_{24-32}$ (VSSPAVQES), $NP_{311-325}$ (QVYSLIRPNENPAHK) and $FliC_{427-441}$ (VQNRFNSAITNLGNT) peptides were synthesized on a Prelude peptide synthesizer (Protein Technologies, Inc., Tuscon, AZ). For all peptide immunizations, 200μg of the peptide was emulsified in 375μg of Complete Freund's adjuvant (CFA) and injected subcutaneously into the flank of a mouse on days 0 and 7 (150μl total volume per injection). CFA was made in house by mixing 20ml of Incomplete Freund's Adjuvant (Becton Dickinson, Franklin Lakes, NJ) and 100mg of desiccated M.Tuberculosis H37 Ra (Becton Dickinson). On days 0 and 2, 300ng of pertussis toxin (Ptx, List Biological Labratories, Campbell CA) was injected intraperionteallly in all immunizations in order to compare both the self and foreign immune responses.

Tetramer Enrichments

Tetramers and monomers were provided by the National Institute of Allergy and Infectious Diseases Tetramer Core Facility at Emory University or were a generous gift of Marc Jenkins. Tetramer enrichment and staining was preformed as previously described (108). Briefly, mouse peripheral lymphoid organs (spleen and inguinal, para-aortic, brachial, axillary, cervical, mesenteric lymph nodes) were processed into a single cell suspension. Cells were then stained with the respective tetramer (PE- and/or APC-conjugated, 4μg/ml) for 60 min at room temperature, washed, stained with anti-PE or anti-APC magnetic microbeads (Miltenyi Biotec, Germany), and enriched on a magnetized LS column (Miltenyi Biotec). The bound and flow-through samples were

then sampled to determine population counts using AccuCheck microbeads (Invitrogen, Carlsbad, CA) and stained for analysis by flow cytometry. Antibodies used are show in Table S1. For intracellular staining, cells were treated with the Tonbo or eBioscience Fixation and Permiabilization kits as per the manufacturer protocol. Samples were collected on an LSR II (Becton Dickinson) and analyzed using FlowJo (Treestar, Ashland, OR).

CD4 T cell adoptive transfer

Splenocytes from naive mice were harvested and processed into a single cell suspension. CD4 T cells were purified following manufacturer instructions using the CD4 T cell negative isolation kit (Miltneyi Biotec). Purified CD4 T cells were analyzed by flow cytometry for purity and counted by flow cytometry using AccuCheck microbeads (Invitrogen). Purified CD4s were injected intravenously (IV) into recipient mice and immunized 24 hours later. Park rate at 24 hours was measured in WT and TCR$\alpha^{-/-}$, it to be ~10 and ~20%, respectively (*Data not shown*).

Nur77 analysis

For experiments comparing donor high- and low-affinity T cells in a WT mouse using tetramers, spleens and lymph nodes from recipient, immunized mice were harvested and processed into single cell suspensions. Tetramer enrichment was performed as described above. Bound samples were then analyzed by flow cytometry. For adoptive transfer limiting dilution experiments in WT mice, Thy1.2 enrichment was performed using anti-Thy1.2 antibody and anti-APC magnetic Microbeads (Miltenyi Biotec) following manufacturer protocol. For Nur77 analysis in WT mice FT samples were used and not enriched. For all cases, prepared samples were stimulated for 18-22

hours in quadruplicate with 10μg/ml of peptide (1 specific peptide, 3 non-specific peptides). Samples were then harvested and stained for analysis of donor (Thy1.2) CD4 T cell Nur77 upregulation by flow cytometry. For analysis of the frequency of Nur77 upregulation, non-specific background was averaged and subtracted from both specific and non-specific samples and then graphed. Discrimination of positive and negative clones for LDA was performed as described in the section on calculations with the values being reported as mean+/- 95% confidence intervals.

For experiments calculating naïve precursor frequency of low-affinity CD4 T cells, spleens from recipient TCR$\alpha^{-/-}$ mice were harvested and processed individually into single cell suspensions. 2-3 x 10^6 splenocytes from each mouse were plated in quadruplicate, with three samples stimulated with 100μg/ml of peptide for 18-22 hours and one sample remaining unstimulated. The unstimulated sample was used for pMHCII tetramer staining to detect higher-affinity CD4 T cells. Stimulated splenocytes were harvested, stained with antibodies shown and analyzed by flow cytometry as described above. Discrimination of positive and negative clones was performed as described in the section on calculations.

Nur77 functional measurement

Spleen and lymph nodes of previously immunized mice were processed into a single cell suspension and counted. Samples were split in half and both set of cells were stimulated with 10μg/ml of peptide at a concentration of 1x10^7 cells per ml in complete media (RPMI 1640, 10% (v/v) FCS**,** 2mM L-glutatmine, 0.05 mM 2-ME and 0.05mg/ml gentamicin sulfate) for 4 hours. One sample received MOG_{35-55} (antigen-specific), while the other received GP_{61-81} (non-specific). Samples were then harvested and tetramer

enrichment was performed as described above. Both bound and flow-through samples were then analyzed by flow cytometry.

TCRβ sequencing

Single cell *Tcrb VDJ* sequencing was performed as previously described(172). In preparation for sequencing, LDA experiments were performed for the $NP_{311-325}$ antigen in $TCR\alpha^{-/-}$ mice (See section on LDA). After restimulation and flow cytometry, the samples were analyzed to determine if they possessed a low-affinity T cell clone (see section on *Calculations*). Single CD4+ T cells from positive and negative LDA samples were then index-sorted by a FACS Aria II (Becton Dickinson) into a 96 well plate containing 2.5µl cDNA master mix (iScript cDNA Synthesis Kit, Bio-Rad). Column 12 of the 96-well plate did not receive cells, thereby acting as a negative control wells for each plate. After production of cDNA, nested *Tcrb VDJ* PCRs were performed on each sample and the negative control column was confirmed by gel electrophoresis. Samples were then sent to Beckman Coulter Genomics (Danvers, MA) for Sanger sequencing. Individual sequences were tabulated and parsed by in-house designed software and then analyzed by IMGT. Non-productive sequences were not analyzed.

TCR Affinity measurement

Spleens from immunized mice were removed on the noted days and processed into a single cell suspension. CD4 T cells were purified using the CD4 T cell positive selection kit (Miltenyi Biotec) as per manufacturer instructions. In parallel, CD4 T cells were counted by flow cytomtery using AccuCheck beads as described above. MP was then performed as previously described. Briefly, RBCs were isolated in accordance with the Institutional Review Board at Emory University and prepared as previously

described(8). RBCs coated with various concentrations of Biotin-X-NHS (EMD) were coated with 0.5 mg/ml streptavidin (Thermo Fisher Scientific, Waltham, MA), followed by 1–2 μg of pMHCII monomer. The pMHCII- coated RBCs were stained with anti-MHC class II PE antibody, and purified T cells were stained with anti-TCR PE antibody. The densities of I-A^b and TCR were calculated using BD QuantiBrite Beads (Becton Dickinson). The micropipette adhesion frequency assay was then preformed as previously described(8). In brief, a pMHC-coated RBC and T cell were placed on opposing micropipettes and brought into contact by micromanipulation for a controlled contact area (Ac) and time (t). The T cell was retracted at the end of the contact period, and the presence of adhesion (indicating TCR–pMHC binding) was observed by elongation of the RBC membrane. This TCR-RBC contact was repeated 25 times and the adhesion frequency (Pa) was calculated. The relative 2D affinity (AcKm) of each cell that had a Pa of greater than 10% was calculated using the Pa at equilibrium (where $t \rightarrow \infty$) using the following equation: $AcKa = -\ln[1-Pa(\infty)]/(mrml)$, where mr and ml reflect the receptor (TCR) and ligand (pMHC) densities, respectively. The total frequency of cells that bound to pMHCII-coated RBCs was tabulated and used for the calculation of antigen-specific CD4 T cell numbers below. Previous reports have shown that as few as 10 cells in a polyclonal population need to be ran to generate an average affinity for the population, while considerably fewer cells (estimated to be 5-7 cells) in a monoclonal repertoire need to be measured for an average affinity(142). For each antigen, the number of binders and cells ran is as follows (shown as binders/cells ran): WT MOG_{35-55} (33/95), KO MOG_{35-55} (27/80), GP_{61-81} (38/174), $FliC_{427-441}$ (11/154), $Aasf_{24-32}$ (11/165), $NP_{311-325}$ (17/249), $85b_{280-294}$ (32/208).

Influenza x31 infections

WT mice were infected intranasally (i.n.) with influenza A/HKx31 (H3N2) at 30,000 EID_{50} (50% egg infectious doses) as previously described(230). Spleens were harvested at day 10-post infection. Magnetic enrichment was performed using CD4 positive selection following manufacturer protocol (Miltenyi Biotec). Purified cells were then stained with 4μg/ml NP311:I-A^b PE tetramer or used in the MP assay to determine the number of antigen-specific cells.

Calculations

For $Nur77^{gfp}$ LDA experiments, all samples were stimulated with their immunized antigen (100μg/ml) and 2-3 other non-specific antigens (100μg/ml). The frequencies of $CD44^+Nur77^{gfp+}CD69^+$ CD4 T cells were tabulated from specific and non-specific antigen controls. Samples were determined to be positive if the frequency of $Nur77^{gfp+}CD69^+$ CD4 T cells in the antigen-specific sample was 3 standard deviations above the mean of the averaged non-specific controls. The number of antigen-specific T cells from the LDA curves was calculated using an online calculator from a previously described method and reported as mean +/- the 95% confidence interval (231).

To calculate the number of CD4 T cells specific for a given antigen by MP, the frequency of non-specific binders was determined by performing the MP assay on CD4 T cells from mice immunized with non-specific peptide in CFA (Fig. S3). These background-binding frequencies were subtracted from the frequencies generated in antigen-specific experiments and total numbers of antigen-specific CD4 T cells were calculated from previously generated absolute counts of CD4 T cells in the spleen.

Statistical Analysis

All data were analyzed using Prism (GraphPad, LaJolla, CA) Software.

Acknowledgments

This work was supported by NIH grant T32 AI007610, RO1 AI096879, RO1 AI110113, and F31 NS086130. Laurel Lawrence maintained the mice used in these experiments and the authors would like to thank the Evavold Lab, Marc Jenkins, Rustom Antia, Veronika Zarnitsyna and Emily Cartwright for helpful discussion. The authors have no conflicts of interest to disclose. RJM designed, performed and analyzed experiments and wrote manuscript. RA performed experiment and discussed findings. HAM performed experiments. BDE designed experiments, discussed findings and wrote manuscript.

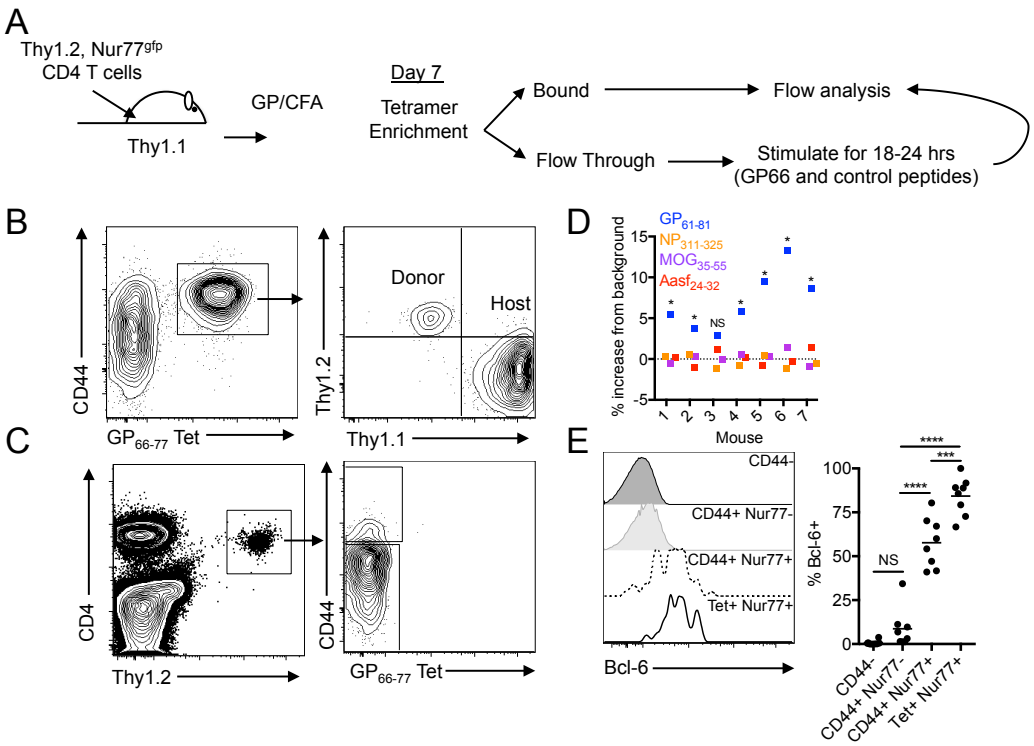
A
Thy1.2, Nur77gfp
CD4 T cells
Thy1.1
GP/CFA
Day 7
Tetramer
Enrichment
Bound
Flow analysis
Flow Through
Stimulate for 18-24 hrs
(GP66 and control peptides)
B
CD44
GP66-77 Tet
Thy1.2
Donor
Host
Thy1.1
C
CD4
Thy1.2
CD44
GP66-77 Tet
D
GP61-81
NP311-325
MOG35-55
Aasf24-32
% increase from background
NS
Mouse
E
CD44-
CD44+ Nur77-
CD44+ Nur77+
Tet+ Nur77+
Bcl-6
% Bcl-6+
NS
CD44-
CD44+ Nur77-
CD44+ Nur77+
Tet+ Nur77+

Fig. 1

Fig. 1. CD4 tetramer limiting dilution reveals low-affinity, antigen-specific CD4 T cells in the naïve repertoire. (**A**) $6x10^6$ $Nur77^{gfp}$ CD4 T cells ($6x10^5$ after a 10% park rate, Thy1.2) were transferred into congenically distinct (Thy1.1) mice and immunized with GP_{61-81} peptide/CFA followed by tetramer enrichment and restimulations. (**B**) Flow cytometry of representative GP66-Tet+ enrichment of secondary lymphoid organs from day 7 immunized mice with a positive donor (Thy1.2) clone identified. (**C**) After tetramer enrichment, the unbound cells were independently stimulated with 100μg/ml of specific (GP_{61-81}) or non-specific ($Aasf_{24-32}$, MOG_{35-55} or $NP_{311-325}$) peptides and gated to identify donor $CD44^+$ Tet- $Thy1.2^+$ CD4 T cells by flow cytometry. (**D**) Percent change over averaged background of $Nur77^{gfp+}CD69^+$ CD4 T cells after stimulation with individual antigens (n=7, two independent experiments, *= 3-Stdev above background average, NS=no significance). (**E)** Bcl-6 expression measured by flow cytometry of CD4 T cells from day 5 immunized mice within identified subsets. Frequency of cells expressing Bcl-6 within each subset identified (points represent individual mice, n=6-7, two experiments, NS=no significance, ***$p<0.001$,**** $p<0.0001$).

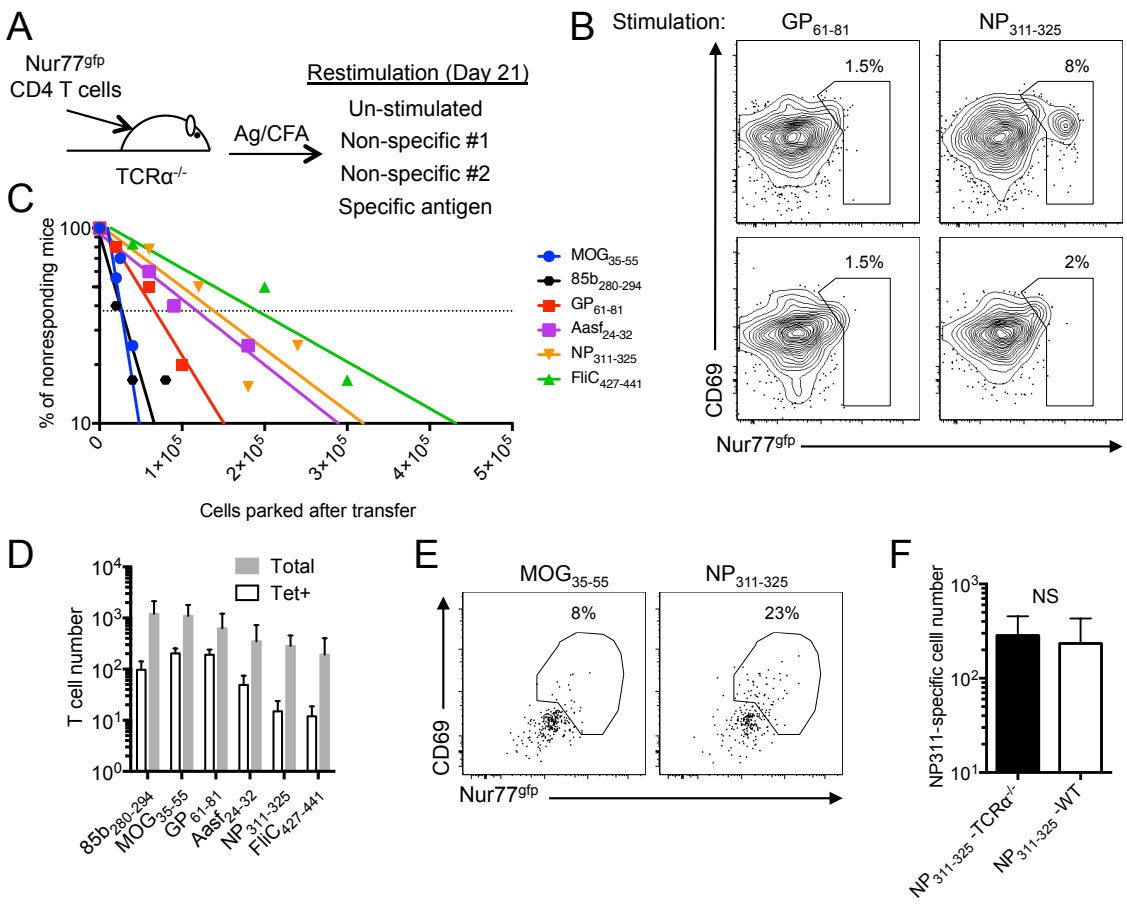
A
Nur77gfp
CD4 T cells
TCRα-/-
Ag/CFA
Restimulation (Day 21)
Un-stimulated
Non-specific #1
Non-specific #2
Specific antigen
B
Stimulation:
GP61-81
NP311-325
1.5%
8%
1.5%
2%
CD69
Nur77gfp
C
% of nonresponding mice
100
10
0
1×10^5
2×10^5
3×10^5
4×10^5
5×10^5
Cells parked after transfer
MOG35-55
85b280-294
GP61-81
Aasf24-32
NP311-325
FliC427-441
D
T cell number
Total
Tet+
85b280-294
MOG35-55
GP 61-81
Aasf24-32
NP311-325
FliC427-441
E
MOG35-55
NP311-325
8%
23%
CD69
Nur77gfp
F
NP311-specific cell number
NS
NP311-325 -TCRα-/-
NP311-325 -WT

Fig. 2

Fig. 2. Increased number of antigen-specific naïve precursor identified using an *in vivo* limiting dilution assay. (**A**) Varied numbers of purified Nur77^{gfp} CD4 T cells were transferred into individual TCR$\alpha^{-/-}$ mice, immunized with peptide antigen in CFA and allowed to expand for 21 days before peptide rechallenge (**B**) Day 21 flow cytometry analysis of antigen-specificity on donor CD4 T cells after $NP_{311-325}$ immunization showing CD69/Nur77 expression after antigen rechallenge with either control (GP_{61-81}-left panel) or priming antigen ($NP_{311-325}$-right panel). $NP_{311-325}$ positive clone shown on top row with negative clone shown on bottom row. (**C**) Positive clones were identified when the antigen-specific upregulation of CD69/Nur77 were three standard deviations (SDs) above the background mean and were graphed as a function of initial cells transferred after accounting for a 20% park rate in lymphophenic mice (n= 4-12 mice per concentration per antigen). Dotted line represents 37% mark of nonresponding mice. (**D**) Tabulated pMHCII tetramer and Nur77 LDA calculated naïve CD4 T cells number for a single antigen, represented as mean +/- 95% confidence interval. FliC and Aasf Tet+ values are taken from previously published work (Marc Jenkins, personal communication, Nelson et al., 2014). (**E**) Limiting dilution experiments in WT mice after immunization with $NP_{311-325}$/CFA, with flow cytometry plots showing CD69 and Nur77 expression for background (MOG_{35-55}) or antigen-specific stimulation ($NP_{311-325}$) (Representative sample). (**F**) Enumeration of naïve LDA for $NP_{311-325}$-specific T cells in TCR$\alpha^{-/-}$ or WT mice (four independent experiments, 3-4 T cell dilutions per experiment from 4 independent experiments, data represented as mean +/- 95% confidence level, NS=no significance).

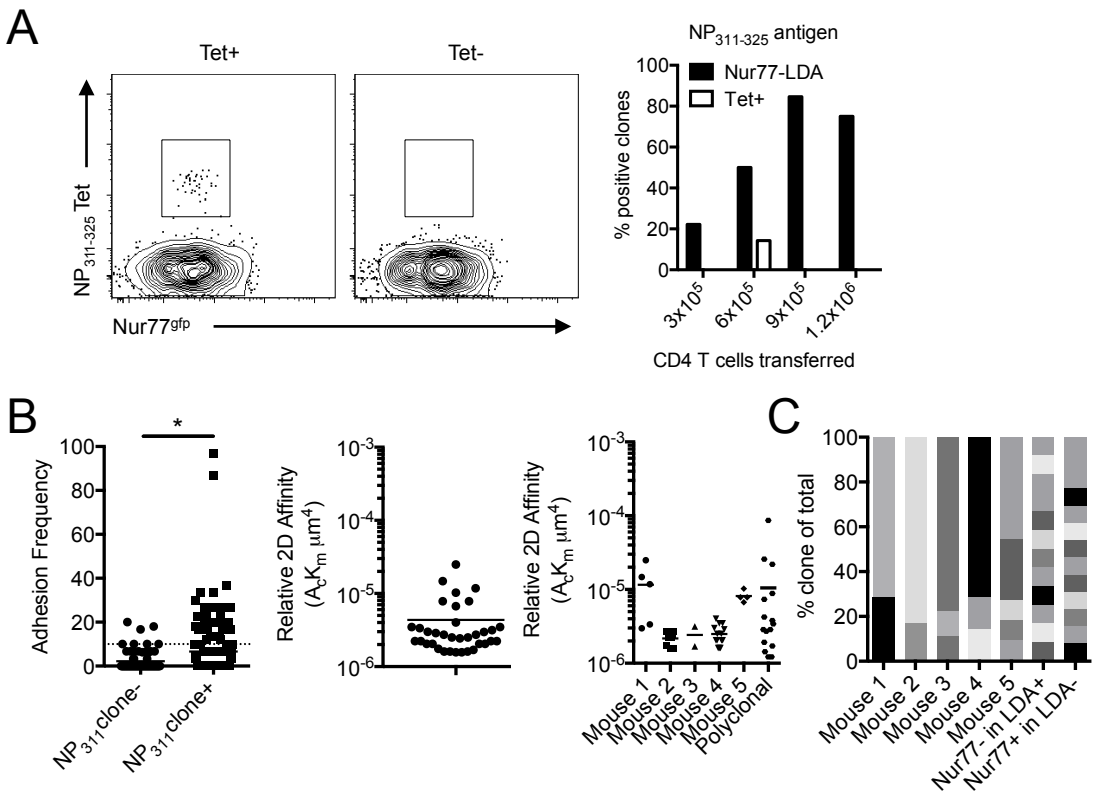
A
Tet+
Tet-
NP311-325 Tet
Nur77gfp
NP311-325 antigen
Nur77-LDA
Tet+
% positive clones
3x10^5
6x10^5
9x10^5
1.2x10^6
CD4 T cells transferred
B
Adhesion Frequency
NP 311clone-
NP 311clone+
Relative 2D Affinity (AcKm µm4)
Mouse 1
Mouse 2
Mouse 3
Mouse 4
Mouse 5
Polyclonal
C
% clone of total
Nur77- in LDA+
Nur77+ in LDA-

Fig. 3

Fig. 3 . *In vivo* limiting dilution assay identifies single, low-affinity T cell clones. (**A**) Representative $NP_{311-325}$ Tet staining in $TCR\alpha^{-/-}$ LDA mice with both a Tet+ positive (left) and negative (right), with only 1 out of 34 mice possessing a Tet+ positive clone. (**B**) MP on single CD4 T cells isolated from positive and negative LDA mice as identified by CD69/Nur77 (data combined from 2 independent experiments, n=2-3 mice, Student's T-test, **p*=0.0073). MP affinities on individual positive LDA clones following $NP_{311-325}$/CFA immunization along with a separate analysis of the polyclonal repertoire (single points represent individual cells). (**C**) Single cell TCRβ sequencing from LDA positive and control mice. Individual colors represent unique TCRβ CDR3 sequences, with each column representing a single mouse.

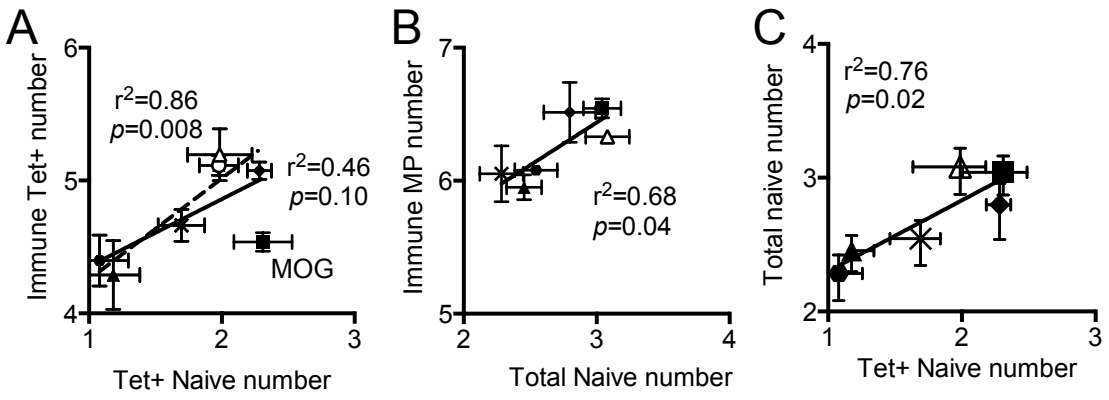
A
Immune Tet+ number
r2=0.86
p=0.008
r2=0.46
p=0.10
MOG
Tet+ Naive number
B
Immune MP number
r2=0.68
p=0.04
Total Naive number
C
Total naive number
r2=0.76
p=0.02
Tet+ Naive number

Fig. 4

Fig. 4. Total precursor numbers predict expansion of CD4 T cells independent of self or foreign antigen specificity. Each point is a unique antigen-specific population: MOG_{38-49} (n), GP_{66-77} (u), $Aasf_{24-32}$ (X), $FliC_{427-442}$ (⬣), $NP_{311-325}$ (▲), $85b_{280-294}$ (Δ), MOG_{38-49} from MOG KO (¢). (**A**) Number of naïve Tet+ CD4 T cells (log transformed) compared with Tet+ CD4 T cells 14 days after immunization (log transformed) (n=5-6 mice per group, data represented as mean+/-SEM). (**B**) Number of antigen-specific CD4 T cells (log transformed) identified by MP after immunization correlated with previously calculated precursor numbers (log transformed) (expanded data: twelve experiments, 2-3 mice per point, data represented as mean+/-SEM). (**C**) Correlation of the number of naïve T cells (both log transformed) as identified by tetramer and LDA (Data represented as mean+/-SEM).

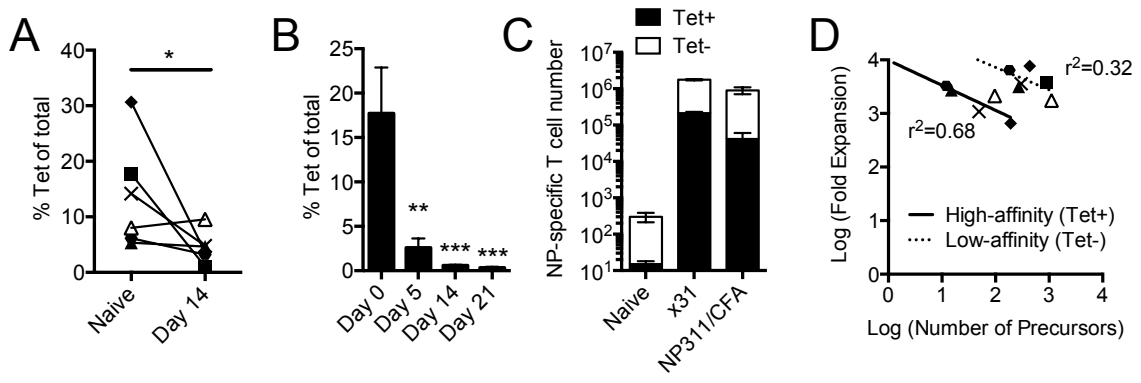
A
% Tet of total
40
30
20
10
0
*
Naive
Day 14
B
% Tet of total
25
20
15
10
5
0
**
***
***
Day 0
Day 5
Day 14
Day 21
C
NP-specific T cell number
Tet+
Tet-
Naive
x31
NP311/CFA
D
Log (Fold Expansion)
Log (Number of Precursors)
r2=0.32
r2=0.68
High-affinity (Tet+)
Low-affinity (Tet-)

Fig. 5

Fig. 5. Low-affinity T cells predominate CD4 T cell immune responses. (**A**) Frequency of Tet+ CD4 T cells in the naïve and day 14 immunized repertoires (data shown as mean frequency for each antigen, Paired Student's T-test, *p<0.05). (**B**) Frequency of MOG-Tet+ cells in the total MP+ T cells during the immune response to $MOG_{35—55}$/CFA immunization (Data shown as mean+/-SEM, One-way ANOVA, **p<0.01, ***p<0.001 with day 0 as a reference value). (**C)** Enumeration of Tet+ and Tet- NP311-specific CD4 T cell contribution from either naïve, day 10 post x31 influenza infection, or NP311/CFA immunizations (naïve data taken from Fig. 4A, expanded data contain 4 independent experiments, with 2 mice each, data represented as mean+/-SEM). (**D**) Plot of precursor number (log transformed) vs fold expansion (log transformed) of high- and low-affinity T cells as identified by tetramer, LDA and MP.

Supplemental Figures:

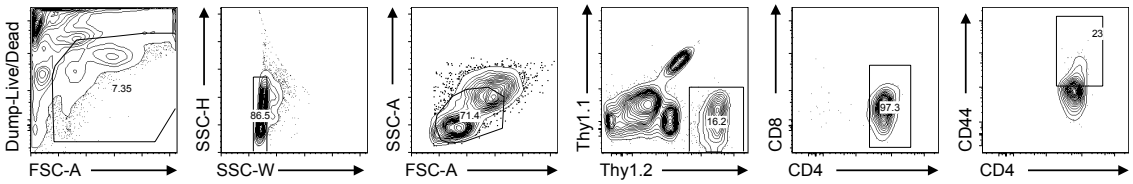

Fig. S1. Identification of antigen-specific donor cells in WT LDA.

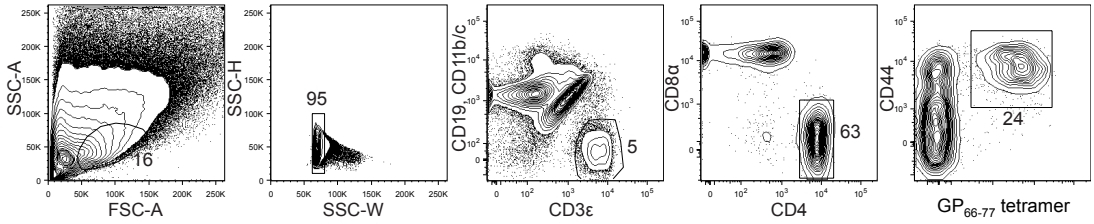

Fig. S2. Identification of antigen-specific CD4 T cells by tetramer.

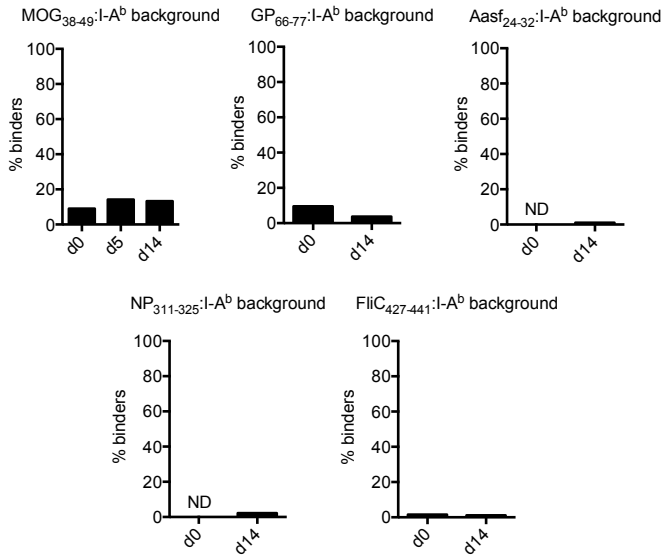

Fig. S3. MP background calculation.

Chapter 4

Discussion

Two main themes run throughout this thesis work. First, the size of the thymocyte-selecting niche contributes to the generation of a normal immune repertoire. The selecting niche controls population frequency and functionality, for both effector and regulatory antigen-specific populations. Second, TCR:pMHCII affinity controls many functions of the T cell-mediated immune response, but the signal that TCR generates can be impacted by factors other than affinity alone.

Thymocyte development is critically dependent on the expression of thymic antigens (78). For CD8 T cells, replacement of a subunit of the thymoproteasome with a component of the proteasome found in the periphery results in severe alteration of the CD8 repertoire (66, 187). It is unclear how the switching of subunits alters the peptide production, but the CD8 T cells are fundamentally altered in their ability to respond to antigen, becoming more self reactive, and have altered CD8 T cell numbers (66). It is hypothesized that CD8 T cells need to see two distinct peptides for development and survival/activation (78). This idea is fully consistent with our findings, as we show both CD4 effectors and regulatory T cells possess the ability to distinguish the selecting and priming ligand. However, it is unclear how T cells perform this task.

For CD4 T cells, alterations in the peptide producing machinery have not been successful at changing the repertoire. Instead, groups have used single peptide selection systems, or the H2-DM KO mouse to understand how changing selecting ligands alters the immune repertoire (86, 232). As expected, these results have shown that the repertoire is altered when only one peptide is present. In the NOD model, alterations in the positive

selection niche are hypothesized to generate a more autoreactive CD4 T cell repertoire (85). Changes in Erk activity found in the NOD background lead to the generation of less γδ and more αβ T cells, thereby oversaturating the positive selecting niche environment. This increase in precursors, with no alterations in peptide availability, leads to a competitive niche environment. In the environment where T cells need selection signals to survive, only those thymocytes with competitive TCRs can mature. This most likely means higher-affinity TCR interactions are enriched, though it has never been measured. Alternatively, thymocytes with broadly cross-reactive TCRs would be enriched and have the increased ability to cause autoimmunity. Modeling performed for human CD8 TCR:MHCI interactions has suggested that TCRs selected on a smaller peptide repertoire are higher-affinity and more likely to control infections (233). The group suggested reduced negative selection of these TCRs was the culprit of increasing the TCR reactivity, though our and the NOD data suggest reduction in the positive selection niche may also be contributing. Regardless of which selection mechanism is responsible, the T cells produced in a more competitive environment are overall more reactive to self-antigens and are more likely to cause autoimmune disease.

For regulatory T cells (Tregs), the role of positive selection and how it affects functionality is better understood (77, 234, 235). Tregs are in the group of T cells that are agonist selected, along with iNKT, IEL, and natural T_H17 T cells (77). High-avidity interactions drive the formation of Tregs, with the higher-avidity receptor thought to give them greater functional suppressive capabilities (236–239). Groups have shown Tregs, as compared to effector T cells, express higher amounts of Nur77 during steady state, implying Tregs are receiving stronger signals through their TCRs (208, 240). Many

groups have suggested the suppressive ability of the Treg is highly linked to their higher-affinity TCR, as Tregs express molecules suggestive of constant, strong activation (236, 238, 241). Additionally, it is hypothesized that the higher-affinity TCR on Tregs would be able to outcompete effector T cells for pMHCII, thereby preventing effector activation (242). The validity of affinity and TCR competition will be discussed at a later time point. An extension of this idea is that the higher the affinity of the TCR is expressed by Tregs, the better suppressors they will be. However, this is not the case. Foxp3 CNS3 KO Tregs were found to be made from higher-avidity TCRs, as readout by Nur77, but these higher-avditiy Tregs are much worse suppressors than Tregs with CNS3 (240). As well, we have shown Treg affinity does not directly correlate with function (*Chapter 2)*. Instead we find Tregs can distinguish their selecting antigen and activating antigen and better suppress upon exposure to their selecting antigen. This is similar to the way that CD8 T cells can distinguish their selecting and activating ligands, signifying that some conserved mechanism may exist across all T cells.

From the findings in CD4 and CD8 T cell development, the important role of the thymocyte-selecting niche is clear. For optimal repertoire generation, you must control the input thymocyte numbers as well as the factors needed for their survival (i.e. cytokine or ligand density). Yet, how does a T cell differentiate between selecting ligand and agonist ligand? Several mechanisms likely exist and can be separated by alterations to internal signaling machinery or to the TCR/CD3 complex. TCR signaling has been shown to discriminate different signals generated by TCR:pMHC interactions. One such mechanism has been proposed for binding partners Themis and SHP1 (61, 137, 141). Themis and SHP1 are implicated in generating a negative feedback loop to create a

digital output during varied TCR signaling generated by differences in TCR:pMHCII affinity (54, *Chapter 1*). Loss of Themis or SHP1 leads to the negative selection of thymocytes that should be normally positively selected. Alterations in other molecules such as Tec kinases can also lead to changes in the repertoire due to differences in their ability to signal (243).

Outside of signaling, changes to the TCR occur during thymocyte development that can alter their ability to signal. TCR density is reduced on thymocytes, with higher expression upon emigration into the periphery (*Unpublished data*). It is unclear if the alterations in density can affect signaling or if organization of the TCR changes but these changes in TCR density likely alter some function of thymocytes. Glycosylation of the TCR has also been shown to be important in distinguishing TCR signaling during selection (244). Another important regulator in TCR signaling is the composition of the lipid bilayer membrane. How can the membrane be affecting TCR function and signaling? One has to first think of the transmembrane receptors and the lipid membrane. Several hundred lipid species exist in the cellular membrane, with >30% of the human genome encoding for transmembrane genes. The possibility exists that the properties of the membranes lipids could alter the way TCRs function, are oriented or even clustered in the membrane. It was previously shown that cholesterol binds to TCRβ chain, with this interaction being necessary for TCR nanoclustering and binding to multivalent p-MHC complexes (245, 246). Recent evidence has demonstrated cholesterol has an even more important role than initially believed, serving as a negative allosteric regulator for TCR (247). Unbinding of the cholesterol:TCRβ complex allows for the CD3 complex to switch from a resting to a primed state with the enhanced ability to have its paired CD3ζ

chains phosphorylated (247). This work showed that the CD3 complex had to be in the primed state for TCR signaling to initiate, and without cholesterol dissociation, no signaling could occur. It is not clear if cholesterol binding to TCR is altered during thymocyte development, but it could be contributing to difference in TCR density and signaling discussed above.

Even though cholesterol has not been directly implicated in thymocyte development, the replacement of cholesterol with modified cholesterol sulfate has affects on the composition of the T cell repertoire (248). The replacement of cholesterol with cholesterol sulfate was found to alter the clustering of TCR on the surface of cells, causing reductions in the native CD3ζ phosphorylation and TCR signaling. It was found that two genes changing expression patterns during T cell development differentially regulated the incorporation of cholesterol sulfate into the membrane of thymocytes. Altered expression of these enzymes leads to the absence of incorporation of cholesterol sulfate into thymocyte membranes, which led to increased negative selection. While addition of cholesterol sulfate led to reduced signaling and a reduction in positive selection. Overall, these data demonstrate the importance of the lipid bilayer in the regulation of TCR activation and signaling.

Below the lipid membrane, factors such as the actin cytoskeleton are also necessary for TCR signaling and consequently T cell repertoire generation (249, 250). The link between TCR signal strength and repertoire generation is critical, as these two processes are fundamental in the formation of a functional immune system. Actin is implicated in TCR signaling for its ability to generate cellular forces that are hypothesized to be important for full T cell activation (249). The TCR:pMHC force

interaction may be a very important step in the discrimination of individual pMHCs and the amplification of TCR activation. Previous results have shown that the application of force to the TCR can increase lifetimes of TCR:pMHCI bonds, thereby generating enhanced Ca^{2+} signaling in T cells (32). It is currently unknown if there are differences in how a single T cell responds to its selecting- or priming-ligand under force, but it could potentially be a way that T cells discriminate between these two ligands.

The next question is how does TCR affinity for pMHC fit into these ideas and processes? In the most simplified form, there are three parts of a TCR:pMHCII bond that are important for the generation of a functional response. There is bond formation, bond lifetime and bond rupture (32, 54, 251, 252). The likelihood of bond formation under equilibrium is the affinity of a TCR:pMHCII interaction, k_{off}/k_{on} (5, 8). It does not tell how long this bond will last, or the strength of the bond. Kinetic segregation models suggest the bonds with the longest lifetime would be the best, as time is an important variable and is needed to exclude phosphatases from the synapse space (54). Serial engagement models would suggest a faster k_{off} would generate better signals, as this would allow for rapid association and dissociation events (53). Lastly, conformational change models would suggest those TCR:pMHCII interactions with the longest bond lifetime may be able to generate the best signal. TCR affinity is involved with all these models, but would play different roles under each one.

TCR affinity has been linked to many functions of a T cell, with most immunologists believing higher-affinity TCR interactions equates to a better T cell response. This idea likely arose from models of B cell affinity maturation as well as models of TCR:pMHC interactions with APLs. During the immune response, B cells undergo somatic

hypermutation in a germinal center reaction to increase the affinity of the Ig receptor (253). This process is believed to be random, with the majority of the Ig rearrangements resulting in failure and death of the cell progeny. Cells that rearrange higher affinity Ig receptors end up leaving the germinal center to become plasma cells (253). Higher-affinity Ig is better at neutralizing and binding to antigens, thereby mediating enhanced protection. APL OT-I data has further supported the idea that higher-affinity equates to enhancement of a response (73, 93, 94). Groups have shown that for the OT-I CD8 TCR-Tg T cell, different affinity ligands equate to altered magnitudes and quality of responses. A paper by Zehn and colleagues (73) led to the conclusion that higher-affinity ligands for the OT-I TCR generate greater primary OT-I expansion as seen in the blood of *Listeria monocytogenes-APL* infected animals. However, several key points are not addressed in this work. First, the OT-I system is a single TCR recognizing different epitopes. It is known that different affinity TCRs undergo different naïve tolerance induction, thereby changing their ability to respond to cognate antigen (26, 74). These different tolerance mechanisms may potentially alter the basal activity of T cells with varied affinities and may dampen or enhance signaling by an individual TCR. A group has shown that for individual TCRs with different affinity but binding to the same antigen, little differences are seen in the primary immune response, in contrast to what is seen in the OT-I APL experiments (205). Second, the endogenous repertoire plays a role in the expansion of the OT-I T cells, as shown in their own supplemental data, but they do not show if there is differing contribution by different APLs (73). Finally, they also only shown this finding for *Listeria monocytogenes*, and do not try different antigen/adjuvant systems. From our own experiments, we find adjuvant can control the ratio of high-to-low affinity T cells in

an immune response (*Chapter 3*). Overall, these discussed factors led to the belief that higher-affinity T cells are better T cells, which is likely an oversimplification of the data. Instead, we propose that certain differentiation and functional outcomes are dependent upon TCR affinity, and that particular functions are more likely to arise from lower-affinity bonds, while others are more likely to occur following higher-affinity interactions. As well, all of these outcomes are probability based and almost any T cell can, most likely, take on various fates depending on the circumstances.

Other groups have suggested affinity controls the expansion and proliferation of activated T cells (27, 73). Proliferation is the culmination of multiple signaling pathways and extrinsic factors to cause sustained cellular replication. Lymphocytes are unique in the way they proliferate, as they undergo a preparatory phase where no cellular division occurs (104, 254). During this time (24-36 hours post stimulus), the lymphocyte is reprogramming its metabolic pathways to be ready for the intense metabolic stress of division (104, 255). After this reprogramming phase, lymphocytes can double every 6-8 hours. Lymphocyte proliferation will then be slowed and halted by numerous factors, such as lack of antigen, growth factors, shrinking niche size or end point differentiation (256, 257). The amount of proliferation a T cell undergoes has previously been suggested to be controlled by TCR affinity, as discussed above. But based on our data, we hypothesize that contribution of the T cells in an expanding repertoire is not controlled by TCR affinity. Several findings support this conclusion. First, single TCR-Tg T cells do not always expand to the same clone size (215, 216). Second, tracking of high- and low-affinity T cells, as defined by TCR-tetramer, show similar accumulation during the immune response, and do not change relative abundance during the primary expansion

(*Chapter 3*). Third, different affinity TCRs recognizing the same antigen do not accumulate proportionally to their affinity (205). Lastly, groups have shown that the timing of T cell activation is important in blast size, as cells that see antigen first are better responders (256). These data point towards factors other than TCR affinity controlling expansion and burst size. In thymocyte selection, mechanisms exist to normalize the TCR signal output from variable input (TCR affinity). This is controlled by a double negative feedback loop partially controlled by Themis and SHP-1 (54, *Chapter 1)*. Based on our data, we believe something similar is occurring during peripheral T cell activation. We hypothesize that at extremely low TCR affinities, there is little proliferation and the T cells are mostly ignorant to antigen (Figure 1). Once a certain threshold has been reached, TCR affinity has very little impact on the expansion capacity, that is, until it reaches exceptionally high-affinity interactions where death is much more likely to occur. Data comparing TCRs of different affinities responding to the same antigens show positive correlations between TCR strength and negative regulator expression (26, 74). These data could suggest that T cells are able to normalize their output signals (proliferation or function) so T cell population diversity can be maintained.

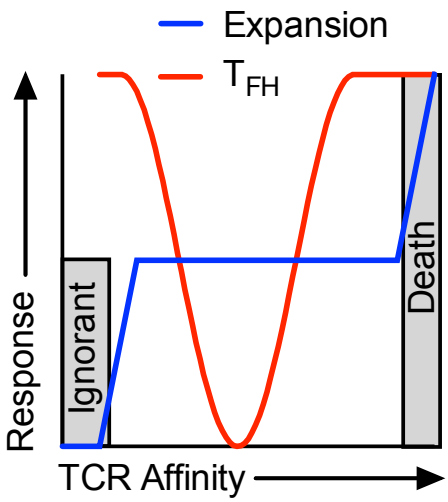

Figure 1. Model of T cell response as a function of TCR affinity. Both T cell expansion and T cell differentiation (T_{FH}) are shown in this model, suggesting one is dependent upon TCR affinity (T_{FH}), while expansion is independent of affinity.

Our data support the conclusion that TCR affinity does not control primary T cell expansion, but affinity still contributes to other factors during T cell activation and differentiation. We are not arguing that a certain affinity generates only one type of T cell, but that having a certain affinity gives the cells a higher probability of taking on a particular phenotype. Previous works have shown that TCR affinity hierarchy correlates with differentiation, as low to high affinity TCRs give a increased likelihood of $T_H2<T_H1<T_H17=T_{FH}$ differentiation (28, 97, 98, 100). T_{FH} cell differentiation is particularly interesting because groups have found these cells are more likely to arise from TCRs that are either highest or lowest-affinity (28, 97, 98). Huseby and colleagues suggests this is due to differences in the production and usage of IL-2, as IL-2 signaling inhibits T_{FH} production (98, 222). In lower-affinity T cells, less autocrine IL-2 is generated, thereby allowing upregulation of Bcl-6 and T_{FH} development. In higher-affinity T cells, IL-2 receptor signaling can be reduced, thereby allowing for Bcl-6 expression in this cell type. In the above Figure 1, we have added in the likelihood of T_{FH} development and how it relates to affinity of TCR interactions.

Along with T_H differentiation, affinity has also been suggested to affect memory T cell formation (93, 148). For CD8 T cells using an APL model, lower-affinity TCR:pMHCI interactions generate better memory T cells, while the higher-affinity TCRs go on to make a larger short-lived effector population (93). Though, as mentioned before, the APL models have many caveats. Recent work using single cell transfers of T cells have been instrumental in our understanding of how TCR characteristics instruct functionality (27, 97, 207). These models have led to arguments against any relationship between affinity and memory differentiation, as they showed all CD4 T cells during

immune activation could generate memory (207). However, this work did not comment or examine the differences in efficiency of the memory formation based on affinity. Just as for T_H cells, memory T differentiation is also likely to be probability based and on a spectrum, with some cells more likely to generate one type of subset of T cell over another. However, the endogenous repertoire and the properties of its TCRs have been ignored in these single cell analyses. It is known that antigen-specific T cell populations vary in their affinity, which is positively correlated with the number of their naïve precursors (27). This is possibly due to their ability to be negatively selected by cross-reactive self-antigens, with higher-affinity T cell populations being less cross-reactive, and therefore undergoing less negative selection (27). If this were true, one would predict that individual antigen-specific populations would possess unique abilities to differentiate to T cell memory subsets. We have found data to suggest this hypothesis is true, that diverse affinity populations have a variable likelihood to differentiate into memory T cells that is positively correlated with affinity (*Unpublished data*). Understanding that the endogenous repertoire is different between antigens suggests that the endogenous repertoire may also affect the single cells transferred differently as well, as has been seen for different TCR-Tg T cells (97). However, the differences seen in the differentiation of TCR-Tg T cells was attributed to the properties of the TCR, and not the endogenous population. We have shown that the transfer of the same TCR-Tg T cell into different hosts with unique T cell repertoires alter the differentiation of the T cells (*Unpublished data).* Understanding of the endogenous repertoire and the affinity of the antigen-specific repertoire will be essential going forward for designing immunotherapeutics.

Together, this work has shown that the TCR:pMHC affinity can contribute to a multitude of T cell functions and outcomes. However, intracellular signaling is equally important in discriminating high- and low-affinity signals. As suggested in previous paragraphs, I believe that TCR affinity gives the framework for how a single T cell will respond to antigen by increasing the probability for certain outcomes to occur. Along with the intrinsic events of the TCR on that single cell, extrinsic events (other T cells of the same antigen, adjuvants) can also influence the outcomes of the antigen-specific population. This plasticity in T cell differentiation is necessary for maintaining the diversity of the immune response and allowing for all effector functions to occur for any given response.

References

1. Maehle, A., C. Prüll, and R. F. Halliwell. 2002. The emergence of the drug receptor theory. *Nat. Rev. Drug Discov.* 1: 637–641.

2. Murphy, K., and C. Weaver. 2016. *Janeway's Immunobiology*, 9th ed.

3. Zarnitsyna, V. I., B. D. Evavold, L. N. Schoettle, J. N. Blattman, and R. Antia. 2013. Estimating the Diversity, Completeness, and Cross-Reactivity of the T Cell Repertoire. *Front. Immunol.* 4: 485.

4. Burnet, M. 1958. *The Clonal Selection Theory of Acquired Immunity*,.

5. Zhu, C., N. Jiang, J. Huang, V. I. Zarnitsyna, and B. D. Evavold. 2013. Insights from in situ analysis of TCR-pMHC recognition: response of an interaction network. *Immunol. Rev.* 251: 49–64.

6. Stone, J. D., and D. M. Kranz. 2013. Role of T cell receptor affinity in the efficacy and specificity of adoptive T cell therapies. *Front. Immunol.* 4: 1–16.

7. Kuo, S. C., and D. a Lauffenburger. 1993. Relationship between receptor/ligand binding affinity and adhesion strength. *Biophys. J.* 65: 2191–2200.

8. Huang, J., V. I. Zarnitsyna, B. Liu, L. J. Edwards, N. Jiang, B. D. Evavold, and C. Zhu. 2010. The kinetics of two-dimensional TCR and pMHC interactions determine T-cell responsiveness. *Nature* 464: 932–6.

9. Huppa, J. B., M. Axmann, M. A. Mörtelmaier, B. F. Lillemeier, E. W. Newell, M. Brameshuber, L. O. Klein, G. J. Schütz, and M. M. Davis. 2010. TCR-peptide-MHC interactions in situ show accelerated kinetics and increased affinity. *Nature* 463: 963–7.

10. Patching, S. G. 2014. Surface plasmon resonance spectroscopy for characterisation of membrane protein-ligand interactions and its potential for drug discovery. *Biochim. Biophys. Acta* 1838: 43–55.

11. Chesla, S. E., P. Selvaraj, and C. Zhu. 1998. Measuring two-dimensional receptor-ligand binding kinetics by micropipette. *Biophys. J.* 75: 1553–1572.

12. Liu, B., S. Zhong, K. Malecek, L. a. Johnson, S. a. Rosenberg, C. Zhu, and M. Krogsgaard. 2014. 2D TCR-pMHC-CD8 kinetics determines T-cell responses in a self-antigen-specific TCR system. *Eur. J. Immunol.* 44: 239–250.

13. Adams, J. J., S. Narayanan, B. Liu, M. E. Birnbaum, A. C. Kruse, N. a. Bowerman, W. Chen, A. M. Levin, J. M. Connolly, C. Zhu, D. M. Kranz, and K. C. Garcia. 2011. T cell receptor signaling is limited by docking geometry to peptide-major histocompatibility complex. *Immunity* 35: 681–693.

14. Altman, J. D., P. a Moss, P. J. Goulder, D. H. Barouch, M. G. McHeyzer-Williams, J. I. Bell, a J. McMichael, and M. M. Davis. 1996. Phenotypic analysis of antigen-specific T lymphocytes. *Science* 274: 94–96.

15. Hamad, A. R., S. M. O'Herrin, M. S. Lebowitz, A. Srikrishnan, J. Bieler, J. Schneck, and D. Pardoll. 1998. Potent T cell activation with dimeric peptide-major histocompatibility complex class II ligand: the role of CD4 coreceptor. *J. Exp. Med.* 188: 1633–1640.

16. Crawford, F., H. Kozono, J. White, P. Marrack, and J. Kappler. 1998. Detection of antigen-specific T cells with multivalent soluble class II MHC covalent peptide complexes. *Immunity* 8: 675–682.

17. Kersh, A. E., L. J. Edwards, and B. D. Evavold. 2014. Progression of Relapsing-Remitting Demyelinating Disease Does Not Require Increased TCR Affinity or Epitope Spread. *J. Immunol.* 193: 4429–4438.

18. Sabatino, J. J., J. Huang, C. Zhu, and B. D. Evavold. 2011. High prevalence of low affinity peptide-MHC II tetramer-negative effectors during polyclonal CD4+ T cell responses. *J. Exp. Med.* 208: 81–90.

19. Stone, J. D., M. N. Artyomov, A. S. Chervin, A. K. Chakraborty, H. N. Eisen, and D. M. Kranz. 2011. Interaction of streptavidin-based peptide-MHC oligomers (tetramers) with cell-surface TCRs. *J. Immunol.* 187: 6281–90.

20. Malherbe, L., C. Hausl, L. Teyton, and M. G. McHeyzer-Williams. 2004. Clonal selection of helper T cells is determined by an affinity threshold with no further skewing of TCR binding properties. *Immunity* 21: 669–679.

21. Kim, C., T. Wilson, K. F. Fischer, and M. A. Williams. 2013. Sustained interactions between T cell receptors and antigens promote the differentiation of CD4+ memory T cells. *Immunity* 39: 508–520.

22. Dougan, S. K., M. Dougan, J. Kim, J. a Turner, S. Ogata, H.-I. Cho, R. Jaenisch, E. Celis, and H. L. Ploegh. 2013. Transnuclear TRP1-specific CD8 T cells with high or low affinity TCRs show equivalent anti-tumor activity. *Cancer Immunol. Res.* 1: 99–111.

23. al-Ramadi, B. K., M. T. Jelonek, L. F. Boyd, D. H. Margulies, and a L. Bothwell. 1995. Lack of strict correlation of functional sensitization with the apparent affinity of MHC/peptide complexes for the TCR. *J. Immunol.* 155: 662–673.

24. Zhong, S., K. Malecek, L. a Johnson, Z. Yu, E. Vega-Saenz de Miera, F. Darvishian,

K. McGary, K. Huang, J. Boyer, E. Corse, Y. Shao, S. a Rosenberg, N. P. Restifo, I. Osman, and M. Krogsgaard. 2013. T-cell receptor affinity and avidity defines antitumor response and autoimmunity in T-cell immunotherapy. *Proc. Natl. Acad. Sci. U. S. A.* 110: 6973–8.

25. Derby, M. a, J. Wang, D. H. Margulies, and J. a Berzofsky. 2001. Two intermediate-avidity cytotoxic T lymphocyte clones with a disparity between functional avidity and MHC tetramer staining. *Int. Immunol.* 13: 817–824.

26. Mandl, J. N., J. P. Monteiro, N. Vrisekoop, and R. N. Germain. 2013. T cell-positive selection uses self-ligand binding strength to optimize repertoire recognition of foreign antigens. *Immunity* 38: 263–74.

27. Nelson, R. W., D. Beisang, N. J. Tubo, T. Dileepan, D. L. Wiesner, K. Nielsen, M. Wüthrich, B. S. Klein, D. I. Kotov, J. A. Spanier, B. T. Fife, J. J. Moon, and M. K. Jenkins. 2014. T cell receptor cross-reactivity between similar foreign and self peptides influences naïve cell population size and autoimmunity. *Immunity* 95–107.

28. Fazilleau, N., L. J. McHeyzer-Williams, H. Rosen, and M. G. McHeyzer-Williams. 2009. The function of follicular helper T cells is regulated by the strength of T cell antigen receptor binding. *Nat. Immunol.* 10: 375–84.

29. Puech, P. H., D. Nevoltris, P. Robert, L. Limozin, C. Boyer, and P. Bongrand. 2011. Force measurements of TCR/pMHC recognition at T cell surface. *PLoS One* 6.

30. Chervin, A. S., J. D. Stone, P. D. Holler, A. Bai, J. Chen, H. N. Eisen, and D. M. Kranz. 2009. The impact of TCR-binding properties and antigen presentation format on T cell responsiveness. *J. Immunol.* 183: 1166–78.

31. Kim, S. T., K. Takeuchi, Z. Y. J. Sun, M. Touma, C. E. Castro, A. Fahmy, M. J. Lang, G. Wagner, and E. L. Reinherz. 2009. The αβ T cell receptor is an anisotropic mechanosensor. *J. Biol. Chem.* 284: 31028–31037.

32. Liu, B., W. Chen, B. D. Evavold, and C. Zhu. 2014. Accumulation of dynamic catch bonds between TCR and agonist peptide-MHC triggers T cell signaling. *Cell* 157: 357–68.

33. Daniels, M. A., and S. C. Jameson. 2000. Critical role for CD8 in T cell receptor binding and activation by peptide/major histocompatibility complex multimers. *J. Exp. Med.* 191: 335–46.

34. Artyomov, M. N., M. Lis, S. Devadas, M. M. Davis, and A. K. Chakraborty. 2010. CD4 and CD8 binding to MHC molecules primarily acts to enhance Lck delivery. *Proc. Natl. Acad. Sci. U. S. A.* 107: 16916–16921.

35. Wooldridge, L., H. A. van den Berg, M. Glick, E. Gostick, B. Laugel, S. L. Hutchinson, A. Milicic, J. M. Brenchley, D. C. Douek, D. A. Price, and A. K. Sewell. 2005. Interaction between the CD8 coreceptor and major histocompatibility complex class I stabilizes T cell receptor-antigen complexes at the cell surface. *J. Biol. Chem.* 280: 27491–501.

36. Jiang, N., J. Huang, L. J. Edwards, B. Liu, Y. Zhang, C. D. Beal, B. D. Evavold, and C. Zhu. 2011. Two-Stage Cooperative T Cell Receptor-Peptide Major Histocompatibility Complex-CD8 Trimolecular Interactions Amplify Antigen Discrimination. *Immunity* 34: 13–23.

37. Garcia, K. C., C. A. Scott, A. Brunmark, F. R. Carbone, P. A. Peterson, I. A. Wilson,

and L. Teyton. 1996. CD8 enhances formation of stable T-cell receptor/MHC class I molecule complexes. *Nature* 384: 356–358.

38. Wyer, J. R., B. E. Willcox, G. F. Gao, U. C. Gerth, S. J. Davis, J. I. Bell, P. A. van der Merwe, and B. K. Jakobsen. 1999. T cell receptor and coreceptor CD8 alphaalpha bind peptide-MHC independently and with distinct kinetics. *Immunity* 10: 219–25.

39. Slifka, M. K., and J. L. Whitton. 2001. Functional avidity maturation of CD8(+) T cells without selection of higher affinity TCR. *Nat. Immunol.* 2: 711–717.

40. Holler, P. D., and D. M. Kranz. 2003. Quantitative Analysis of the Contribution of TCR/pepMHC Affinity and CD8 to T Cell Activation. *Immunity* 18: 255–264.

41. Laugel, B., H. A. van den Berg, E. Gostick, D. K. Cole, L. Wooldridge, J. Boulter, A. Milicic, D. A. Price, and A. K. Sewell. 2007. Different T Cell Receptor Affinity Thresholds and CD8 Coreceptor Dependence Govern Cytotoxic T Lymphocyte Activation and Tetramer Binding Properties. *J. Biol. Chem.* 282: 23799–23810.

42. Harding, S., P. Lipp, and D. R. Alexander. 2002. A therapeutic CD4 monoclonal antibody inhibits TCR-zeta chain phosphorylation, zeta-associated protein of 70-kDa Tyr319 phosphorylation, and TCR internalization in primary human T cells. *J. Immunol.* 169: 230–8.

43. Pullar, C. E., P. J. Morris, and K. J. Wood. 2003. Altered proximal T-cell receptor signalling events in mouse CD4+ T cells in the presence of anti-CD4 monoclonal antibodies: Evidence for reduced phosphorylation of Zap-70 and LAT. *Scand. J. Immunol.* 57: 333–341.

44. Kamperschroer, C., and D. G. Quinn. 1999. Quantification of epitope-specific MHC

class-II-restricted T cells following lymphocytic choriomeningitis virus infection. *Cell. Immunol.* 193: 134–146.

45. Harrington, L. E., R. Van Der Most, J. Lindsay, R. Ahmed, and J. L. Whitton. 2002. Recombinant Vaccinia Virus-Induced T-Cell Immunity : Quantitation of the Response to the Virus Vector and the Foreign Epitope Recombinant Vaccinia Virus-Induced T-Cell Immunity : Quantitation of the Response to the Virus Vector and the Foreign Epitope. *J. Virol.* 76: 3329–3337.

46. Varga, S. M., and R. M. Welsh. 1998. Detection of a high frequency of virus-specific CD4+ T cells during acute infection with lymphocytic choriomeningitis virus. *J. Immunol.* 161: 3215–3218.

47. Murali-Krishna, K., J. D. Altman, M. Suresh, D. J. D. Sourdive, A. J. Zajac, J. D. Miller, J. Slansky, and R. Ahmed. 1998. Counting antigen-specific CD8 T cells: A reevaluation of bystander activation during viral infection. *Immunity* 8: 177–187.

48. Williams, M. a., E. V. Ravkov, and M. J. Bevan. 2008. Rapid Culling of the CD4+ T Cell Repertoire in the Transition from Effector to Memory. *Immunity* 28: 533–545.

49. Martinez, R. J., N. Zhang, S. R. Thomas, S. L. Nandiwada, M. K. Jenkins, B. a Binstadt, and D. L. Mueller. 2012. Arthritogenic self-reactive CD4+ T cells acquire an FR4hiCD73hi anergic state in the presence of Foxp3+ regulatory T cells. *J. Immunol.* 188: 170–81.

50. McDermott, D. S., and S. M. Varga. 2011. Quantifying antigen-specific CD4 T cells during a viral infection: CD4 T cell responses are larger than we think. *J. Immunol.* 187: 5568–76.

51. Blanchfield, J. L., S. K. Shorter, and B. D. Evavold. 2013. Monitoring the Dynamics of T Cell Clonal Diversity Using Recombinant Peptide:MHC Technology. *Front. Immunol.* 4: 170.

52. Viola, A., and A. Lanzavecchia. 1996. T cell activation determined by T cell receptor number and tunable thresholds. *Science* 273: 104–106.

53. Valitutti, S., S. Müller, M. Cella, E. Padovan, and A. Lanzavecchia. 1995. Serial triggering of many T-cell receptors by a few peptide-MHC complexes. *Nature* 375: 148–151.

54. Davis, S. J., and P. A. van der Merwe. 2006. The kinetic-segregation model: TCR triggering and beyond. *Nat. Immunol.* 7: 803–809.

55. Anton van der Merwe, P., S. J. Davis, A. S. Shaw, and M. L. Dustin. 2000. Cytoskeletal polarization and redistribution of cell-surface molecules during T cell antigen recognition. *Semin. Immunol.* 12: 5–21.

56. Kalergis, a M., N. Boucheron, M. a Doucey, E. Palmieri, E. C. Goyarts, Z. Vegh, I. F. Luescher, and S. G. Nathenson. 2001. Efficient T cell activation requires an optimal dwell-time of interaction between the TCR and the pMHC complex. *Nat. Immunol.* 2: 229–234.

57. Sugawara, T., T. Moriguchi, E. Nishida, and Y. Takahama. 1998. Differential roles of ERK and p38 MAP kinase pathways in positive and negative selection of T lymphocytes. *Immunity* 9: 565–574.

58. Mariathasan, S., a. Zakarian, D. Bouchard, a. M. Michie, J. C. Zuniga-Pflucker, and P. S. Ohashi. 2001. Duration and Strength of Extracellular Signal-Regulated Kinase

Signals Are Altered During Positive Versus Negative Thymocyte Selection. *J. Immunol.* 167: 4966–4973.

59. Fischer, A. M., C. D. Katayama, G. Pagès, J. Pouysségur, and S. M. Hedrick. 2005. The role of Erk1 and Erk2 in multiple stages of T cell development. *Immunity* 23: 431–443.

60. McNeil, L. K., T. K. Starr, and K. a Hogquist. 2005. A requirement for sustained ERK signaling during thymocyte positive selection in vivo. *Proc. Natl. Acad. Sci. U. S. A.* 102: 13574–13579.

61. Fu, G., J. Casas, S. Rigaud, V. Rybakin, F. Lambolez, J. Brzostek, J. A. H. Hoerter, W. Paster, O. Acuto, H. Cheroutre, K. Sauer, and N. R. J. Gascoigne. 2013. Themis sets the signal threshold for positive and negative selection in T-cell development. *Nature* 504: 441–5.

62. Stepanek, O., A. S. Prabhakar, C. Osswald, C. G. King, A. Bulek, D. Naeher, M. Beaufils-Hugot, M. L. Abanto, V. Galati, B. Hausmann, R. Lang, D. K. Cole, E. S. Huseby, A. K. Sewell, A. K. Chakraborty, and E. Palmer. 2014. Coreceptor Scanning by the T Cell Receptor Provides a Mechanism for T Cell Tolerance. *Cell* 159: 333–345.

63. Stritesky, G. L., Y. Xing, J. R. Erickson, L. a Kalekar, X. Wang, D. L. Mueller, S. C. Jameson, and K. A. Hogquist. 2013. Murine thymic selection quantified using a unique method to capture deleted T cells. *Proc. Natl. Acad. Sci. U. S. A.* 110: 4679–84.

64. Fulton, R. B., S. E. Hamilton, Y. Xing, J. A. Best, A. W. Goldrath, K. A. Hogquist, and S. C. Jameson. 2014. The TCR's sensitivity to self peptide–MHC dictates the ability of naive CD8+ T cells to respond to foreign antigens. *Nat. Immunol.* 16: 107–117.

65. Bettini, M., L. Blanchfield, A. Castellaw, Q. Zhang, M. Nakayama, M. P. Smeltzer, H. Zhang, K. A. Hogquist, B. D. Evavold, and D. A. A. Vignali. 2014. TCR Affinity and Tolerance Mechanisms Converge To Shape T Cell Diabetogenic Potential. *J. Immunol.* 193: 571–579.

66. Xing, Y., S. C. Jameson, and K. a Hogquist. 2013. Thymoproteasome subunit-β5T generates peptide-MHC complexes specialized for positive selection. *Proc. Natl. Acad. Sci. U. S. A.* 110: 6979–84.

67. Persaud, S. P., C. R. Parker, W.-L. Lo, K. S. Weber, and P. M. Allen. 2014. Intrinsic CD4+ T cell sensitivity and response to a pathogen are set and sustained by avidity for thymic and peripheral complexes of self peptide and MHC. *Nat. Immunol.* 15: 266–74.

68. Hogquist, K. A., and S. C. Jameson. 2014. The self-obsession of T cells: how TCR signaling thresholds affect fate "decisions" and effector function. *Nat. Immunol.* 15: 815–823.

69. Brownlie, R. J., and R. Zamoyska. 2013. T cell receptor signalling networks: branched, diversified and bounded. *Nat. Rev. Immunol.* 13: 257–69.

70. Rosenthal, K. M., L. J. Edwards, J. J. Sabatino, J. D. Hood, H. A. Wasserman, C. Zhu, and B. D. Evavold. 2012. Low 2-dimensional CD4 T cell receptor affinity for myelin sets in motion delayed response kinetics. *PLoS One* 7: e32562.

71. Stefanová, I., B. Hemmer, M. Vergelli, R. Martin, W. E. Biddison, and R. N. Germain. 2003. TCR ligand discrimination is enforced by competing ERK positive and SHP-1 negative feedback pathways. *Nat. Immunol.* 4: 248–254.

72. Salmond, R. J., R. J. Brownlie, V. L. Morrison, and R. Zamoyska. 2014. The tyrosine

phosphatase PTPN22 discriminates weak self peptides from strong agonist TCR signals. *Nat. Immunol.* 15: 875–883.

73. Zehn, D., S. Y. Lee, and M. J. Bevan. 2009. Complete but curtailed T-cell response to very low-affinity antigen. *Nature* 458: 211–4.

74. Hebeisen, M., L. Baitsch, D. Presotto, P. Baumgaertner, P. Romero, O. Michielin, D. E. Speiser, and N. Rufer. 2013. SHP-1 phosphatase activity counteracts increased T cell receptor affinity. *J. Clin. Invest.* 123: 1044–1065.

75. Kumar, D., Y. Feng, R. J. Mallis, X. Li, D. B. Keskin, R. E. Hussey, S. K. Brady, J.-H. Wang, G. Wagner, E. L. Reinherz, and M. J. Lang. 2015. Force-dependent transition in the T-cell receptor β -subunit allosterically regulates peptide discrimination and pMHC bond lifetime. *Proc. Natl. Acad. Sci.* 112: 1517–1522.

76. Husson, J., K. Chemin, A. Bohineust, C. Hivroz, and N. Henry. 2011. Force generation upon T cell receptor engagement. *PLoS One* 6: e19680.

77. Stritesky, G. L., S. C. Jameson, and K. A. Hogquist. 2012. Selection of self-reactive T cells in the thymus. *Annu. Rev. Immunol.* 30: 95–114.

78. Klein, L., B. Kyewski, P. M. Allen, and K. A. Hogquist. 2014. Positive and negative selection of the T cell repertoire: what thymocytes see (and don't see). *Nat. Rev. Immunol.* 14: 377–91.

79. Jenkins, M. K., and J. J. Moon. 2012. The Role of Naive T Cell Precursor Frequency and Recruitment in Dictating Immune Response Magnitude. *J. Immunol.* 188: 4135–4140.

80. Chu, H. H., J. J. Moon, K. Takada, M. Pepper, J. A. Molitor, T. W. Schacker, K. A.

Hogquist, S. C. Jameson, and M. K. Jenkins. 2009. Positive selection optimizes the number and function of MHCII-restricted CD4+ T cell clones in the naive polyclonal repertoire. *Proc. Natl. Acad. Sci. U. S. A.* 106: 11241–5.

81. Moon, J. J., H. H. Chu, M. Pepper, S. J. McSorley, S. C. Jameson, R. M. Kedl, and M. K. Jenkins. 2007. Naive CD4(+) T cell frequency varies for different epitopes and predicts repertoire diversity and response magnitude. *Immunity* 27: 203–13.

82. Jenkins, M. K., H. H. Chu, J. B. McLachlan, and J. J. Moon. 2010. On the composition of the preimmune repertoire of T cells specific for Peptide-major histocompatibility complex ligands. *Annu. Rev. Immunol.* 28: 275–294.

83. Hogquist, K. A., S. C. Jameson, W. R. Heath, J. L. Howard, M. J. Bevan, and F. R. Carbone. 1994. T cell receptor antagonist peptides induce positive selection. *Cell* 76: 17–27.

84. Merkenschlager, M., C. Benoist, and D. Mathis. 1994. Evidence for a single-niche model of positive selection. *Proc. Natl. Acad. Sci. U. S. A.* 91: 11694–8.

85. Mingueneau, M., W. Jiang, M. Feuerer, D. Mathis, and C. Benoist. 2012. Thymic negative selection is functional in NOD mice. *J. Exp. Med.* 209: 623–37.

86. Ignatowicz, L., J. Kappler, and P. Marrack. 1996. The repertoire of T cells shaped by a single MHC/peptide ligand. *Cell* 84: 521–9.

87. Taniguchi, R. T., J. J. DeVoss, J. J. Moon, J. Sidney, a. Sette, M. K. Jenkins, and M. S. Anderson. 2012. Detection of an autoreactive T-cell population within the polyclonal repertoire that undergoes distinct autoimmune regulator (Aire)-mediated selection. *Proc. Natl. Acad. Sci.* 2–7.

88. Liston, A., S. Lesage, J. Wilson, L. Peltonen, and C. C. Goodnow. 2003. Aire regulates negative selection of organ-specific T cells. *Nat. Immunol.* 4: 350–4.

89. Yu, W., N. Jiang, P. J. R. Ebert, B. A. Kidd, S. Muller, P. J. Lund, J. Juang, K. Adachi, T. Tse, M. E. Birnbaum, E. W. Newell, D. M. Wilson, G. M. Grotenbreg, S. Valitutti, S. R. Quake, and M. M. Davis. 2015. Clonal Deletion Prunes but Does Not Eliminate Self-Specific alpha beta CD8+ T Lymphocytes. *Immunity* 42: 929–941.

90. Quiel, J., S. Caucheteux, A. Laurence, N. J. Singh, G. Bocharov, S. Z. Ben-Sasson, Z. Grossman, and W. E. Paul. 2011. Antigen-stimulated CD4 T-cell expansion is inversely and log-linearly related to precursor number. *Proc. Natl. Acad. Sci. U. S. A.* 108: 3312–3317.

91. Busch, D. H., and E. G. Pamer. 1999. T cell affinity maturation by selective expansion during infection. *J. Exp. Med.* 189: 701–710.

92. Zehn, D., and M. J. Bevan. 2006. T cells with low avidity for a tissue-restricted antigen routinely evade central and peripheral tolerance and cause autoimmunity. *Immunity* 25: 261–70.

93. Knudson, K. M., N. P. Goplen, C. A. Cunningham, M. A. Daniels, and E. Teixeiro. 2013. Low-Affinity T cells are programmed to maintain normal primary responses but are impaired in their recall to low-affinity ligands. *Cell Rep.* 4: 554–565.

94. King, C. G., S. Koehli, B. Hausmann, M. Schmaler, and E. Palmer. 2013. T Cell Affinity Regulates Asymmetric Division , Effector Cell Differentiation , and Tissue Pathology. *Immunity* 37: 709–720.

95. Vrisekoop, N., J. P. Monteiro, J. N. Mandl, and R. N. Germain. 2014. Revisiting

Thymic Positive Selection and the Mature T Cell Repertoire for Antigen. *Immunity* 41: 181–190.

96. Lee, H.-M., J. L. Bautista, J. Scott-Browne, J. F. Mohan, and C.-S. Hsieh. 2012. A broad range of self-reactivity drives thymic regulatory T cell selection to limit responses to self. *Immunity* 37: 475–86.

97. Tubo, N. J., A. J. Pagán, J. J. Taylor, R. W. Nelson, J. L. Linehan, J. M. Ertelt, E. S. Huseby, S. S. Way, and M. K. Jenkins. 2013. Single Naive CD4(+) T Cells from a Diverse Repertoire Produce Different Effector Cell Types during Infection. *Cell* 153: 785–96.

98. Keck, S., M. Schmaler, S. Ganter, L. Wyss, S. Oberle, E. S. Huseby, D. Zehn, and C. G. King. 2014. Antigen affinity and antigen dose exert distinct influences on CD4 T-cell differentiation. *Proc. Natl. Acad. Sci.* 111: 14852–14857.

99. Baumgartner, C. K., H. Yagita, and L. P. Malherbe. 2012. A TCR affinity threshold regulates memory CD4 T cell differentiation following vaccination. *J. Immunol.* 189: 2309–17.

100. van Panhuys, N., F. Klauschen, and R. N. Germain. 2014. T-Cell-Receptor-Dependent Signal Intensity Dominantly Controls CD4(+) T Cell Polarization In Vivo. *Immunity* 1–12.

101. Brogdon, J. L., D. Leitenberg, and K. Bottomly. 2002. The Potency of TCR Signaling Differentially Regulates NFATc/p Activity and Early IL-4 Transcription in Naive CD4+ T Cells. *J. Immunol.* 168: 3825–3832.

102. Caserta, S., J. Kleczkowska, A. Mondino, and R. Zamoyska. 2010. Reduced

functional avidity promotes central and effector memory CD4 T cell responses to tumor-associated antigens. *J. Immunol.* 185: 6545–6554.

103. O'Sullivan, D., G. J. W. van der Windt, S. C.-C. Huang, J. D. Curtis, C.-H. Chang, M. D. Buck, J. Qiu, A. M. Smith, W. Y. Lam, L. M. DiPlato, F.-F. Hsu, M. J. Birnbaum, E. J. Pearce, and E. L. Pearce. 2014. Memory CD8(+) T Cells Use Cell-Intrinsic Lipolysis to Support the Metabolic Programming Necessary for Development. *Immunity* 41: 75–88.

104. Wang, R., C. P. Dillon, L. Z. Shi, S. Milasta, R. Carter, D. Finkelstein, L. L. McCormick, P. Fitzgerald, H. Chi, J. Munger, and D. R. Green. 2011. The Transcription Factor Myc Controls Metabolic Reprogramming upon T Lymphocyte Activation. *Immunity* 35: 871–882.

105. van der Windt, G. J. W., D. O'Sullivan, B. Everts, S. C.-C. Huang, M. D. Buck, J. D. Curtis, C.-H. Chang, A. M. Smith, T. Ai, B. Faubert, R. G. Jones, E. J. Pearce, and E. L. Pearce. 2013. CD8 memory T cells have a bioenergetic advantage that underlies their rapid recall ability. *Proc. Natl. Acad. Sci. U. S. A.* 110: 14336–41.

106. Man, K., M. Miasari, W. Shi, A. Xin, D. C. Henstridge, S. Preston, M. Pellegrini, G. T. Belz, G. K. Smyth, M. a Febbraio, S. L. Nutt, and A. Kallies. 2013. The transcription factor IRF4 is essential for TCR affinity-mediated metabolic programming and clonal expansion of T cells. *Nat. Immunol.* 14: 1155–65.

107. Nikolich-Zugich, J., M. K. Slifka, and I. Messaoudi. 2004. The many important facets of T-cell repertoire diversity. *Nat. Rev. Immunol.* 4: 123–132.

108. Moon, J. J., H. H. Chu, J. Hataye, A. J. Pagán, M. Pepper, J. B. McLachlan, T. Zell,

and M. K. Jenkins. 2009. Tracking epitope-specific T cells. *Nat. Protoc.* 4: 565–81.

109. Langman, R. E., and M. Cohn. 1987. The E-T (elephant-tadpole) paradox necessitates the concept of a unit of B-cell function: the protection. *Mol. Immunol.* 24: 675–697.

110. Wooldridge, L., J. Ekeruche-Makinde, H. a van den Berg, A. Skowera, J. J. Miles, M. P. Tan, G. Dolton, M. Clement, S. Llewellyn-Lacey, D. a Price, M. Peakman, and A. K. Sewell. 2012. A single autoimmune T cell receptor recognizes more than a million different peptides. *J. Biol. Chem.* 287: 1168–77.

111. Birnbaum, M. E., J. L. Mendoza, D. K. Sethi, S. Dong, J. Glanville, J. Dobbins, E. Ozkan, M. M. Davis, K. W. Wucherpfennig, and K. C. Garcia. 2014. Deconstructing the peptide-MHC specificity of T cell recognition. *Cell* 157: 1073–87.

112. Holler, P. D., a R. Lim, B. K. Cho, L. a Rund, and D. M. Kranz. 2001. CD8(-) T cell transfectants that express a high affinity T cell receptor exhibit enhanced peptide-dependent activation. *J. Exp. Med.* 194: 1043–1052.

113. Donermeyer, D. L., K. S. Weber, D. M. Kranz, and P. M. Allen. 2006. The study of high-affinity TCRs reveals duality in T cell recognition of antigen: specificity and degeneracy. *J. Immunol.* 177: 6911–6919.

114. Holler, P. D., L. K. Chlewicki, and D. M. Kranz. 2003. TCRs with high affinity for foreign pMHC show self-reactivity. *Nat. Immunol.* 4: 55–62.

115. O'Sullivan, J. a., A. Zloza, F. J. Kohlhapp, T. V. Moore, A. T. Lacek, N. O. Dulin, and J. a. Guevara-Patiño. 2011. Priming with very low-affinity peptide ligands gives rise to CD8 + T-cell effectors with enhanced function but with greater susceptibility to

transforming growth factor (TGF)β-mediated suppression. *Cancer Immunol. Immunother.* 60: 1543–1551.

116. Khan, N., M. Cobbold, J. Cummerson, and P. a H. Moss. 2010. Persistent viral infection in humans can drive high frequency low-affinity T-cell expansions. *Immunology* 131: 537–548.

117. Lyman, M. a, C. T. Nugent, K. L. Marquardt, J. a Biggs, E. G. Pamer, and L. a Sherman. 2005. The fate of low affinity tumor-specific CD8+ T cells in tumor-bearing mice. *J. Immunol.* 174: 2563–2572.

118. Rees, W., J. Bender, T. K. Teague, R. M. Kedl, F. Crawford, P. Marrack, and J. Kappler. 1999. An inverse relationship between T cell receptor affinity and antigen dose during CD4(+) T cell responses in vivo and in vitro. *Proc. Natl. Acad. Sci. U. S. A.* 96: 9781–9786.

119. Srinivasan, A., J. Foley, and S. J. McSorley. 2004. Massive number of antigen-specific CD4 T cells during vaccination with live attenuated Salmonella causes interclonal competition. *J. Immunol.* 172: 6884–6893.

120. Majstoravich, S., J. Zhang, S. Nicholson-Dykstra, S. Linder, W. Friedrich, K. a. Siminovitch, and H. N. Higgs. 2004. Lymphocyte microvilli are dynamic, actin-dependent structures that do not require Wiskott-Aldrich syndrome protein (WASp) for their morphology. *Blood* 104: 1396–1403.

121. Sechi, A. S., and J. Wehland. 2004. Interplay between TCR signalling and actin cytoskeleton dynamics. *Trends Immunol.* 25: 257–265.

122. Miguel, L., D. M. Owen, C. Lim, C. Liebig, J. Evans, A. I. Magee, and E. C. Jury.

2011. Primary human CD4+ T cells have diverse levels of membrane lipid order that correlate with their function. *J. Immunol.* 186: 3505–3516.

123. Nagafuku, M., K. Okuyama, Y. Onimaru, a. Suzuki, Y. Odagiri, T. Yamashita, K. Iwasaki, M. Fujiwara, M. Takayanagi, I. Ohno, and J. -i. Inokuchi. 2012. PNAS Plus: CD4 and CD8 T cells require different membrane gangliosides for activation. *Proc. Natl. Acad. Sci.* 109: E336–E342.

124. Zhang, J., A. K. Somani, and K. A. Siminovitch. 2000. Roles of the SHP-1 tyrosine phosphatase in the negative regulation of cell signalling. *Semin. Immunol.* 12: 361–78.

125. Carter, J. D., G. M. Calabrese, M. Naganuma, and U. Lorenz. 2005. Deficiency of the Src homology region 2 domain-containing phosphatase 1 (SHP-1) causes enrichment of CD4+CD25+ regulatory T cells. *J. Immunol.* 174: 6627–38.

126. Mauldin, I. S., K. S. Tung, and U. M. Lorenz. 2012. The tyrosine phosphatase SHP-1 dampens murine Th17 development. *Blood* 119: 4419–29.

127. Iype, T., M. Sankarshanan, I. S. Mauldin, D. W. Mullins, and U. Lorenz. 2010. The protein tyrosine phosphatase SHP-1 modulates the suppressive activity of regulatory T cells. *J. Immunol.* 185: 6115–27.

128. Carter, J. D., B. G. Neel, and U. Lorenz. 1999. The tyrosine phosphatase SHP-1 influences thymocyte selection by setting TCR signaling thresholds. *Int. Immunol.* 11: 1999–2014.

129. Lorenz, U. 2009. SHP-1 and SHP-2 in T cells: two phosphatases functioning at many levels. *Immunol Rev* 228: 342–359.

130. Green, M. C., and L. D. Shultz. 1975. Motheaten, an Immunodeficient Mutant of the Mouse. *J. Hered.* 66: 250–258.

131. Kilgore, N. E., J. D. Carter, U. Lorenz, and B. D. Evavold. 2003. Cutting edge: dependence of TCR antagonism on Src homology 2 domain-containing protein tyrosine phosphatase activity. *J. Immunol.* 170: 4891–5.

132. Schnell, F. J., N. Alberts-Grill, and B. D. Evavold. 2009. CD8+ T cell responses to a viral escape mutant epitope: active suppression via altered SHP-1 activity. *J. Immunol.* 182: 1829–1835.

133. Wasserman, H. A., C. D. Beal, Y. Zhang, N. Jiang, C. Zhu, and B. D. Evavold. 2008. MHC variant peptide-mediated anergy of encephalitogenic T cells requires SHP-1. *J. Immunol.* 181: 6843–9.

134. Johnson, D. J., L. I. Pao, S. Dhanji, K. Murakami, P. S. Ohashi, and B. G. Neel. 2013. Shp1 regulates T cell homeostasis by limiting IL-4 signals. *J. Exp. Med.* 210: 1419–31.

135. Fowler, C. C., L. I. Pao, J. N. Blattman, and P. D. Greenberg. 2010. SHP-1 in T cells limits the production of CD8 effector cells without impacting the formation of long-lived central memory cells. *J. Immunol.* 185: 3256–67.

136. Fu, G., S. Vallée, V. Rybakin, M. V McGuire, J. Ampudia, C. Brockmeyer, M. Salek, P. R. Fallen, J. A. H. Hoerter, A. Munshi, Y. H. Huang, J. Hu, H. S. Fox, K. Sauer, O. Acuto, and N. R. J. Gascoigne. 2009. Themis controls thymocyte selection through regulation of T cell antigen receptor-mediated signaling. *Nat. Immunol.* 10: 848–856.

137. Lesourne, R., S. Uehara, J. Lee, K. Song, L. Li, J. Pinkhasov, Y. Zhang, N. Weng, K.

F. Wildt, L. Wang, R. Bosselut, and P. E. Love. 2009. Themis, a T cell-specific protein important for late thymocyte development. *Nat. Immunol.* 10: 840–848.

138. Johnson, A. L., L. Aravind, N. Shulzhenko, A. Morgun, S. Choi, T. L. Crockford, T. Lambe, H. Domaschenz, E. M. Kucharska, L. Zheng, C. G. Vinuesa, M. J. Lenardo, C. C. Goodnow, R. J. Cornall, and R. H. Schwartz. 2009. Themis is a member of a new metazoan gene family and is required for the completion of thymocyte positive selection. *Nat. Immunol.* 10: 831–9.

139. Paster, W., A. M. Bruger, K. Katsch, C. Grégoire, R. Roncagalli, G. Fu, N. R. J. Gascoigne, K. Nika, A. Cohnen, S. M. Feller, P. C. Simister, K. C. Molder, S. Cordoba, O. Dushek, and B. Malissen. 2015. A THEMIS : SHP 1 complex promotes T-cell survival. *EMBO J.* 34: 393–409.

140. Paster, W., C. Brockmeyer, G. Fu, P. C. Simister, B. de Wet, A. Martinez-Riaño, J. a H. Hoerter, S. M. Feller, C. Wülfing, N. R. J. Gascoigne, and O. Acuto. 2013. GRB2-mediated recruitment of THEMIS to LAT is essential for thymocyte development. *J. Immunol.* 190: 3749–56.

141. Gascoigne, N. R., and O. Acuto. 2015. THEMIS: a critical TCR signal regulator for ligand discrimination. *Curr. Opin. Immunol.* 33: 86–92.

142. Martinez, R. J., and B. D. Evavold. 2015. Lower Affinity T Cells are Critical Components and Active Participants of the Immune Response. *Front. Immunol.* 6: 1–10.

143. Xing, Y., and K. A. Hogquist. 2012. T-cell tolerance: central and peripheral. *Cold Spring Harb. Perspect. Biol.* 4.

144. Hu, Q., S. A. Nicol, A. Y. W. W. Suen, and T. A. Baldwin. 2012. Examination of

thymic positive and negative selection by flow cytometry. *J. Vis. Exp.* 1–7.

145. Puls, K. L., K. A. Hogquist, N. Reilly, and M. D. Wright. 2002. CD53, a thymocyte selection marker whose induction requires a lower affinity TCR-MHC interaction than CD69, but is up-regulated with slower kinetics. *Int. Immunol.* 14: 249–58.

146. Zhang, J., A. K. Somani, D. Yuen, Y. Yang, P. E. Love, and K. A. Siminovitch. 1999. Involvement of the SHP-1 tyrosine phosphatase in regulation of T cell selection. *J. Immunol.* 163: 3012–21.

147. Daniels, M. A., E. Teixeiro, J. Gill, B. Hausmann, D. Roubaty, K. Holmberg, G. Werlen, G. a Holländer, N. R. J. Gascoigne, and E. Palmer. 2006. Thymic selection threshold defined by compartmentalization of Ras/MAPK signalling. *Nature* 444: 724–9.

148. Krummey, S. M., R. J. Martinez, R. Andargachew, D. Liu, M. Wagener, J. E. Kohlmeier, B. D. Evavold, C. P. Larsen, and M. L. Ford. 2016. Low-Affinity Memory CD8+ T Cells Mediate Robust Heterologous Immunity. *J. Immunol.* 196: 2838–46.

149. Weinreich, M. A., and K. A. Hogquist. 2008. Thymic Emigration: When and How T Cells Leave Home. *J. Immunol.* 181: 2265–2270.

150. Rausch, P., M. Basic, A. Batra, S. C. Bischoff, M. Blaut, T. Clavel, J. Gläsner, S. Gopalakrishnan, G. A. Grassl, C. Günther, D. Haller, M. Hirose, S. Ibrahim, G. Loh, J. Mattner, S. Nagel, O. Pabst, F. Schmidt, B. Siegmund, T. Strowig, V. Volynets, S. Wirtz, S. Zeissig, Y. Zeissig, A. Bleich, and J. F. Baines. 2016. Analysis of factors contributing to variation in the C57BL/6J fecal microbiota across German animal facilities. *Int. J. Med. Microbiol.* .

151. Tanchot, C., F. a Lemonnier, B. Pérarnau, a a Freitas, and B. Rocha. 1997.

Differential requirements for survival and proliferation of CD8 naïve or memory T cells. *Science* 276: 2057–62.

152. Takeda, S., H. R. Rodewald, H. Arakawa, H. Bluethmann, and T. Shimizu. 1996. MHC class II molecules are not required for survival of newly generated CD4+ T cells, but affect their long-term life span. *Immunity* 5: 217–28.

153. Anderson, M. S., E. S. Venanzi, L. Klein, Z. Chen, S. P. Berzins, S. J. Turley, H. von Boehmer, R. Bronson, A. Dierich, C. Benoist, and D. Mathis. 2002. Projection of an immunological self shadow within the thymus by the aire protein. *Science (80-.).* 298: 1395–401.

154. MacDonald, H. R., R. Schneider, R. Lees, R. Howe, H. Acha-Orbea, H. Festenstein, R. Zinkernagel, and H. Hengartner. 1988. T-cell receptor Vb use predicts reactivity and tolerance to Mlsa-encode antigens. *Nature* 332.

155. Kappler, J. W., N. Roehm, and P. Marrack. 1987. T cell tolerance by clonal elimination in the thymus. *Cell* 49: 273–80.

156. Jordan, M. S., A. Boesteanu, A. J. Reed, A. L. Petrone, A. E. Holenbeck, M. A. Lerman, A. Naji, and A. J. Caton. 2001. Thymic selection of CD4+CD25+ regulatory T cells induced by an agonist self-peptide. *Nat. Immunol.* 2: 301–306.

157. Malhotra, D., J. L. Linehan, T. Dileepan, Y. J. Lee, W. E. Purtha, J. V Lu, R. W. Nelson, B. T. Fife, H. T. Orr, M. S. Anderson, K. A. Hogquist, and M. K. Jenkins. 2016. Tolerance is established in polyclonal CD4+ T cells by distinct mechanisms, according to self-peptide expression patterns. *Nat. Immunol.* .

158. Legoux, F. P., J. Lim, A. W. Cauley, T. Sparwasser, S. S. Way, J. J. Moon, F. P.

Legoux, J. Lim, A. W. Cauley, S. Dikiy, J. Ertelt, and T. J. Mariani. 2015. CD4 + T Cell Tolerance to Tissue-Restricted Self Antigens Is Mediated by Antigen-Specific Regulatory T Cells Rather Than Deletion. *Immunity* 43: 1–13.

159. Meredith, M., D. Zemmour, D. Mathis, and C. Benoist. 2015. Aire controls gene expression in the thymic epithelium with ordered stochasticity. *Nat. Immunol.* 1–11.

160. Brennecke, P., A. Reyes, S. Pinto, K. Rattay, M. Nguyen, R. Küchler, W. Huber, B. Kyewski, and L. M. Steinmetz. 2015. Single-cell transcriptome analysis reveals coordinated ectopic gene-expression patterns in medullary thymic epithelial cells. *Nat. Immunol.* 16.

161. Klein, L., M. Klugmann, K. a Nave, V. K. Tuohy, and B. Kyewski. 2000. Shaping of the autoreactive T-cell repertoire by a splice variant of self protein expressed in thymic epithelial cells. *Nat. Med.* 6: 56–61.

162. Cao, Y., B. A. Goods, K. Raddassi, G. T. Nepom, W. W. Kwok, J. C. Love, and D. A. Hafler. 2015. Functional inflammatory profiles distinguish myelin-reactive T cells from patients with multiple sclerosis. *Sci. Transl. Med.* 7: 287ra74–287ra74.

163. Raddassi, K., S. C. Kent, J. Yang, K. Bourcier, E. M. Bradshaw, V. Seyfert-Margolis, G. T. Nepom, W. W. Kwok, and D. A. Hafler. 2011. Increased frequencies of myelin oligodendrocyte glycoprotein/MHC class II-binding CD4 cells in patients with multiple sclerosis. *J. Immunol.* 187: 1039–46.

164. Venken, K., N. Hellings, R. Liblau, and P. Stinissen. 2010. Disturbed regulatory T cell homeostasis in multiple sclerosis. *Trends Mol. Med.* 16: 58–68.

165. Zozulya, A. L., and H. Wiendl. 2008. The role of regulatory T cells in multiple

sclerosis. *Nat. Clin. Pract. Neurol.* 4: 384–398.

166. Liñares, D., P. Mañá, M. Goodyear, A. M. Chow, C. Clavarino, N. D. Huntington, L. Barnett, F. Koentgen, R. Tomioka, C. C. a. Bernard, M. Freire-Garabal, and H. H. Reid. 2003. The magnitude and encephalogenic potential of autoimmune response to MOG is enhanced in MOG deficient mice. *J. Autoimmun.* 21: 339–351.

167. Moon, J. J., P. Dash, T. H. Oguin, J. L. McClaren, H. H. Chu, P. G. Thomas, and M. K. Jenkins. 2011. Quantitative impact of thymic selection on Foxp3+ and Foxp3− subsets of self-peptide/MHC class II-specific CD4+ T cells. *Proc. ...* 1–6.

168. Bouneaud, C., P. Kourilsky, and P. Bousso. 2000. Impact of negative selection on the T cell repertoire reactive to a self-peptide: a large fraction of T cell clones escapes clonal deletion. *Immunity* 13: 829–40.

169. Denning, T. L., S. W. Granger, S. Granger, D. Mucida, R. Graddy, G. Leclercq, W. Zhang, K. Honey, J. P. Rasmussen, H. Cheroutre, A. Y. Rudensky, and M. Kronenberg. 2007. Mouse TCRalphabeta+CD8alphaalpha intraepithelial lymphocytes express genes that down-regulate their antigen reactivity and suppress immune responses. *J. Immunol.* 178: 4230–9.

170. Bettini, M. L., M. Bettini, M. Nakayama, C. S. Guy, and D. A. A. Vignali. 2013. Generation of T cell receptor-retrogenic mice: improved retroviral-mediated stem cell gene transfer. *Nat. Protoc.* 8: 1837–40.

171. Alli, R., P. Nguyen, and T. L. Geiger. 2008. Retrogenic modeling of experimental allergic encephalomyelitis associates T cell frequency but not TCR functional affinity with pathogenicity. *J. Immunol.* 181: 136–45.

172. Dash, P., J. L. McClaren, T. H. Oguin, W. Rothwell, B. Todd, M. Y. Morris, J. Becksfort, C. Reynolds, S. A. Brown, P. C. Doherty, and P. G. Thomas. 2011. Paired analysis of TCRα and TCRβ chains at the single-cell level in mice. *J. Clin. Invest.* 121: 288–95.

173. Tanaka, S., A. Suto, T. Iwamoto, D. Kashiwakuma, S. Kagami, K. Suzuki, H. Takatori, T. Tamachi, K. Hirose, A. Onodera, J. Suzuki, O. Ohara, M. Yamashita, T. Nakayama, and H. Nakajima. 2014. Sox5 and c-Maf cooperatively induce Th17 cell differentiation via RORγt induction as downstream targets of Stat3. *J. Exp. Med.* 211: 1857–74.

174. Tang, Q., K. J. Henriksen, M. Bi, E. B. Finger, G. Szot, J. Ye, E. L. Masteller, H. McDevitt, M. Bonyhadi, and J. A. Bluestone. 2004. In vitro-expanded antigen-specific regulatory T cells suppress autoimmune diabetes. *J. Exp. Med.* 199: 1455–65.

175. Tarbell, K. V, S. Yamazaki, K. Olson, P. Toy, and R. M. Steinman. 2004. CD25+ CD4+ T cells, expanded with dendritic cells presenting a single autoantigenic peptide, suppress autoimmune diabetes. *J. Exp. Med.* 199: 1467–77.

176. Ouyang, W., W. Liao, C. T. Luo, N. Yin, M. Huse, M. V Kim, M. Peng, P. Chan, Q. Ma, Y. Mo, D. Meijer, K. Zhao, A. Y. Rudensky, G. Atwal, M. Q. Zhang, and M. O. Li. 2012. Novel Foxo1-dependent transcriptional programs control T(reg) cell function. *Nature* 491: 554–9.

177. Luo, C. T., W. Liao, S. Dadi, A. Toure, and M. O. Li. 2016. Graded Foxo1 activity in Treg cells differentiates tumour immunity from spontaneous autoimmunity. *Nature* 529: 532–536.

178. Hedrick, S. M., R. Hess Michelini, A. L. Doedens, A. W. Goldrath, and E. L. Stone. 2012. FOXO transcription factors throughout T cell biology. *Nat. Rev. Immunol. Immunol.* 12: 649–61.

179. Lo, W.-L., N. J. Felix, J. J. Walters, H. Rohrs, M. L. Gross, and P. M. Allen. 2009. An endogenous peptide positively selects and augments the activation and survival of peripheral CD4+ T cells. *Nat. Immunol.* 10: 1155–61.

180. Ebert, P. J. R., S. Jiang, J. Xie, Q.-J. Li, and M. M. Davis. 2009. An endogenous positively selecting peptide enhances mature T cell responses and becomes an autoantigen in the absence of microRNA miR-181a. *Nat. Immunol.* 10: 1162–1169.

181. Locht, C., L. Coutte, and N. Mielcarek. 2011. The ins and outs of pertussis toxin. *FEBS J.* 278: 4668–82.

182. Hinterberger, M., M. Aichinger, O. Prazeres da Costa, D. Voehringer, R. Hoffmann, and L. Klein. 2010. Autonomous role of medullary thymic epithelial cells in central CD4(+) T cell tolerance. *Nat. Immunol.* 11: 512–9.

183. Derbinski, J., J. Gäbler, B. Brors, S. Tierling, S. Jonnakuty, M. Hergenhahn, L. Peltonen, J. Walter, and B. Kyewski. 2005. Promiscuous gene expression in thymic epithelial cells is regulated at multiple levels. *J. Exp. Med.* 202: 33–45.

184. Su, M., Y. Song, Z. He, R. Hu, D. Rood, and L. Lai. 2015. Administration of embryonic stem cell-derived thymic epithelial progenitors expressing MOG induces antigen-specific tolerance and ameliorates experimental autoimmune encephalomyelitis. *J. Autoimmun.* .

185. Gough, S. C. L., and M. J. Simmonds. 2007. The HLA Region and Autoimmune

Disease: Associations and Mechanisms of Action. *Curr. Genomics* 8: 453–65.

186. Huesmann, M., B. Scott, P. Kisielow, and H. von Boehmer. 1991. Kinetics and efficacy of positive selection in the thymus of normal and T cell receptor transgenic mice. *Cell* 66: 533–540.

187. Takada, K., F. Van Laethem, Y. Xing, K. Akane, H. Suzuki, S. Murata, K. Tanaka, S. C. Jameson, A. Singer, and Y. Takahama. 2015. TCR affinity for thymoproteasome-dependent positively selecting peptides conditions antigen responsiveness in CD8+ T cells. *Nat. Immunol.* 1–9.

188. Burns, J. B., B. D. Bartholomew, and S. T. Lobo. 2002. In vivo activation of myelin oligodendrocyte glycoprotein-specific T cells in healthy control subjects. *Clin. Immunol.* 105: 185–91.

189. Lund, J. M., L. Hsing, T. T. Pham, and A. Y. Rudensky. 2008. Coordination of early protective immunity to viral infection by regulatory T cells. *Science* 320: 1220–4.

190. Laidlaw, B. J., W. Cui, R. a Amezquita, S. M. Gray, T. Guan, Y. Lu, Y. Kobayashi, R. a Flavell, S. H. Kleinstein, J. Craft, and S. M. Kaech. 2015. Production of IL-10 by CD4+ regulatory T cells during the resolution of infection promotes the maturation of memory CD8+ T cells. *Nat. Immunol.* 1–11.

191. St-Pierre, C., S. Brochu, J. R. Vanegas, M. Dumont-Lagacé, S. Lemieux, and C. Perreault. 2013. Transcriptome sequencing of neonatal thymic epithelial cells. *Sci. Rep.* 3: 1860.

192. Ford, M. L., and B. D. Evavold. 2003. Regulation of polyclonal T cell responses by an MHC anchor-substituted variant of myelin oligodendrocyte glycoprotein 35-55. *J.*

Immunol. 171: 1247–54.

193. Bailey-Bucktrout, S. L., M. Martinez-Llordella, X. Zhou, B. Anthony, W. Rosenthal, H. Luche, H. J. Fehling, and J. A. Bluestone. 2013. Self-antigen-driven activation induces instability of regulatory T cells during an inflammatory autoimmune response. *Immunity* 39: 949–62.

194. Lefranc, M.-P., V. Giudicelli, C. Ginestoux, N. Bosc, G. Folch, D. Guiraudou, J. Jabado-Michaloud, S. Magris, D. Scaviner, V. Thouvenin, K. Combres, D. Girod, S. Jeanjean, C. Protat, M. Yousfi-Monod, E. Duprat, Q. Kaas, C. Pommié, D. Chaume, and G. Lefranc. 2004. IMGT-ONTOLOGY for immunogenetics and immunoinformatics. *In Silico Biol.* 4: 17–29.

195. Lefranc, M.-P. 2004. IMGT-ONTOLOGY and IMGT databases, tools and Web resources for immunogenetics and immunoinformatics. *Mol. Immunol.* 40: 647–60.

196. Lefranc, M.-P. 2008. IMGT, the International ImMunoGeneTics Information System for Immunoinformatics : methods for querying IMGT databases, tools, and web resources in the context of immunoinformatics. *Mol. Biotechnol.* 40: 101–11.

197. Falcon, S., and R. Gentleman. 2007. Using GOstats to test gene lists for GO term association. *Bioinformatics* 23: 257–8.

198. Subramanian, A., P. Tamayo, V. K. Mootha, S. Mukherjee, B. L. Ebert, M. a Gillette, A. Paulovich, S. L. Pomeroy, T. R. Golub, E. S. Lander, and J. P. Mesirov. 2005. Gene set enrichment analysis: a knowledge-based approach for interpreting genome-wide expression profiles. *Proc. Natl. Acad. Sci. U. S. A.* 102: 15545–50.

199. Love, M. I., W. Huber, and S. Anders. 2014. Moderated estimation of fold change

and dispersion for RNA-seq data with DESeq2. *Genome Biol.* 15: 550.

200. Cohn, M., and R. E. Langman. 1990. The protecton: the unit of humoral immunity selected by evolution. *Immunol. Rev.* 115: 5–261.

201. Wooldridge, L., A. Lissina, D. K. Cole, H. A. van den Berg, D. A. Price, and A. K. Sewell. 2009. Tricks with tetramers: how to get the most from multimeric peptide-MHC. *Immunology* 126: 147–64.

202. Boniface, J. J., J. D. Rabinowitz, C. Wulfing, J. Hampl, Z. Reich, J. D. Altman, R. M. Kantor, C. Beeson, H. M. McConnell, and M. M. Davis. 1998. Initiation of signal transduction through the T cell receptor requires the peptide multivalent engagement of MHC ligands. *Immunity* 9: 459–466.

203. Xiong, Y., P. Kern, H.-C. Chang, and E. L. Reinherz. 2000. T Cell Receptor Binding to a pMHCII Ligand Is Kinetically Distinct from and Independent of CD4. *J. Biol. Chem.* 276: 5659–5667.

204. Savage, P. A., J. J. Boniface, and M. M. Davis. 1999. A kinetic basis for T cell receptor repertoire selection during an immune response. *Immunity* 10: 485–92.

205. Gallegos, A. M., H. Xiong, I. M. Leiner, B. Sušac, M. S. Glickman, E. G. Pamer, and J. W. J. van Heijst. 2016. Control of T cell antigen reactivity via programmed TCR downregulation. *Nat. Immunol.* .

206. Kedl, R. M., W. A. Rees, D. A. Hildeman, B. Schaefer, T. Mitchell, J. Kappler, and P. Marrack. 2000. T cells compete for access to antigen-bearing antigen-presenting cells. *J. Exp. Med.* 192: 1105–1113.

207. Tubo, N. J., B. T. Fife, A. J. Pagan, D. I. Kotov, M. F. Goldberg, and M. K. Jenkins. 2016. Most microbe-specific naïve CD4+ T cells produce memory cells during infection. *Science (80-.).* 351: 511–514.

208. Moran, A. E., K. L. Holzapfel, Y. Xing, N. R. Cunningham, J. S. Maltzman, J. Punt, and K. A. Hogquist. 2011. T cell receptor signal strength in Treg and iNKT cell development demonstrated by a novel fluorescent reporter mouse. *J. Exp. Med.* 208: 1279–89.

209. Waldmann, H., I. Lefkovits, and J. Quintáns. 1975. Limiting dilution analysis of helper T-cell function. *Immunology* 28: 1135–1148.

210. Schubert, D. A., S. Gordo, J. J. Sabatino, S. Vardhana, E. Gagnon, D. K. Sethi, N. P. Seth, K. Choudhuri, H. Reijonen, G. T. Nepom, B. D. Evavold, M. L. Dustin, and K. W. Wucherpfennig. 2012. Self-reactive human CD4 T cell clones form unusual immunological synapses. *J. Exp. Med.* 209: 335–352.

211. Hong, J., S. P. Persaud, S. Horvath, P. M. Allen, B. D. Evavold, and C. Zhu. 2015. Force-Regulated In Situ TCR-Peptide-Bound MHC Class II Kinetics Determine Functions of CD4+ T Cells. *J. Immunol.* 195: 3557–3564.

212. Zhang, S.-Q., P. Parker, K.-Y. Ma, C. He, Q. Shi, Z. Cui, C. M. Williams, B. S. Wendel, A. I. Meriwether, M. A. Salazar, and N. Jiang. 2016. Direct measurement of T cell receptor affinity and sequence from naïve antiviral T cells. *Sci Transl Med* 8: 341ra77–341ra77.

213. Whitmire, J. K., J. K. Whitmire, N. Benning, N. Benning, J. L. Whitton, and J. L. Whitton. 2006. Precursor Frequency, Nonlinear Proliferation, and Functional Maturation

of Virus-Specific CD4+ T Cells. *J. Immunol.* 176: 3028–3036.

214. Hataye, J., J. J. Moon, A. Khoruts, C. Reilly, and M. K. Jenkins. 2006. Naıve and Memory CD4+ T cell Survival Controlled by Clonal Abundance. *Science (80-.).* 312: 114–116.

215. Buchholz, V. R., M. Flossdorf, I. Hensel, L. Kretschmer, B. Weissbrich, P. Gräf, A. Verschoor, M. Schiemann, T. Höfer, and D. H. Busch. 2013. Disparate individual fates compose robust CD8+ T cell immunity. *Science* 340: 630–5.

216. Gerlach, C., J. C. Rohr, L. Perié, N. van Rooij, J. W. J. van Heijst, A. Velds, J. Urbanus, S. H. Naik, H. Jacobs, J. B. Beltman, R. J. de Boer, and T. N. M. Schumacher. 2013. Heterogeneous differentiation patterns of individual CD8+ T cells. *Science* 340: 635–9.

217. Merkenschlager, J., and G. Kassiotis. 2015. Narrowing the gap: preserving repertoire diversity despite clonal selection during the CD4 T cell response. *Front. Immunol.* 6: 1–11.

218. Huang, J., X. Zeng, N. Sigal, P. J. Lund, L. F. Su, H. Huang, Y. Chien, and M. M. Davis. 2016. Detection, phenotyping, and quantification of antigen-specific T cells using a peptide-MHC dodecamer. *Proc. Natl. Acad. Sci.* 201602488.

219. Cameron, B. J., A. B. Gerry, J. Dukes, J. V Harper, V. Kannan, F. C. Bianchi, F. Grand, J. E. Brewer, M. Gupta, G. Plesa, G. Bossi, A. Vuidepot, A. S. Powlesland, A. Legg, K. J. Adams, A. D. Bennett, N. J. Pumphrey, D. D. Williams, G. Binder-Scholl, I. Kulikovskaya, B. L. Levine, J. L. Riley, A. Varela-Rohena, E. a Stadtmauer, A. P. Rapoport, G. P. Linette, C. H. June, N. J. Hassan, M. Kalos, and B. K. Jakobsen. 2013.

Identification of a Titin-derived HLA-A1-presented peptide as a cross-reactive target for engineered MAGE A3-directed T cells. *Sci. Transl. Med.* 5: 197ra103.

220. Linette, G. P., E. A. Stadtmauer, M. V. Maus, A. P. Rapoport, B. L. Levine, L. Emery, L. Litzky, A. Bagg, B. M. Carreno, P. J. Cimino, G. K. Binder-Scholl, D. P. Smethurst, A. B. Gerry, N. J. Pumphrey, A. D. Bennett, J. E. Brewer, J. Dukes, J. Harper, H. K. Tayton-Martin, B. K. Jakobsen, N. J. Hassan, M. Kalos, and C. H. June. 2013. Cardiovascular toxicity and titin cross-reactivity of affinity-enhanced T cells in myeloma and melanoma. *Blood* 122: 863–871.

221. Oestreich, K. J., S. E. Mohn, and A. S. Weinmann. 2012. Molecular mechanisms that control the expression and activity of Bcl-6 in TH1 cells to regulate flexibility with a TFH-like gene profile. *Nat. Immunol.* 13: 405–11.

222. Pepper, M., A. J. Pagán, B. Z. Igyártó, J. J. Taylor, and M. K. Jenkins. 2011. Opposing Signals from the Bcl6 Transcription Factor and the Interleukin-2 Receptor Generate T Helper 1 Central and Effector Memory Cells. *Immunity* 35: 583–595.

223. Gottschalk, R. A., E. Corse, and J. P. Allison. 2010. TCR ligand density and affinity determine peripheral induction of Foxp3 in vivo. *J. Exp. Med.* 207: 1701–11.

224. Sauer, S., L. Bruno, A. Hertweck, D. Finlay, M. Leleu, M. Spivakov, Z. A. Knight, B. S. Cobb, D. Cantrell, E. O'Connor, K. M. Shokat, A. G. Fisher, and M. Merkenschlager. 2008. T cell receptor signaling controls Foxp3 expression via PI3K, Akt, and mTOR. *Proc. Natl. Acad. Sci. U. S. A.* 105: 7797–7802.

225. Mason, D. 1998. A very high level of crossreactivity is an essential feature of the T-cell receptor. *Immunol. Today* 19: 395–404.

226. Yager, E. J., M. Ahmed, K. Lanzer, T. D. Randall, D. L. Woodland, and M. A. Blackman. 2008. Age-associated decline in T cell repertoire diversity leads to holes in the repertoire and impaired immunity to influenza virus. *J. Exp. Med.* 205: 711–723.

227. Woodland, D. L., B. L. Kotzin, and E. Palmer. 1990. Functional consequences of a T cell receptor D beta 2 and J beta 2 gene segment deletion. *J Immunol* 144: 379–385.

228. Messaoudi, I., J. A. Guevara Patiño, R. Dyall, J. LeMaoult, and J. Nikolich-Zugich. 2002. Direct link between mhc polymorphism, T cell avidity, and diversity in immune defense. *Science* 298: 1797–1800.

229. Casrouge, a, E. Beaudoing, S. Dalle, C. Pannetier, J. Kanellopoulos, and P. Kourilsky. 2000. Size estimate of the alpha beta TCR repertoire of naive mouse splenocytes. *J. Immunol.* 164: 5782–5787.

230. McMaster, S. R., J. J. Wilson, H. Wang, and J. E. Kohlmeier. 2015. Airway-Resident Memory CD8 T Cells Provide Antigen-Specific Protection against Respiratory Virus Challenge through Rapid IFN-γ Production. *J. Immunol.* 195: 203–9.

231. Rosenbloom, D. I. S., O. Elliott, A. L. Hill, T. J. Henrich, J. M. Siliciano, and R. F. Siliciano. 2015. Designing and interpreting limiting dilution assays: general principles and applications to the latent reservoir for HIV-1 Daniel. *Open Forum Infect. Dis.* 2.

232. Martin, W. D., G. G. Hicks, S. K. Mendiratta, H. I. Leva, H. E. Ruley, and L. Van Kaer. 1996. H2-M mutant mice are defective in the peptide loading of class II molecules, antigen presentation, and T cell repertoire selection. *Cell* 84: 543–50.

233. Kosmrlj, A., E. L. Read, Y. Qi, T. M. Allen, M. Altfeld, S. G. Deeks, F. Pereyra, M. Carrington, B. D. Walker, and A. K. Chakraborty. 2010. Effects of thymic selection of

the T-cell repertoire on HLA class I-associated control of HIV infection. *Nature* 465: 350–4.

234. Bautista, J. L., C.-W. J. Lio, S. K. Lathrop, K. Forbush, Y. Liang, J. Luo, A. Y. Rudensky, and C.-S. Hsieh. 2009. Intraclonal competition limits the fate determination of regulatory T cells in the thymus. *Nat. Immunol.* 10: 610–7.

235. Lio, C.-W. J., and C.-S. Hsieh. 2008. A two-step process for thymic regulatory T cell development. *Immunity* 28: 100–11.

236. Kieback, E., E. Hilgenberg, U. Stervbo, S. M. Anderton, W. Uckert, S. Fillatreau, E. Kieback, E. Hilgenberg, U. Stervbo, V. Lampropoulou, P. Shen, M. Bunse, and Y. Jaimes. 2016. Thymus-Derived Regulatory T Cells Are Positively Selected on Natural Self-Antigen through Cognate Interactions of High Functional Avidity Article. *Immunity* 44: 1114–1126.

237. Fontenot, J. D., J. P. Rasmussen, M. A. Gavin, and A. Y. Rudensky. 2005. A function for interleukin 2 in Foxp3-expressing regulatory T cells. *Nat. Immunol.* 6: 1142–51.

238. Levine, A. G., A. Arvey, W. Jin, and A. Y. Rudensky. 2014. Continuous requirement for the TCR in regulatory T cell function. *Nat. Immunol.* 15: 1070–8.

239. Fontenot, J. D., M. A. Gavin, and A. Y. Rudensky. 2003. Foxp3 programs the development and function of CD4+CD25+ regulatory T cells. *Nat. Immunol.* 4: 330–6.

240. Feng, Y., J. van der Veeken, M. Shugay, E. V. Putintseva, H. U. Osmanbeyoglu, S. Dikiy, B. E. Hoyos, B. Moltedo, S. Hemmers, P. Treuting, C. S. Leslie, D. M. Chudakov, and A. Y. Rudensky. 2015. A mechanism for expansion of regulatory T-cell repertoire

and its role in self-tolerance. *Nature* 528: 132–6.

241. Vahl, J. C., C. Drees, K. Heger, S. Heink, J. C. Fischer, J. Nedjic, N. Ohkura, H. Morikawa, H. Poeck, S. Schallenberg, D. Rieß, M. Y. Hein, T. Buch, B. Polic, A. Schönle, R. Zeiser, A. Schmitt-Gräff, K. Kretschmer, L. Klein, T. Korn, S. Sakaguchi, and M. Schmidt-Supprian. 2014. Continuous T Cell Receptor Signals Maintain a Functional Regulatory T Cell Pool. *Immunity* 1–15.

242. Vignali, D. A. A., L. W. Collison, and C. J. Workman. 2008. How regulatory T cells work. *Nat. Rev. Immunol.* 8: 523–532.

243. Schaeffer, E. M., C. Broussard, J. Debnath, S. Anderson, D. W. McVicar, and P. L. Schwartzberg. 2000. Tec family kinases modulate thresholds for thymocyte development and selection. *J. Exp. Med.* 192: 987–1000.

244. Zhou, R. W., H. Mkhikian, A. Grigorian, A. Hong, D. Chen, A. Arakelyan, and M. Demetriou. 2014. N-glycosylation bidirectionally extends the boundaries of thymocyte positive selection by decoupling Lck from Ca2+ signaling. *Nat. Immunol.* 15: 1038–1045.

245. Mingueneau, M., A. Sansoni, C. Grégoire, R. Roncagalli, E. Aguado, A. Weiss, M. Malissen, and B. Malissen. 2008. The proline-rich sequence of CD3epsilon controls T cell antigen receptor expression on and signaling potency in preselection CD4+CD8+ thymocytes. *Nat. Immunol.* 9: 522–32.

246. Minguet, S., M. Swamy, B. Alarcón, I. F. Luescher, and W. W. A. Schamel. 2007. Full Activation of the T Cell Receptor Requires Both Clustering and Conformational Changes at CD3. *Immunity* 26: 43–54.

247. Swamy, M., K. Beck-Garcia, E. Beck-Garcia, F. A. Hartl, A. Morath, O. S. Yousefi,

E. P. Dopfer, E. Molnár, A. K. Schulze, R. Blanco, A. Borroto, N. Martín-Blanco, B. Alarcon, T. Höfer, S. Minguet, and W. W. A. Schamel. 2016. A Cholesterol-Based Allostery Model of T Cell Receptor Phosphorylation. *Immunity* 44: 109`–1101.

248. Wang, F., K. Beck-García, C. Zorzin, W. W. A. Schamel, and M. M. Davis. 2016. Inhibition of T cell receptor signaling by cholesterol sulfate, a naturally occurring derivative of membrane cholesterol. *Nat. Immunol.* 17: 844–850.

249. Liu, Y., L. Blanchfield, V. P.-Y. Ma, R. Andargachew, K. Galior, Z. Liu, B. Evavold, and K. Salaita. 2016. DNA-based nanoparticle tension sensors reveal that T-cell receptors transmit defined pN forces to their antigens for enhanced fidelity. *Proc. Natl. Acad. Sci. U. S. A.* 201600163.

250. Tan, Y. X., B. N. Manz, T. S. Freedman, C. Zhang, K. M. Shokat, and A. Weiss. 2013. Inhibition of the kinase Csk in thymocytes reveals a requirement for actin remodeling in the initiation of full TCR signaling. *Nat. Immunol.* 15: 186–194.

251. Boniface, J. J., Z. Reich, D. S. Lyons, and M. M. Davis. 1999. Thermodynamics of T cell receptor binding to peptide-MHC: evidence for a general mechanism of molecular scanning. *Proc. Natl. Acad. Sci. U. S. A.* 96: 11446–11451.

252. Matsui, K., J. J. Boniface, P. Steffner, P. a Reay, and M. M. Davis. 1994. Kinetics of T-cell receptor binding to peptide/I-Ek complexes: correlation of the dissociation rate with T-cell responsiveness. *Proc. Natl. Acad. Sci. U. S. A.* 91: 12862–6.

253. Victora, G. D., and M. C. Nussenzweig. 2012. Germinal Centers. *Annu. Rev. Immunol.* 30: 429–457.

254. Verbist, K. C., C. S. Guy, S. Milasta, S. Liedmann, M. M. Kamiński, R. Wang, and

D. R. Green. 2016. Metabolic maintenance of cell asymmetry following division in activated T lymphocytes. *Nature* 532: 389–93.

255. Wang, R., and D. R. Green. 2012. Metabolic checkpoints in activated T cells. *Nat. Immunol.* 13: 907–915.

256. Bousso, B. P., J. Levraud, and P. Kourilsky. 1999. The Composition of a Primary T Cell Response Is Largely Determined by the Timing of Recruitment of Individual T Cell Clones. *J. Exp. Med.* 189: 1591–1600.

257. Blair, D. a, D. L. Turner, T. O. Bose, Q.-M. Pham, K. R. Bouchard, K. J. Williams, J. P. McAleer, L. S. Cauley, A. T. Vella, and L. Lefrançois. 2011. Duration of antigen availability influences the expansion and memory differentiation of T cells. *J. Immunol.* 187: 2310–2321.